OAK RIDGE
NATIONAL LABORATORY
MANAGED BY UT-BATTELLE
FOR THE DEPARTMENT OF ENERGY

ORNL/TM-2011/399

SUPERHEATER CORROSION IN BIOMASS BOILERS: Today's Science and Technology

September 30, 2010

W. B. A. (Sandy) Sharp
SharpConsultant

UT-BATTELLE
ORNL-27 (4-00)

DOCUMENT AVAILABILITY

Reports produced after January 1, 1996, are generally available free via the U.S. Department of Energy (DOE) Information Bridge.

Web site http://www.osti.gov/bridge

Reports produced before January 1, 1996, may be purchased by members of the public from the following source.

National Technical Information Service
5285 Port Royal Road
Springfield, VA 22161
Telephone 703-605-6000 (1-800-553-6847)
TDD 703-487-4639
Fax 703-605-6900
E-mail info@ntis.gov
Web site http://www.ntis.gov/support/ordernowabout.htm

Reports are available to DOE employees, DOE contractors, Energy Technology Data Exchange (ETDE) representatives, and International Nuclear Information System (INIS) representatives from the following source.

Office of Scientific and Technical Information
P.O. Box 62
Oak Ridge, TN 37831
Telephone 865-576-8401
Fax 865-576-5728
E-mail reports@osti.gov
Web site http://www.osti.gov/contact.html

This report was prepared as an account of work sponsored by an agency of the United States Government. Neither the United States Government nor any agency thereof, nor any of their employees, makes any warranty, express or implied, or assumes any legal liability or responsibility for the accuracy, completeness, or usefulness of any information, apparatus, product, or process disclosed, or represents that its use would not infringe privately owned rights. Reference herein to any specific commercial product, process, or service by trade name, trademark, manufacturer, or otherwise, does not necessarily constitute or imply its endorsement, recommendation, or favoring by the United States Government or any agency thereof. The views and opinions of authors expressed herein do not necessarily state or reflect those of the United States Government or any agency thereof.

ORNL/TM-2011/399

Industrial Technologies Program

SUPERHEATER CORROSION IN BIOMASS BOILERS: TODAY'S SCIENCE AND TECHNOLOGY

W. B. A. (Sandy) Sharp

September, 2010

Prepared by
OAK RIDGE NATIONAL LABORATORY
Oak Ridge, Tennessee 37831-6283
managed by
UT-BATTELLE, LLC
for the
U.S. DEPARTMENT OF ENERGY
under contract DE-AC05-00OR22725

CONTENTS

LIST OF FIGURES v
LIST OF TABLES vii
ACRONYMS ix
ACKNOWLEDGMENTS xi
EXECUTIVE SUMMARY xiii
1. INTRODUCTION 1
1.1 MOTIVATION TO USE RENEWABLE FUELS 1
1.2 INTRODUCTION TO RELATIONSHIP BETWEEN STEAM TEMPERATURE AND HEAT RECOVERED FROM FUEL 3
1.3 INTRODUCTION TO TYPES OF BOILERS USED TO BURN BIOMASS 3
1.4 INTRODUCTION TO CORROSION ISSUES IN BIOMASS FUEL BOILER SUPERHEATERS 5
1.5 INTRODUCTION TO HIGH TEMPERATURE CORROSION MECHANISMS IN SUPERHEATER ALLOYS 5
1.5.1 Rate Limiting Steps 5
1.5.2 Effects of Alloying Elements 7
1.5.3 Effects of Sulfur 7
1.5.4 Effects of Chlorine 7
2. CORROSION IN BLACK LIQUOR RECOVERY BOILER SUPERHEATERS 9
2.1 INTRODUCTION 9
2.2 PARTICLE CARRYOVER AND STICKY DEPOSITS 10
2.3 CORROSION RESISTANCE OF CANDIDATE ALLOYS 11
2.4 CORROSION CONTROL STRATEGIES 13
2.5 SUMMARY 14
3. CORROSION IN Na_2SO_4-NaCL GAS TURBINE ENVIRONMENTS, ESPECIALLY NEAR AND ABOVE THE FIRST MELTING TEMPERATURE OF DEPOSITS 15
3.1 INTRODUCTION TO GAS TURBINE MATERIALS 15
3.2 CORROSION IN GAS TURBINE ENVIRONMENTS 15
3.3 SUMMARY 16
4. CORROSION IN COAL-FIRED BOILER SUPERHEATERS, ESPECIALLY NEAR AND ABOVE THE FIRST MELTING TEMPERATURE OF FLUE GAS DEPOSITS 17
4.1 INTRODUCTION 17
4.2 MATERIALS FOR ULTRA-SUPERCRITICAL COAL-FIRED POWER PLANTS 17
4.2.1 US Research to Develop Materials for Ultra-supercritical Coal-fired Power Plants 17
4.2.2 Research in Other Countries to Develop Materials for Ultra-supercritical Coal-fired Power Plants 19
4.3 EFFECT OF CHLORINE IN COAL ON BOILER CORROSION 20
4.3.1 Effect of Temperature Gradients 22
4.4 FOULING TENDENCY AND ASH DISPOSAL 24
4.5 EFFECTS OF OXYFUEL COMBUSTION 25
4.6 EFFECTS ON CORROSION OF CO-FIRING BIOMASS WITH COAL 26
4.7 SUMMARY 31
5. CORROSION IN SUPERHEATERS OF BOILERS BURNING MUNICIPAL WASTE AND TIRE-DERIVED FUEL, ESPECIALLY NEAR AND ABOVE THE FMT 32
5.1 CO-FIRING WASTES WITH FOSSIL FUELS 32
5.2 EFFECTS OF CHLORINE IN COMBUSTED WASTES 32
5.3 EFFECTS OF ZINC AND LEAD IN COMBUSTED WASTES 33
5.4 CORROSION MONITORING IN WASTE-TO-ENERGY PLANTS 35

5.5 EFFECTS ON CORROSION OF CO-FIRING TIRE-DERIVED FUEL WITH COAL 35
5.6 SUMMARY 35
6. CORROSION IN SUPERHEATERS OF BOILERS BURNING AGRICULTURAL BIOMASS, ESPECIALLY NEAR AND ABOVE THE FIRST MELTING TEMPERATURE 37
6.1 POLICY ISSUES DRIVING THE USE OF BIOMASS FUELS 37
6.2 CHARACTERISTICS OF BIOMASS FUELS 38
6.3 EVALUATING BIOMATERIALS AS BOILER FUELS 39
6.3.1 Wood Products as Biomass Fuels 39
6.3.2 Straw as a Biomass Fuel 40
6.3.3 Rice Husk as a Biomass Fuel 42
6.3.4 Salix as a Biomass Fuel 43
6.3.5 Rapeseed as a Biomass Fuel 43
6.3.6 Uncommon Biomass Fuels 43
6.4 CO-FIRING BIOMASS WITH OTHER FUELS 43
6.5 EVALUATING MATERIALS PERFORMANCE IN BIOMASS BOILER SUPERHEATERS 44
6.6 EFFECTS OF BIOMASS CHLORINE ON SUPERHEATER CORROSION MECHANISMS 46
6.7 FUEL TREATMENTS TO REDUCE CORROSION 49
6.7.1 Introduction 49
6.7.2 Sulfation Additives 50
6.7.3 Leaching 52
6.8 OPERATIONAL MODIFICATIONS TO REDUCE CORROSION 53
6.8.1 Slagging Superheater 53
6.9 DESIGN MODIFICATIONS TO REDUCE CORROSION 53
6.9.1 “Chorine Trap” 53
6.9.2 Easily Replaced Superheater Tubes 54
6.9.3 Remove Superheater from Corrosive Flue Gas Environment 54
6.9.4 Add an Insulating Layer to Raise the Surface Temperature of Superheater Tubes Above the Dew Point of Alkali Chlorides 55
6.10 COATINGS TO REDUCE CORROSION 57
6.11 PREDICTION OF CORROSION IN CFBS 57
6.12 SUMMARY 59
7. DISCUSSION AND CONCLUSIONS 61
7.1 STATUS OF SCIENCE AND TECHNOLOGY OF OPERATING BIOMASS BOILERS AT OR ABOVE THE MELTING TEMPERATURE OF ASH DEPOSITS 61
7.2 FINDINGS APPLICABLE THE LABORATORY AND FIELD TESTING IN THIS PROJECT OR FUTURE PROJECTS 61
8. REFERENCES 64
APPENDIX A A-1
SUPERHEATER CORROSION AND ALLOY PERFORMANCE IN CURRENT GENERATION HIGH PRESSURE RECOVERY BOILERS A-3

LIST OF FIGURES

Fig. 1. Total and renewable energy consumption in the U.S. in 2009. 2
Fig. 2. Temperature dependence of corrosion of Type 310 stainless steel exposed for 3 days in a recovery boiler superheater. 9
Fig. 3. Empirical relationship between high temperature corrosion rate and coal chlorine. 20
Fig. 4. Effects of coal chlorine content and heat flux on high temperature corrosion rates. 23
Fig. 5. Composition of fly ash (top triangle) and bottom ash deposits (lower triangle) in deposits from wheat straw-fired grate boilers, a coal-fired CFB boiler and a straw-coal co-fired boiler. 28
Fig. 6. Sulfur/chlorine ratios in boiler fuels. 44
Fig. 7. Metso tube containing a thermally-insulating layer to raise its surface temperature above the dew point of NaCl vapor 56
Fig. 8. Effects of increasing superheater tube temperature on concentrations of potential corrosives. 56

LIST OF TABLES

Table 1. Fireside environments and steam temperatures in modern boilers burning biomass, coal and municipal waste 39
Table 2. Typical superheater tube materials in LP/HP kraft recovery boilers 3
Table 3. Reported cases of accelerated lower tube bend corrosion of replacement alloys 5
Table 4. Superheater tube materials in HT/HP recovery boilers in Japan 6
Table 5. Laboratory superheater tube corrosion testing for HT/HP recovery boilers 7

ACRONYMS

ACAA	American Coal Ash Association
AES	Auger Electron Spectroscopy
BFB	Bubbling Fluidized Bed
CFB	Circulating Fluidized Bed
CVD	Chemical Vapor Deposition
DOE	Department of Energy
EU	European Union
FBHE	Fluidized Bed Heat Exchanger
FMT	First Melting Temperature
HP	High Pressure
HT	High Temperature
HVOF	High Velocity Oxy-Fuel
IDT	Initial Deformation Temperature
MSW	Municipal Solid Waste
NPE	Non-process Element
NREL	National Renewable Energy Laboratory
PREWIN	Performance, Reliability and Emissions Reduction in Waste Incinerators
SCR	Selective Catalytic Reduction
STA	Simultaneous Thermal Analysis
TDF	Tire-derived Fuel
PVC	Polyvinyl Chloride
UK	United Kingdom
US	United States
VTT	VTT Technical Research Centre of Finland
WSI	Welding Services Incorporated
WTE	Waste-to-Energy

ACKNOWLEDGMENTS

This research was provided by the Department of Energy's Office of Energy Efficiency and Renewable Energy's Industrial Technologies Program, carried out at the Oak Ridge National Laboratory, managed by UT-Battelle, LLC, for the U. S. Department of Energy under contract #DE-AC05-00OR22725.

EXECUTIVE SUMMARY

This report broadens a previous review of published literature on corrosion of recovery boiler superheater tube materials to consider the performance of candidate materials at temperatures near the deposit melting temperature in advanced boilers firing coal, wood-based fuels, and waste materials as well as in gas turbine environments. Discussions of corrosion mechanisms focus on the reactions in fly ash deposits and combustion gases that can give corrosive materials access to the surface of a superheater tube.

Setting the steam temperature of a biomass boiler is a compromise between wasting fuel energy, risking pluggage that will shut the unit down, and creating conditions that will cause rapid corrosion on the superheater tubes and replacement expenses.

The most important corrosive species in biomass superheater corrosion are chlorine compounds and the most corrosion resistant alloys are typically FeCrNi alloys containing 20 to 28%Cr. Although most of these materials contain many other additional additions, there is no coherent theory of the alloying required to resist the combination of high temperature salt deposits and flue gases that are found in biomass boiler superheaters that may cause degradation of superheater tubes.

After depletion of chromium by chromate formation or chromic acid volatilization exceeds a critical amount, the protective scale gives way to a thick layer of Fe_2O_3 over an unprotective $(FeCrNi)_3O_4$ spinel. This oxide is not protective and can be penetrated by chlorine species that cause further acceleration of the corrosion rate by a mechanism called active oxidation. Active oxidation, cited as the cause of most biomass superheater corrosion under chloride ash deposits, does not occur in the absence of these alkali salts when the chloride is present as HCl gas.

Although a deposit is more corrosive at temperatures where it is molten than at temperatures where it is frozen, increasing superheater tube temperatures through the measured first melting point of fly ash deposits does not necessarily produce a step increase in corrosion rate. The corrosion rate typically accelerates at temperatures below the first melting temperature and mixed deposits may have a broad melting temperature range. Although the environment at a superheater tube surface is initially that of the ash deposits, this chemistry typically changes as the deposits mature. The corrosion rate is controlled by the environment and temperature at the tube surface, which can only be measured indirectly. Some results are counter-intuitive.
Two boiler manufacturers and a consortium have developed models to predict fouling and corrosion in biomass boilers in order to specify tube materials for particular operating conditions. It would be very useful to compare the predictions of these models regarding corrosion rates and recommended alloys in the boiler environments where field tests will be performed in the current program.

Manufacturers of biomass boilers have concluded that it is more cost-effective to restrict steam temperatures, to co-fire biofuels with high sulfur fuels and/or to use fuel additives rather than try to increase fuel efficiency by operating with superheater tube temperatures above melting temperature of fly ash deposits. Similar strategies have been developed for coal fired and waste-fired boilers. Additives are primarily used to replace alkali metal chloride deposits with higher melting temperature and less corrosive alkali metal sulfate or alkali aluminum silicate deposits.

Design modifications that have been shown to control superheater corrosion include adding a radiant pass (empty chamber) between the furnace and the superheater, installing cool tubes immediately upstream of the superheater to trap high chloride deposits, designing superheater banks for quick

replacement, using an external superheater that burns a less corrosive biomass fuel, moving circulating fluidized bed (CFB) superheaters from the convective pass into the hot recirculated fluidizing medium and adding an insulating layer to superheater tubes to raise their surface temperature above the dew point temperature of alkali chlorides. All these design changes offer advantages but introduce other challenges. For example, operating with superheater temperatures above the dew point of alkali chlorides could require the use of creep-resistant tube alloys and does not eliminate chloride corrosion.

Improved test methods that can be applied within this project include automated dimensional metrology to make a statistical analysis of depth of penetration and corrosion product thickness, and simultaneous thermal analysis measurements to quantify the melting of complex ashes and avoid the unreliability of the standard ash fusion test.

Other important developments in testing include the installation of individually-temperature-controlled superheater loops for corrosion testing in operating boilers and temperature gradient testing. Several laboratories have shown that increases in temperature gradient increase corrosion rates at a given tube temperature. Although constant temperature laboratory tests can be useful for identifying and comparing the corrosion resistance of candidate alloys, field testing or thermal gradient laboratory testing may be more appropriate for simulating conditions in operating boilers.

1. INTRODUCTION

Industrial boilers make process steam, provide heating and cooling, and generate electricity. These boilers can use biomass fuels as an alternative to fossil fuels such as natural gas, coal, and fuel oil. However, biomass fuels often contain significant amounts of elements such as chlorine, potassium, sodium and sulfur that form deposits on the superheater tubes that heat the steam produced in the boiler to its final temperature. Because these deposits have low melting points, standard operating practice for biomass boilers has been to limit the temperature of superheater tubes substantially below that of fossil fuel-fired boilers in order to avoid the possibility that deposits could be molten on superheater tube surfaces and cause accelerated corrosion. However, reducing the superheater tube temperature limits the energy that can be derived from a fuel far below the current efficiencies of advanced fossil fuel fired boilers. The project funded under Department of Energy (DOE) Award DE-FC36-04GO17884 will investigate corrosion mitigation strategies that could improve the efficiency of biomass-fueled boilers, in order to increase the use of renewable energy and reduce the country's dependence on imported fossil fuels. This report reviews current understanding of the science and technology of superheater corrosion in biomass boilers in order to establish the state of the art. This will support the project goals of finding ways to reduce corrosion and extend the life of superheater tubes operating at temperatures above the melting point of ash deposits.

After an introduction to the underlying issues, the report first considers corrosion in black liquor recovery boilers, expanding and updating a literature survey from a previous project. Current knowledge of corrosion and of corrosion control in related environments in gas turbines, coal fired boilers and waste-fired boilers is then summarized, with particular reference to molten deposits. The rest of the report is a detailed survey of corrosion in biomass boiler superheaters. Most of the experience and technology in this field is European and the author has had personal discussions with many of the leaders in this field in Sweden, Finland, Germany and the United Kingdom (UK).

1.1 MOTIVATION TO USE RENEWABLE FUELS

Interest in generating energy from biomass fuels is growing because of the desire to reduce US dependence on foreign oil. In 2009, renewable energy accounted for only 8% of the total energy consumed in the United States (US) [101]. Figure 1 shows the sources from which the US obtained its energy in 2009 [101].

Between 2008 and 2009 the country's total energy consumption decreased 4.6%, to 94.8 quadrillion British Thermal Units (Btu). During this period the energy produced from coal and petroleum decreased 0.15 and 0.15 quadrillion Btu, respectively, while renewable energy consumption rose 0.3 quadrillion Btu. The largest increases in renewable fuels were 0.17 trillion Btu from biomass fuels, 0.17 trillion Btu from hydroelectric and 0.15 trillion Btu from wind. The largest decreases in renewable fuel types were 0.15 quadrillion Btu for wood and wood-derived fuels.

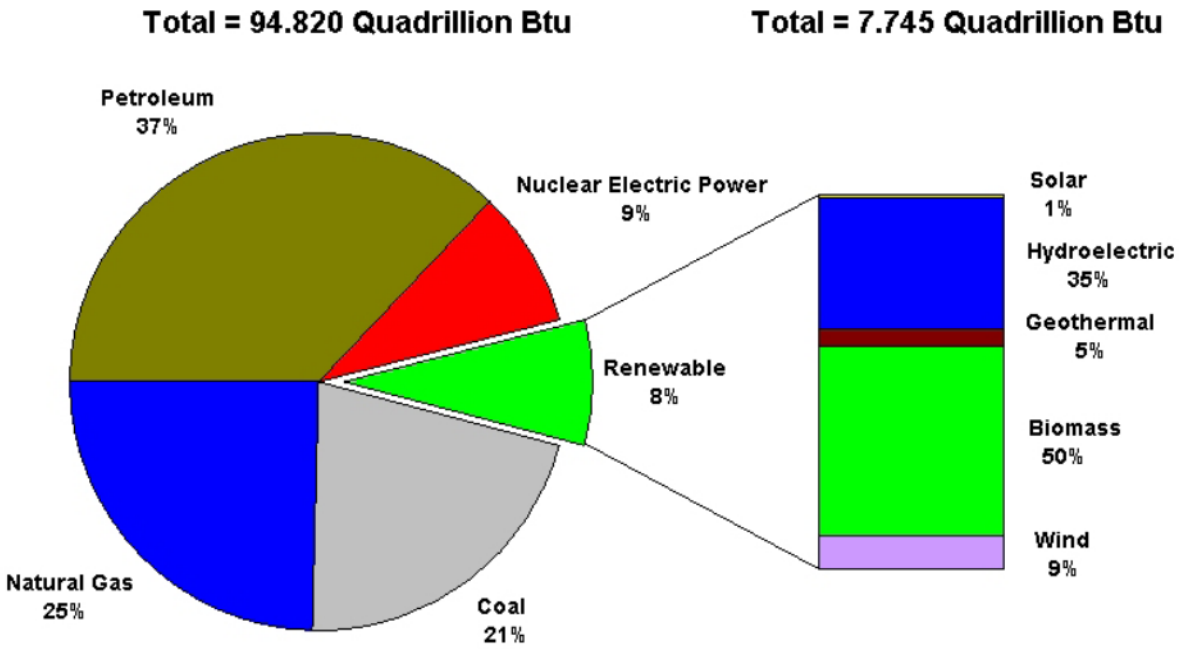

Fig. 1. Total and renewable energy consumption in the U.S. in 2009.

The increased use of biomass fuels between 2008 and 2009 (12%) was much less than the 38% growth rate of the previous year, partly because policy changes made exporting biomass fuels less favorable.

In contrast, Europe responded vigorously to the Kyoto Protocol by committing to reduce greenhouse gas emissions between 2008 and 2012 compared to 1990 levels. Without Europe's current use of biomass, between 2% and 8% more CO_2 would be emitted. Europe's additional use of biomass fuels could further reduce CO_2 emissions by 7%, to 28% [47].

Calculations by Mann and Spath of the National Renewable Energy Laboratory (NREL) [133] indicate that replacing 5% and 15% of an Illinois No. 6 coal with urban waste biomass could reduce power plant greenhouse gas emissions by 7% and 22% respectively per unit of electricity produced. However, there are significant barriers to the utilization of biomass by conventional coal-fired utilities in the US [47]. These can be grouped into materials handling issues, operational issues and agglomeration, fouling and corrosion issues. Weber and Zygarlicke [47] have summarized the availability of biomass fuels (agricultural wastes, forest residuals and wood residuals, municipal wastes and energy crops). The materials handling issues begin with the fact that electricity generation from biomass requires much greater volumes of biomass fuels than of coal. Many biomass materials also have much higher contents of corrosives (e.g. alkali salts and chlorine) and erosives (e.g. silica) than coal. The mechanisms by which alkali salts and chlorine cause corrosion will be discussed in detail in this review. Lastly, sticky (partially-molten) deposits on heat exchange surfaces restrict heat transfer on superheater tubes and form difficult-to-purge clinkers in the lower furnace. Weber and Zygarlicke note that the final and perhaps most important barrier to the development of biomass power in the US is economic. The US's deregulated power industry pursues a least-cost approach to electricity generation, avoiding investment risks. This approach makes it difficult for biomass fuel projects to compete.

Discussions about carbon neutrality have increased in importance with concerns about the role of carbon dioxide in global warming. Carbon dioxide concentrations are increasing because of fossil fuel burning and deforestation. Biomass fuels and other plant-based materials store carbon only for months or years, unlike fossil fuels, which store carbon for millions of years. So, when plant-based substances are burned, the carbon dioxide they have converted into plant material is essentially recycled, moving from air to the plant and back to the air. The carbon removed from the air by the plants cancels out the carbon emitted by the plant when it is burned. Although the harvesting and transportation of the biomass to the boiler uses petroleum-based fuels for transportation and electricity for cutting and chipping, making energy by burning recently grown biomaterials is much more nearly carbon neutral than making energy by burning fossil fuels1.

Turning from renewable fuels to waste fuels, Lee, Themelis and Castaldi reported that, in 2007, 88 waste-to-energy (WTE) plants were operating in the US [158]. They burned about 143,000,000 metric tons2 of municipal solid wastes and generated about 45,000,000,000 kWh of electricity and an equal amount of energy for district heating and industrial use. Capital and maintenance costs accounted for about 60% and 15% of the annual cost of operating a WTE facility. Maintenance costs due to corrosion ranged from $0.23 per ton to $8.17 per ton of MSW combusted, with a typical cost of about $4 per short ton3. These wastes contain from about 0.5% to 0.75% of chlorine, half of which comes from chlorinated plastics, mostly PVC.

1.2 INTRODUCTION TO RELATIONSHIP BETWEEN STEAM TEMPERATURE AND HEAT RECOVERED FROM FUEL

The energy extracted by converting heat into work in the Rankine steam cycle used by industrial boilers is limited by the difference between the maximum and minimum steam temperatures in the steam cycle. These temperatures in turn are limited by the alloys used to manufacture the boiler tubes. Unless supercritical steam pressures are used, steam cycle limits are typically from the temperatures at which tube materials began to creep to water condenser temperatures. Historic limits for stainless steels in coal-fired power stations have been about 565°C (1049°F) and condenser temperatures are around 30°C (86°F). This presents a theoretical maximum efficiency of about 63%. The most efficient coal-fired power stations achieve efficiencies of only about 45%. Combined cycle plants achieve higher efficiencies by using the exhaust gases from a gas turbine generator to heat a steam boiler that produces additional electric power.

1.3 INTRODUCTION TO TYPES OF BOILERS USED TO BURN BIOMASS

Biomass fuels are burned in three main types of boilers (plus combined heat and power, CHP), which are called grate fired, bubbling bed and circulating fluidized bed units. The design and operation of these boilers are described in the handbook written by Babcock and Wilcox [62]. These boilers are normally operated solely to generate electricity but can be operated to simultaneously generate a combination of heat and power.

Grate-fired boilers ("stokers") are used for fuels that are burned as coarse particles. The fuel particles are mechanically or pneumatically fed onto the upper track of a belt-type grate, which consists of a large number of closely-spaced parallel bars linked by joints. The fuel is dried and burned as the

---

1 Confusion arises because the same term "carbon neutral" is used to describe carbon off-setting in which amounts of carbon emitted into the air as a result of human activity are offset by tree planting or other activities that produce a corresponding lowering of carbon dioxide emitted elsewhere.
2 1 metric ton is 2205 lbs.
3 1 short ton is 2000 lbs.

grate moves through the bottom of the furnace. Lighter fractions and small fuel particles burn in suspension. A cut-off gate directs the ash into a hopper as the grate belt leaves the furnace cavity, turns down and returns back to the feed side of the boiler. Primary combustion air blown into the fuel from below the grate helps to keep the belt cool.

In fluidized bed combustion, fuel particles burn while they are suspended in an upward-blowing gas stream. The furnace cavity contains a granular material like sand. As the rate of upward flow is increased, a condition is reached where the sand particles are suspended and the bed behaves like a fluid. The mixture of upward air flow and the tumbling of the particles provides uniform mixing, even flow and good heat transfer to the wall tubes. Excessive upward air flow begins to form bubbles of air in the bed. This substantially increases the volume of the air-solids mixture that forms the bed and produces turbulent flow. Fluidized bed boilers can handle a wider variety of fuels than conventional boilers. Fluidized bed boilers are of two types, bubbling bed boilers and circulating fluidized bed boilers. Bubbling fluidized beds normally operate with a restricted combustion air in a reducing atmosphere. They are normally used to burn lower-quality fuels that contain substantial volatile matter. Most of the fluidizing medium remains in the furnace. In circulating fluidized bed boilers, the combustion gases carry fluidizing particles out of the furnace. These hot particles are removed in a cyclone and returned to the bottom of the furnace though a recirculation loop called the loop seal because the fluidizing particles are separated from the flue gases.

The inorganic ash particles that remain after the organic components of a fuel have been combusted either fall to the bottom of the furnace, where they fall into a hopper, or are carried forward with the flue gases as fly ash particles. Some of the fly ash is collected in hoppers under the economizer and air heater tubes and the rest is removed by electrostatic precipitators or bag filters.

Limestone can be added to boilers to reduce SOx emissions. This reaction produces calcium sulfate. Contact between the hot calcium sulfate particles and the tubes also increases heat transfer.

Slag-tap furnaces were originally developed to burn fuels with low ash melting temperatures. Molten ash forms on the lower furnace walls and continuously drains out through openings ("slag taps") in the furnace floor, just as molten smelt drains out though smelt spouts in the bottom of a black liquor recovery boiler. Although slag-tap units have the advantage of producing much less fly ash, their high furnace temperatures emit more NOx than is allowed by today's permits.

In contrast the lower combustion temperatures in fluidized bed boilers have much less tendency to produce molten deposits on the fireside of even the hottest (i.e. the superheater) tubes. Because of their lower combustion temperatures, fluidized bed boilers produce lower NOx emissions than grate-fired boilers. However, as will be discussed later, fuels containing high concentrations of alkali metal salts, and chlorides may still cause corrosion and fouling in the hottest tubes.

For a boiler to generate power from biomass fuels over an extended period of years, its tubes must be made from materials that resist corrosion and cracking. Fireside corrosion and internal corrosion of tubes in the furnace wall and economizer can cause substantial problems, but this report will focus on resistance to fireside corrosion in the superheater tubes[4], where the steam receives its final heating before it leaves the boiler to generate power in the turbo-generator.

4 In addition, fluidizing media (typically sand) can erode tubes in and around a fluidized bed furnace.

1.4 INTRODUCTION TO CORROSION ISSUES IN BIOMASS FUEL BOILER SUPERHEATERS

Fireside corrosion of superheater tubes is generally more severe than steam-side corrosion[5] in biomass boilers. Flue gases produced in biomass boilers are relatively corrosive because they contain relatively high concentrations of alkali, sulfur and chlorine gases and particles. Stainless superheater tubes suffer higher corrosion rates at much lower temperatures than in coal-fired boilers. This has forced biomass fueled boiler operators to keep steam conditions far below those used with clean coal fuels. The National Renewable Energy Laboratory has made a preliminary survey of the extent and nature of corrosive alkali deposits formed in boilers burning annual crop fuels [41]. Low melting temperature particles carried over with the flue gases (e.g. alkali metal chlorides and sulfates) and corrosive gases released by combustion processes (e.g. HCl and Cl_2) not only cause corrosion, but also form deposits that limit the rate of heat transfer to the steam in the tubes.

Molten superheater deposits are much more corrosive to superheater tubes than solid deposits. Superheater deposits typically melt progressively over a broad temperature range. Although fly ash particles typically do not stick on tubes unless the surface temperature is high enough to melt 15 to 20% of the deposit, most boiler operators are careful avoid operating with maximum superheater tube temperatures hotter than the first melting temperature (FMT) of fireside ash deposits. Sticky deposits cause two types of problem. They cause fireside corrosion and they agglomerate by attracting other deposits like a fly paper. This build-up of deposits, called fouling, can lead to pluggage where the deposits become so voluminous that the passages between adjacent boiler tubes become clogged and the operators are forced to shut the boilers down for cleaning. This can also produce a condition called slagging, where the outer surface of an ash deposit on a superheater tube is hotter than the temperature at which the deposit is fully molten, and molten ash flows off the outer surface of the deposit.

Lokare and others [22] investigated ash deposition rates for a wide range of biomass fuels and fuel blends in the Multifuel Flow Reactor at Brigham Young University. One to one blends of biomass fuels with base fuels straw and grain screening showed lower deposition rates than the base fuels alone. Differences between the deposition rates and predictions from a simple model of ash deposition that assumed each ash species would behave independently confirmed that there had been substantial interactions between the fuel components.

1.5 INTRODUCTION TO HIGH TEMPERATURE CORROSION MECHANISMS IN SUPERHEATER ALLOYS

1.5.1 Rate Limiting Steps

When a superheater alloy is heated in a simple oxidizing environment, an oxide film thickens on its surface and progressively isolates the alloy from its environment. If the oxide remains crack-free and stable, the rate of reaction is often inversely proportional to the oxide thickness. This "parabolic rate law" is analogous to transport of heat through a metal plate (inversely proportional to the thickness of the plate). The parabolic rate law arises when the rate of an oxidation reaction is limited by ionic diffusion through a thickening oxide film [162]. Although electrons must also move across the film

5 The few cases where biomass fuel boiler superheater tubes have suffered internal (steam side) corrosion have been traced to operational errors that have allowed either oxygenated feedwater to cause pitting or contaminated feedwater to cause stress-corrosion cracking.

to sustain the oxidation process, most metal oxides (with the notable exception of Al_2O_3 [6]) are good electronic conductors, leaving ionic diffusion through the semiconductor oxide "electrolyte" between the tube alloy and its environment as the rate limiting step.

Although this simple model of oxidation first laid out by Wagner in 1933 [162] applies to pure metals, alloy oxidation is more complex. When an alloy is first exposed to an oxidizing environment, all the metal atoms on its surface will tend to be oxidized. To the extent that these oxides form a barrier to further oxidation, subsequent reactions will oxidize only the most reactive elements in the alloy, such as chromium and aluminum. However, homogenization of the corrosion product by thermal interdiffusion will produce solutions of the less reactive elements in the oxide of the more reactive elements. The minor constituents in the surface oxide alter the corrosion rate by acting as dopants in the semiconductor oxide and changing the diffusion rates of anions and cations across this oxide. Sharp has shown that these effects explain relative oxidation rates in simple iron-chromium-nickel alloys [87]. Addition of nickel first increased, and then decreased, the oxidation rate of iron-chromium alloys. This was explained as follows. Cr_2O_3 has a minimum conductivity when it contains 4 m/o Fe_2O_3. Dissolving divalent Ni^{2+} into the n-type Cr_2O_3 formed on Fe-18Cr-Ni alloys when the Cr_2O_3 contains > 4 m/o Fe_2O_3 increases the anion defect concentration, increasing compressive stresses in the oxide so that it blisters and cracks, forming local $(Cr,Fe)_3O_4$ spinels. Alloys that contained much more nickel, also contained < 4 m/o Fe_2O_3[7] in the initial Cr_2O_3 film, which was therefore a p-type semiconductor. Dissolving divalent Ni^{2+} into this p-type Cr_2O_3 reduced its defect concentration and the reduced corresponding oxidation rate of the alloy. Oxide defect structures do not only determine the effect of alloying elements. They also change in the presence of temperature gradients, and accelerate corrosion rates in temperature gradients compared to corrosion rates under isothermal conditions, as we will see in Section 4.3.1 [144].

Although the primary method of controlling high temperature oxidation is to add alloying elements that produce oxides with low ionic conductivity, some potentially beneficial additions may embrittle the alloy (e.g. silicon) or be prohibitively expensive (e.g. rare earth metals such as cerium or yttrium). However, small additions of these elements can nucleate subscale oxide barriers that slow the rate of Cr_2O_3. Small concentrations of aluminum offer the same type of protection, by forming oxide particles that gradually spread across the scale/alloy interface to reduce the rate of subsequent reactions. The role of alloying elements will be discussed in the next section.

Alloy grain boundaries have imperfect lattice structures that allow much more rapid diffusion of atoms than can occur in the bulk of the alloy. For this reason, the initial oxidation rate at grain boundaries is typically higher than in the grain centers. Whether the oxide at the grain boundary becomes more or less protective as a result, depends on the composition of the oxide that is produced and the extent to which it inhibits the easy inward diffusion of corrosive species down the grain boundary. Yttrium additions appear to inhibit this rapid diffusion in the imperfect grain boundary structure. Yttrium and cerium additions also increase the adhesion of Cr_2O_3 and Al_2O_3, thereby increasing resistance to spalling during thermal cycling.

Another important factor in the ability of an oxide to protect a metal substrate is the ratio of the volume of the oxide formed to the volume of metal consumed to form it. If the oxide has a much higher volume than the metal that formed it the oxide it likely to blister, crack or spall to relieve the stress, especially under thermal cycling conditions. Also, if the oxide volume is less than the volume

---

6 Al_2O_3 is an electrical insulator and its resistivity increases with purity. Its low electronic conductivity gives rise to inverse logarithmic oxidation rates that rapidly stifle oxidation rather than parabolic oxidation rates.
7 Interestingly, the Fe 16-19%Cr 400-series ferritic stainless steels produce oxides with compositions very close to this diffusion rate minimum.

of metal consumed, tensile stresses produce cracks that make the oxide non-protective. The ratio of oxide volume to consumed metal volume is known as the Pilling-Bedworth ratio, after the researchers who first demonstrated this classification [161].

1.5.2 Effects of Alloying Elements

Stott has documented the effects of common alloying additions to high temperature alloys based on iron, nickel and cobalt [85]. Chromium oxide (Cr_2O_3) provides reasonable protection in air or oxygen at temperatures up to about 900°C (1652°F) above which it reacts to a higher oxidation state and volatilizes as CrO_3. For applications at these temperatures, aluminum or silicon is added to the alloy to form a healing layer of Al_2O_3 or SiO_2 at the metal/scale interface. To form Al_2O_3 scales on Fe-Al, Ni-Al or Co-Al materials, the alloy needs to contain 6-12% of aluminum. The addition of an element such as chromium that produces an oxide of intermediate stability and enables Al_2O_3 to form on alloys that contain less aluminum. For example Fe-15% Cr alloy can establish an Al_2O_3 layer with the addition of only 3-4% aluminum. Silicon additions to Fe-Cr alloys form internal oxide particles that can grow and coalesce into a healing layer, but silicon is less effective in this regard than aluminum. For example Fe-15-30%Cr-Si alloys initially form Cr_2O_3, but this gives way to an outer layer of iron oxides, an inner Cr_2O_3 scale and a healing layer of SiO_2 at the alloy/scale interface. Stott also notes that the differential thermal expansion stresses that produce spalling of oxides are more severe on austenitic than on ferritic alloys and more severe with Al_2O_3 scales than with Cr_3O_3 scales. Alloying elements such as Mn, Ti, Mo, Nb have lesser effects on the oxidation of Cr_2O_3-forming alloys and this is also discussed [85].

1.5.3 Effects of Sulfur

The corrosive effects of sulfur gases on boiler tube alloys depend largely on their oxygen concentration [163]. Although sulfide scales may be formed in reducing (air-deficit) combustion environments, SO_x gases form only oxides. In coal-fired boilers the presence of sulfur gases substantially increases the corrosion rate. Ni-Cr alloys are more resistant than Fe-Cr alloys because they show less tendency to form low melting temperature metal-metal sulfide eutectics. This will be discussed in more detail with regard to corrosion in gas turbines in Section 3.

Boiler fuels that release sulfur gases almost always also produce fly ash deposits on the fire side of the tubes. In coal-fired boilers the most corrosive components of these ash deposits are alkali metal sulfates, pyrosulfates and chlorides. Corrosion by coal ash components in the highly oxidizing environment created by combustion gases containing sulfur is very complex. In biomass boilers, alkali chlorides are the most aggressive species. Sulfur compounds are often added during the combustion of biomass in order to convert alkali chlorides to less corrosive alkali sulfates.

1.5.4 Effects of Chlorine

Sodium chloride is present in the ashes of some coals (particularly bituminous or brown coals), usually with sodium sulfate. Many of the corrosion challenges posed by biomass fuels arise from the significant alkali chlorides contents. Fundamental studies of superheater corrosion mechanisms and studies of corrosion in straw-burning boilers have helped to clarify the mechanisms involved. These will be discussed in Section 6.5.2. Austenitic steels are generally more resistant than ferritic steels to corrosion by chloride salts [163]. Sodium chloride attack typically produces intergranular corrosion with an “orange peel” appearance. At higher temperatures otherwise protective Cr_2O_3 can volatilize as $CrCl_3$ or CrO_2Cl_2, and volatilization rates can be increased in the presence of water vapor. Volatilization effects will be discussed in more detail in Section 6.6. Silicon additions reduce the

corrosion resistance of nimonic alloys, possibly by restricting the outward diffusion of chromium. Alloys that form Al_2O_3 scales are generally resistant to chloride corrosion [163].

2. CORROSION IN BLACK LIQUOR RECOVERY BOILER SUPERHEATERS

2.1 INTRODUCTION

Previous research on superheater corrosion by the current research team [31] included a review by Kish of published research on superheater corrosion and alloy performance in current generation high temperature, high pressure recovery boilers. Dr. Kish's report[8] is included as an appendix to the current review. A summary of conclusions and comments from recent publications is included here.

Rates of corrosion in black liquor recovery boiler superheaters increase with the temperature of the tubes and therefore with the final steam temperature of the unit. Many pulp mills have installed boilers with low or moderate steam temperatures to avoid corrosion problems both in the reducing environment of the lower furnace and in the oxidizing environment of the upper furnace. However, operating with a low steam temperature reduces the energy extracted from the fuel, as noted in our previous discussion of Rankine cycle efficiencies in Section 1.2. Calculations by Vakkilainen [135] show that increasing recovery boiler steam conditions from typical current values of 80 bar (1160 pounds per square inch (psi)) and 480°C (896°F) to 104 bar (1508 psi) and 520°C (968°F) would increase electrical output by about 7%.

Standard textbooks (e.g. [111]) state that corrosion in recovery boiler superheaters is generally not a problem when the exit steam temperature is kept below about 450°C (842°F). Small temperature increases that raise superheater tube temperatures above the FMT of surface ash deposits can produce large increases in corrosion rate. Figure 2 presents corrosion data from probe tests by Estes [118] that showed four- or five-fold increases in the corrosion rate of Type 310 stainless steel coupons in a recovery boiler superheater over a 3°C (5°F) increase in metal temperature.

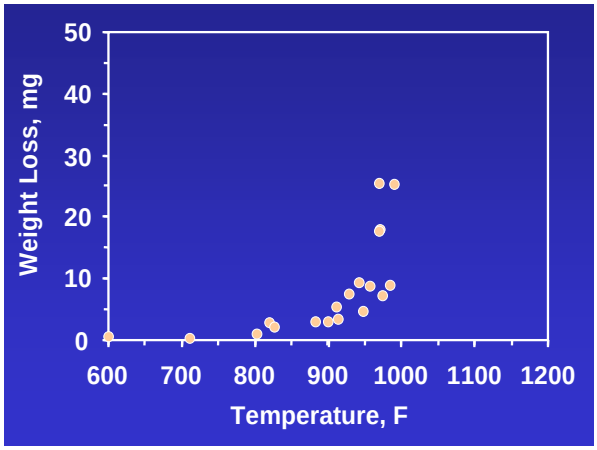

Fig. 2. Temperature dependence of corrosion of Type 310 stainless steel exposed for 3 days in a recovery boiler superheater.

Most operators establish their steam temperature so as to keep the temperature of fireside ash deposits comfortably below their melting point [112-115]. Kish notes that today's recovery boilers operate with steam temperatures up to about 500°C (932°F). Mäkipää and others suggest that the maximum temperature for recovery boiler superheater alloys will probably be about 525°C (977°F) [114].

8 Pages 53 to 59 of reference [31]

Clement and Grace have made a very comprehensive review of superheater design and performance in recovery boilers, paying particular attention to issues raised by high temperature and high pressure operation. Their first paper [137] discusses the history of superheater development, design and metallurgy, and notes that most of the experience with high temperature and high pressure boilers comes from Finland and Japan. They recommend that at least two stages of attemperation be installed in superheaters designed to operate at temperatures above 482°C (900°F). In their second paper Grace and Clement reported a survey of failures in superheaters of North American recovery boilers [138]. The greatest causes of superheater failure were fatigue cracking, corrosion thinning and tie failures. Fatigue cracking and tie failures occur at antinodes where vibrating tubes are constrained. Thermal fatigue cracking is typically caused by large and sudden heating and cooling cycles. Fireside attachments to composite tubes are particularly vulnerable. In high temperature recovery boiler superheaters, corrosion thinning is the predominant failure mechanism. This is typically most severe at the front corner of the bottom bends of the tubes in the hottest platens[9]. Clement and Grace recommend that the chlorine concentration in the black liquor solids should be kept below 0.5% to reduce plugging and increase superheater life. Tie failures, tube warpage and short term overheat can be avoided by careful startup procedures. With regard to fouling, only about half the North American recovery boiler fleet can operate for a year without shutting down to remove fouling deposits with a water wash or a chill and blow.

2.2 PARTICLE CARRYOVER AND STICKY DEPOSITS

The volume of particles carried over in a recovery boiler increases when the firing load is increased, when the flue gas velocity is high, and when the char bed is hot. High loads and high flue gas velocities increase the carryover of unburned liquor particles. Inadequate addition of combustion air (i.e. from secondary and tertiary air ports) makes it more likely that the carryover particles will be incompletely burned. Tran has shown that these incompletely burned liquor particles can destabilize protective oxides and initiate corrosion on the windward side of superheater tubes [40].

Particle carryover can be reduced by adopting high-solids firing methods which produce larger liquor spray droplets. However, high-solids firing also increases the production of small fume particles by increasing the bed temperature.

Superheater deposits in Kraft recovery boilers consist primarily of sodium sulfate and sodium carbonate, but potassium salts including chlorides and sulfides may also be present. These deposits usually melt over a wide temperature range because they are complex mixtures. Their first melting temperature (FMT) depends on the liquor composition and firing practice, but is generally between 520 and 580°C (968 and 1076°F). Hupa and others [39] have shown that the critical parameters governing superheater fouling and corrosion are the sticky temperature (when 15% of the deposit on the tube surface is molten) and the flow temperature (when 70% of the outermost deposit is molten so that no further thickening can take place). Field studies have shown that particles carried over in recovery boiler flue gases do not stick onto tube surfaces in their path unless their liquid content exceeds about 15%.

Tran, Backman, Hupa and others have made detailed studies of the relationship between the compositions of recovery boiler deposits and their sticky temperatures [117]. If the particles are sticky at the operating temperature of the superheater tubes, deposits can build up rapidly. The thicker the deposit, the higher its fireside temperature, and the more likely it will be to attract additional deposits. Sticky deposits can bridge the gaps between adjacent tubes and block the

9 These bottom bends experience not only the highest heat flux but also erosion from particles entrained in the flue gases

passages between adjacent superheater tube platens. This diverts all the flue gases though the remaining unblocked passages, causing excessive heating of the tubes in these so-far-unblocked passages. In extreme cases, overheating of the tubes in the unblocked passage can melt their fireside deposits and plug the whole upper furnace. To avoid pluggage problems, recovery boiler operators can monitor tube temperatures at the discharge of each platen to be sure that they are safely below the FMT. Additional safeguards include monitoring the composition of the black liquor solids and maintaining the efficiency of the soot blowers.

2.3 CORROSION RESISTANCE OF CANDIDATE ALLOYS

The corrosion resistance of alloys in recovery boiler superheater environments depends on the gaseous and solid chemicals that are present in the flue gas. If the flue gas was simply hot air, and if molten deposits and unburned liquor particles were not present, rates of superheater corrosion would depend only on the tube temperature. The corrosion rate would be controlled by the transport of reagents through the thickening oxide scale on the fireside of the tubes. But in fact deposits are present and the fuel gases can contain corrosives such as SO_x, Cl_2 and HCl [112]. In such cases, or when tube temperatures are too high for corrosion rates on unalloyed carbon steel to be manageable, superheater tubes need to contain alloying elements that form oxides that are adherent, coherent and have lower ionic diffusion coefficients. Chromium is the most important alloying element. Although chromium initially oxidizes more rapidly than iron, chromium oxides are much more protective than iron oxides. Commonly used recovery boiler superheater tube materials, in order of increasing corrosion resistance, are as follows:

Carbon steel
T11 steel (1.25% Cr, 0.5% Mo)
T22 steel (2.25% Cr, 1% Mo)
Type 304 (19% Cr, 10% Ni) and Type 347H stainless steel (19% Cr, 11% Ni, 0.5% Nb)
Alloy 310 (25 % Cr, 20% Ni) and Alloy 28 (27% Cr, 31% Ni, 3.5% Mo)

The ferritic steels T11 and T22 are only useful at temperatures significantly below the FMT. At temperatures close to the FMT, austenitic 300-series stainless steels have been successful. For temperatures at or just above the first melting point of deposits, iron-nickel-chromium alloys (e.g. Alloy 800H) and nickel-chromium-molybdenum alloys (e.g. Alloy 625) have been used with mixed success. However, no alloys have yet been found that would enable recovery boilers to operate with steam temperatures high enough to achieve fuel energy efficiencies comparable to those of coal-fired utility boilers.

Because the austenitic stainless steels would be vulnerable to waterside stress-corrosion cracking if feedwater contaminated by chlorides entered the superheater, some mills prefer to avoid the use of solid austenitic superheater tubes. Composite superheater tubes with a Type 310 stainless steel outer layer over a pressure-bearing SA-213T22 inner tube achieve this goal. Mills more confident in their water quality choose less expensive solid tube materials like 347H. The author has overseen successful installations of both solid Type 347H and co-extruded 310 over T-22 recovery boiler superheater tubes.

Kish's review documents field experience with stainless steel and nickel-based alloy tube materials in recovery boilers. A 1982 Finnish study [119] found corrosion rates of about 0.1 millimeter (mm)/year (0.004" per year) on Types 304, 304L, 321 and Type 347 stainless steel. There were no significant differences in corrosion rate between these alloys.

Next generation high temperature/high pressure recovery boilers developed in Japan and Finland are being built with more advanced superheater alloys. The latest recovery boiler superheater alloy developed in Japan, MN25R, contains 25% Cr, 15% Ni, Mo, up to 1.5%Si, and N [120]. Laboratory and field testing in Finland have evaluated alloys such as 347H, AC-66, Alloy 28, HR-11N, Alloy 625 and Alloy 67. At temperatures above the FMT the corrosion rates of these alloys accelerate to rates that seem to depend on the percentage of molten phase in the surface deposit. The pitting and intergranular nature of the corrosion is consistent with a mechanism involving molten chloride-containing salts on the surface of the alloy. Alloying with chromium increases corrosion resistance, particularly if molybdenum and nitrogen are also present.

Kish reviewed experience with alloys used to replace corroded superheater tubes (i.e. Types 304 and 347H stainless steel, composite Type 310-clad T-22 and Incoloy 800H). He found documented cases of accelerated corrosion of all these alloys, with the exception of Alloy 28, in lower superheater tube bends.

Kish concluded that corrosion rates of superheater alloys below the FMT are less consistent than corrosion rates above the FMT. Although the role of chlorine seems to be pre-eminent, it is difficult to compare field data from different research groups because the boiler environments are rarely well-characterized. Laboratory test data are also difficult to compare, because different researchers use different experimental methods. For example few researchers have controlled the partial pressure of steam in the test environment although soot blowers clearly produce cycles of increased water vapor in superheater environments and water vapor has been shown to increase the corrosion of nickel-chromium alloys in simulated low-NO_x coal-fired boiler environments [76, 77].

Vakkilainen [67] has reviewed alloys that could be useful for recovery boiler superheaters operating at temperatures of above 500°C (932°F). His candidate list includes Type 347H and 310stainless steels, grades HR2M and HR3C from Sumitomo and YUS 170 from Nippon Steel and the Sanicro alloys 28, 63, 67 and Super 625[10]. For coatings, Vakkilainen suggested WSI's weld-applied Unifuse 310 or 52 alloys.

Skrifvars, Westén-Karlsson, Hupa and Salmenoja [73, 74] recently reported laboratory tests of six candidate alloys for recovery boiler superheaters. In the first part of the study [73], mixtures of Na_2SO_4, K_2SO_4 and NaCl, chosen to have FMTs ranging from 522 to 884°C (972 to 1623°F), were applied to the six alloys in one week tests at 450 to 600°C (842 to 1112°F). The weight percentage of the molten portion of each mixture had previously been measured as a function of the exposure temperature.

The alloy samples (T-22, T-91, Esshete 1250, Sanicro 28, HR11N and Sanicro 63) were pre-oxidized in air for 24 hours at 200°C (392°F). Additional tests were performed without the salt layer. The thickness of the corrosion layer was evaluated by automated image analysis. Pure Na_2SO_4 deposits corroded only the lowest alloy (T-22). When even 0.3 w/o chlorine was added, corrosion began below the FMT on T-22, T-91 and Esshete 1250. Additions of 1.3 w/o chlorine initiated corrosion below the FMT on Sanicro 28. Substituting 10 w/o potassium for sodium in the 0.3 w/o chlorine salt substantially increased the thickness of the corrosion layer. Corrosion product thicknesses produced in tests ranging up to 5 weeks showed corrosion rates slowing with test duration although the data were somewhat scattered. A series of tests on a single steel at a single temperature (530°C; 986°F) showed that the thickness of the corrosion product increased as the salt contained a greater percentage of molten phases.

---

10 For completeness, the Mitsubishi Heavy Industries alloy MN25R could be added to this list. Mitsubishi has said that this alloy may be suitable for temperatures of up to 540°C (1004°F) [137]

The second part of the study by Skrifvars, Westén-Karlsson, Hupa and Salmenoja [74] reported laboratory studies to investigate corrosion of superheater alloys T-22, Esshete 1250, and Alloy 625 under synthetic alkali chloride deposits. The authors concluded that one-week laboratory tests were sufficient to show differences in corrosion resistance of substrate materials and of applied salts. The influence of chloride on corrosion depended on whether or not the added chlorides brought the FMT below the surface temperature of the test sample. Chlorine-containing Na and K salts produced molten deposits that corroded all the steels at temperatures above the FMT. These chlorine-containing salts also corroded T-22 and Esshete 1250, apparently by solid state reactions, at temperatures below the FMT. These two steels that corroded showed indications of iron volatilization, possibly as iron chloride, which produced porous condensed iron oxide deposits on the outside of the oxide layer and of salt particles. At 575°C, indications of condensed chromium and nickel oxides were also found in tests on Alloy 625. Chlorine-free Na and K salts did not corrode any of the steels. Alloy 625 proved the most corrosion resistant of the alloys tested. Skrifvars' experiments [74] were made in an air environment without added water vapor. Data from Chalmers University of Technology suggest that environments without water vapor are likely to underestimate the corrosion in real environments, because water vapor increases the volatilization of chromic oxide.

2.4 CORROSION CONTROL STRATEGIES

In 2001, Salmenoja and Turiemo [136, 115] made a thorough review of the combustion processes and of the corrosion mechanisms that need to be understood in order to control superheater corrosion in recovery boilers. Their papers include data showing that corrosion rates in superheater environments begin to increase at temperatures at least 50°C (120°F) below the FMT of tube deposits. Accelerated corrosion below the FMT has been studied in other types of boilers and also in gas turbines, where it is referred to as Type 2 hot corrosion (see Section 3.2). However, the accelerated corrosion could also be an artifact of deposit sampling. The authors caution that deposit sampling procedures can allow sulfides to become oxidized to sulfates, which leads to overestimation of the FMT. This is important because it shows that conventional measurements of the FMT of recovery boiler fly ash may not provide reliable predictions of the onset of rapid superheater corrosion.

The fact that solid salt deposits accelerate corrosion at temperatures blow the FMT [73] suggests that the active oxidation mechanism can be initiated by as little as 0.3% chloride, particularly if potassium is present. It is possible that the fluxing of Cr_2O_3 to form K_2CrO_4 or Na_2CrO_4 may allow chlorine to reach the alloy surface. Skrifvars points out that the sensitivity of the corrosion rate to very low concentrations of chlorine in salt deposits represents a major challenge to pulp mills that plan to purge chlorides from liquor systems in order to raise steam temperatures [73].

Once its recovery boiler is built and its liquor system and load have been established, a pulp mill has few options to reduce rates of superheater corrosion. The FMT of fly ash deposits can be raised by reducing the chloride and potassium content of the black liquor, e.g. by reducing the amount of chloride-bearing bleach plant wastes recycled to the black liquor or by increasing the purging of recovery boiler precipitator catch. Unfortunately, both these options carry financial penalties. Therefore, setting the maximum superheater steam temperature becomes a compromise between wasting fuel energy, risking pluggage that will shut down the unit, and creating conditions that will cause rapid corrosion of the superheater tubes. Recovery boiler operators have historically accepted the loss of fuel efficiency caused by low steam efficiency in order to keep well away from superheater pluggage and corrosion problems. However, increasing concern about fuel efficiency (described in Sections 1.1 and 1.2) has promoted research to overcome the barriers presented by fouling and

corrosion. Biomass boiler additives have been developed to increase the FMT of superheater deposits by changing their composition, new boiler designs have been developed to remove the superheater from the flue gases and new alloys that might resist the corrosive environment have been developed. The remainder of this report will discuss options like these as well as opportunities to use more corrosion-resistant alloys.

2.5 SUMMARY

Finnish and Japanese researchers have concluded that tube temperatures above the FMT produce such high corrosion rates that superheater corrosion control should focus on the removal of the corrosive materials from the liquor cycle. The boiler manufacturers add systems to remove corrosive materials from the liquor cycle rather than designing the superheater to operate at temperatures above the FMT of fly ash deposits. For example, several Japanese mills remove chloride and potassium by selective dissolution and precipitation [120]. Part of the precipitator catch is added to water at 40-45°C (104-113°F). This dissolves all the K_2SO_4 and NaCl and some of the Na_2SO_4. When ice is added to cool the solution to 15°C, $Na_2SO_4 \cdot 10H_2O$ crystallizes and can be separated from the solution that remains enriched in potassium and chloride. This process can halve the concentration of potassium and chloride in the precipitator catch. Reducing the concentration of these elements in the liquor cycle reduces the likelihood of sticky deposits and superheater corrosion.

3. CORROSION IN Na_2SO_4-NaCL GAS TURBINE ENVIRONMENTS, ESPECIALLY NEAR AND ABOVE THE FIRST MELTING TEMPERATURE OF DEPOSITS

3.1 INTRODUCTION TO GAS TURBINE MATERIALS

Gas turbine environments present one extreme environment for high temperature alloys. Like the steam-raising boilers discussed in the rest of this report, gas turbine designers want to increase operating temperatures to achieve greater fuel efficiency. However, gas turbine alloys need to retain their strength at even higher temperatures than boiler tubes. Because turbine blades do not need good thermal conductivity, they are made with insulating coatings and internal cooling. This enables the turbines to operate with combustion temperatures that are well above the melting point of the alloys used for engine parts. The high temperature creep resistance and corrosion resistance of the blade alloys are maximized by alloying and their directional properties are improved by directional solidification or single crystal formation. Typical alloys are nickel-based with 10-15%Cr; 8-10%Co; 3-12% Al; 2-8%W; 1-2%Mo; 1-4%Ti, Si, Ta, Re, Hf, Nb, Y. A thermal barrier coating is applied to the surface of the turbine blade or guide vane and air or steam flows through internal channels for cooling. The ceramic thermal barrier coating is attached by a bond coat which both provides oxidation protection and hinders the outward diffusion of substrate atoms. Bond coats may be aluminides, aluminides with a 5-10 μm sub-layer of platinum, or MCrAlY[11] materials in which aluminum and chromium provide corrosion resistance and the yttrium increases the adherence of the coating to the substrate. The ceramic barrier coating is typically a material like Y_2O_3-stablized ZrO_2. This can be applied by chemical vapor deposition (CVD), sputtering, plasma spray or physical vapor deposition.

3.2 CORROSION IN GAS TURBINE ENVIRONMENTS

The gas turbine alloy technology described above has been developed in light of an understanding of the corrosion mechanisms produced by fuel impurities such as sulfides and chlorides [152]. Sulfur from the fuel reacts with sodium chloride from ingested air to form corrosive sodium sulfate deposits. To minimize sodium sulfate formation, the sulfur content of jet fuel is generally limited to 0.3 w/o. Where corrosion occurs, it appears as an outer layer of porous oxides over a Cr-depleted matrix that contains Cr-rich sulfides. Corrosion by molten sodium sulfate, known as Type 1 hot corrosion, occurs between the melting point temperature and dew point temperature of Na_2SO_4, i.e. between about 800 and 950°C (1470 to 1740°F).

Type 1 corrosion depends on the solubility of the oxide formed on the alloy in molten Na_2SO_4 [153]. Thermochemistry studies of the oxide solutions have been used to develop phase stability diagrams showing the solubility of the various metal compounds in Na_2SO_4 at various temperatures in plots similar to the Pourbaix diagrams developed for aqueous solutions [86]. The solubility of most oxides in molten Na_2SO_4 depends on the activity of the Na_2O in the Na_2SO_4 (which is generally proportion to the SO_3 concentration). The oxide dissolves either by an acidic or basic dissolution mechanism, depending on the basicity of the salt. For example nickel is dissolved by acid fluxing as Ni^{2+} ions:

$$NiO + Na_2SO_4 \rightarrow Ni^{2+} + SO_4^{2-} + Na_2O$$

and by basic fluxing as NiO_2^{2-} ions:

11 M is used to designate a metal.

$$NiO + Na_2SO_4 \rightarrow 2Na^+ + NiO_2^{2-} + SO_3$$

In acid fluxing the NiO dissolves by giving up oxide ions while in basic fluxing it dissolves by accepting oxide anions. A graph of oxide solubility versus salt basicity (-log a_{Na2O}) shows a minimum where the acidic and basic dissolution curves intersect. In reality, the reactions are more complex. Oxides on alloys contain multiple constituents, each with its own solubility as a function of basicity. Some corrosion processes will produce sulfides that can subsequently oxidize.

In some cases, NaCl can be present in the Na_2SO_4 deposits. For example sea water aerosols may be ingested into gas turbines used in marine environments. Chlorine adds two types of problems [153]. Parts per million concentrations of chlorine can make Cr_2O_3 and Al_2O_3 scales more likely to crack or spall while larger concentrations of chlorine can degrade M-Cr-Al-Y alloys rapidly by an active oxidation mechanism.

The practical consequence of these hot corrosion reactions is that corrosion rates in gas turbines are very sensitive to the concentration of SO_3 and NaCl in the combustion gas environment. Readers are referred to standard texts [151,153] for more information.

Accelerated corrosion can also occur below the apparent deposit melting temperature. This is called Type 2 hot corrosion and occurs in the presence of small concentrations of SO_3 at temperatures between about 700 and 800°C (1290 and 1470°F). Type 2 hot corrosion is referred to by some authors as gas-phase-induced acidic fluxing [153]. It appears to occur when the formation of Cr_2O_3 or Al_2O_3 is inhibited by the formation of $NiSO_4$-Na_2SO_4 or $CoSO_4$-Na_2SO_4 eutectics [151]. Luthra and Shores [51] reported that the SO_2 concentration required to form liquid Na_2SO_4-$NiSO_4$ on NiO was 5x 10^{-4} atmospheres at 750°C (1382°F), but that the Na_2SO_4 – 38%$NiSO_4$- eutectic has a melting point as low as 671°C (1240°F).

Beltran and Saegusa reported tests of candidate alloys for gas turbines in Type 2 hot corrosion environments [52]. The test environment contained 76% O_2, 0.15% SO_2 (balance N_2) and deposits were applied in an aqueous Na_2SO_4 mist containing 1 mole% $PbSO_4$ and 15 mole% of K_2SO_4. The most corrosion-resistant materials were Inconel alloys 671, 718 and 617. Pitting corrosion eventually gave way to the formation of a multilayered non-adherent surface oxide. Co-based alloys had lower corrosion resistance than Fe- or Ni-base alloys. Chromium was the most beneficial alloying element, while aluminized diffusion coatings provided little or no corrosion protection.

3.3 SUMMARY

These studies of high temperature alloy-salt-gas reactions in gas turbine environments show the importance of reactions that dissolve protective oxides and of reactions that form low melting temperature eutectics. Molten salts accelerate the degradation of corroded metals by mechanisms known collectively as "hot corrosion". These reactions have been studied in detail with relation to gas turbine environments, both at temperatures above the melting point of sodium sulfate (Type 1 hot corrosion) and at lower temperatures where gas reactions can produce alkali metal/alloy metal sulfate ternary eutectics (Type 2 hot corrosion). Protection against hot corrosion can be achieved by operating at above the salt dew point temperature, by using high chromium alloys[12] or by using protective metallic coatings very rich in aluminum or in aluminum and chromium [151].

12 Lai [152] comments that titanium additions seem to improve hot corrosion resistance while molybdenum and aluminum are considered detrimental.

4. CORROSION IN COAL-FIRED BOILER SUPERHEATERS, ESPECIALLY NEAR AND ABOVE THE FIRST MELTING TEMPERATURE OF FLUE GAS DEPOSITS

4.1 INTRODUCTION

The amount of electricity derived from coal burned in conventional coal-fired utility boilers depends strongly on their steam temperature and pressure. Research to increase the operating temperatures and operating pressures of utility boilers has been a focus of research, particularly since the energy crisis of the 1970's. Other parallel initiatives have sought to reduce CO_2 and NO_x emissions.

The main enabling technology required to build ultra-supercritical boilers to operate with steam temperatures of 760°C (1400°F) and steam pressures of 35 megapascals (Mpa) (5000 psi) is the development of stronger alloys that resist fireside corrosion at high temperatures.

4.2 MATERIALS FOR ULTRA-SUPERCRITICAL COAL-FIRED POWER PLANTS

4.2.1 US Research to Develop Materials for Ultra-supercritical Coal-fired Power Plants

In 2001, Blough and Seitz [88] evaluated the corrosion resistance of 10 superheater alloys in a coal fired boiler at temperatures simulating those of an advanced-cycle coal-fired unit (620 to 727°C; 1148 to 1341°F). The samples were exposed on retractable probes for periods of 6 months, 15½ months and nearly 22 months. Previous work had shown that Cr additions of up to 25% increased the corrosion resistance of the alloy. Al and Si additions were also beneficial, but less so. Nickel additions up to about 35% seemed also to be beneficial. The wastage rate increased with increases in the alkali concentration in the ash and with the SO_2 concentration in the flue gas. At the highest test temperature the best performing alloys were HR3C, Inconel 671, Fe_3Al and 253MA. After nearly 22 months exposure, all four of these alloys showed annualized corrosion rates of less than 0.0031" per year (79 microns per year) in the higher temperature tests (temperatures between 677 and 727°C; 1250 and 1341°F). The lower temperature tests (temperatures between 621 to 677°C; 1150 to 1250°F) did not show significantly lower corrosion rates, probably because the molten alkali–iron-trisulfate corrosion began to dissociate at the highest test temperatures. Molten alkali-iron-trisulfates are normally stable between about 600 and 700°C (1112 and 1292°F).

In 2003, Natesan, Purohit and Rink [89] evaluated the corrosion resistance of candidate alloys in coal ash environments. For iron-based alloys, the corrosion rate dependence on temperature followed a bell-shaped curve with a peak at about 725°C (1337°F). The actual rate depended on the alloy composition. The most corrosion-resistant iron-base alloy was HR3C (Fe-25Cr-20Ni-0.4Si-Nb-N). Although several of the alloys had adequate corrosion resistance (corrosion rates less than about 0.2mm per year (0.008" per year) at temperatures below the FMT of the sulfates in the coal ash environment[13], additions of NaCl produced catastrophic corrosion at 650 and 800°C (1202 and 1472°F). The authors conclude that this type of fly ash composition cannot be handled by iron-based alloys. Boiler operators desiring to burn such fuels should instead blend them with less aggressive fuels to keep the concentration of alkali sulfates and chlorides in the blended fuel below set limits. Nickel-based alloy candidates showed less weight loss than the iron-base alloys, but their attack was more localized as pitting. The outer portion of the scale was enriched in chromium and iron, and the inner portion was enriched in nickel and sulfur. The authors attributed the corrosion of the nickel-

13 Na_2SO_4 itself does not melt until the temperature reaches 884°C (1623°F).

based alloys to Type 2 hot corrosion involving the formation of a eutectic between Na_2SO_4 and $NiSO_4$. This mechanism is independent of effects of NaCl on the salt chemistry.

Other tests of candidate alloys under simulated fireside coal ash deposits were published by Baker and Smith in 2004 [93]. Twenty-eight alloys were tested at 700 and 775°C (1292 and 1427°F) under deposits containing Na_2SO_4 and K_2SO_4 in a gas mixture containing 1% SO_2. The average alloy wastage decreased as the Cr content of the alloy increased, up to about 29% Cr. The alloys most resistant to corrosion in the laboratory tests were 690, 671 and 188. In field tests in a supercritical coal-fired boiler, the best performers were Alloy 671, weld overlays of Alloy 52, Alloy 72 and Alloy 740. Alloy 740 easily met the stress-rupture criteria anticipated for 750°C (1382°F) operation.

Viswanathan and others have described the U.S. program to develop materials for ultra-supercritical coal power plants [100]. This program addresses economics, material strength, resistance to creep and thermal fatigue, fireside and steamside corrosion resistance, fabricability and weldability.

Reports of progress towards these national goals were published in 2005 and 2006 [100, 90]. With regard to creep resistance, these reports conclude that the strongest solid solution-strengthened nickel-based alloys (e.g. the modified 617 alloy known as CCA617) could operate at temperatures of up to 720°C (1328°F). Age-hardenable nickel-based alloys (e.g. Inconel 740 [93]) would be required at temperatures above 720°C (1328°F). Although these alloys have excellent creep resistance, their service temperatures are likely to be limited by other factors such as fireside corrosion, steamside corrosion and fabricability. Steam side oxidation and oxide exfoliation reduce the tube cross-section and can cause mechanical damage in the turbine. Also, the formation of insulating oxides increases the surface temperature of the tube, which will accelerate both fire side and steam side oxidation, and potentially cause premature creep-rupture.

Because ferritic steels cannot resist corrosion in molten alkali sulfate fly ash deposits at temperatures above 538°C (1000°F), the hottest tubes will need to be made out of austenitic steels or nickel-based alloys. Viswanathan lists 17 materials capable of operating at temperatures above 700°C (1300°F) and 9 alloys that might reach the goals of the US program. Because the high strength steels available for waterwall tubes require post-weld heat treatment, weldable high-strength alloys clad or overlaid with high-chromium alloys for corrosion resistance may be more suitable.

Another status report on this research program was published by Hack and Stanko in 2005 [94]. They concluded that commercial alloys would have had adequate corrosion resistance for ultra-supercritical plants burning Western coals. However, some of the high strength nickel alloys (especially those strengthened by Mo) could suffer corrosion in units burning high-sulfur Eastern and Midwestern coals. For such applications, more corrosion-resistant coatings such as weld overlay, diffusion coatings or laser cladding might be required. Units burning high-sulfur coals would probably require fireside corrosion protection for waterwall tubes made from 9-12% Cr ferritic steels.

In related work published in 2006, Kiser, Hinshaw and Orsini [122] reviewed field experience with nickel-based alloys and laboratory results in a new test environment simulating low NO_x combustion environments. The use of low-NO_x burners produced more reducing combustion gases that contain significant concentrations of H_2S potentially residing in sulfur-rich deposits on waterwall tubes. The environments are not unlike those in the lower furnace of black liquor recovery boilers, and low alloy ferritic steels had inadequate corrosion resistance in this environment.

The low-NO_x test environment consisted of the following gases:

Reducing Cycle: N_2-16%CO_2-10%H_2O-5%CO-2%H_2S (flow rate 500 sccm).
Oxidizing Cycle: N_2-17.2%CO_2-10.75%H_2O (No CO or H_2S).

The test consisted of repeated cycles: 4 days of the reducing cycle followed by 3 days of the oxidizing cycle. The test temperature was 1000°F (1832°F) and samples were removed, cooled to room temperature and weighed after 500, 1000, 3000 and 9000 hours. Tested materials included weld overlays ERNiCrFeAl-1 and ERNiCr-4 (Ni-39Cr-10Fe-0.5Ti) as well as a selection of high temperature creep resistant superheater alloys (Clad Alloy 671, Alloy 740, 310HCbN, Alloy 800, Alloy 825, Alloy HR120, Alloy 709, Fe_3Al, Type 347HFG and Alloy 52 (ERNiCr-7)). In 2 ½- year field exposures in a boiler at Niles, Ohio, the most corrosion-resistant alloys were those with the highest chromium contents. The authors quoted previous research by the US Institute of Fuel showing that in coal ash environments the best performer was a 50%Cr, 50%Ni alloy (e.g. Alloy 671). The authors documented 6 case histories of the successful use of Alloy 671 as co-extruded tubing in power plant superheaters. ERNiCr-4 was included because it offered the highest chromium content that could be applied as a crack-free weld overlay with a high deposition rate. 46,000 hours of exposure in a reheater environment at 649°C (1200°F) produced an annualized corrosion rate of only 13 microns per year (0.0005" per year) on ERNiCr-4 overlay.

Gagliano, Stanko and Hack published an update on the US program to develop materials for advanced steam cycles in 2008 [106]. They reported research (a) to measure the fireside corrosion resistance and specifically the Type 2 hot corrosion resistance of alloys that have sufficient strength for superheater and reheater tubes in ultra-supercritical boilers and (b) to determine the fireside corrosion resistance of alloys, weld overlays and coatings that have sufficient strength for waterwall tube applications in ultra-supercritical boilers. Controlled temperature probes, each containing 30 ring coupons placed end-to-end, were installed in three coal-fired utility boilers. Coupon temperatures ranged from 650 to 870°C (1200 to 1600°F). Preliminary visual inspection did not indicate any significant metal loss. Alloys evaluated at 650°C (1200°F) included 800HT, 740, 617, 347HFG, 230, HR6W, HR3C, 304H, 33WO/230, and 622WO/230. Alloys evaluated at 870°C (1600°F) included 72WO/230, 740, 52WO/230, HR6W, 50/50LC, HR3C and SiCr/304H. This research is continuing**.**

4.2.2 Research in Other Countries to Develop Materials for Ultra-supercritical Coal-fired Power Plants

Masuyama has published a historical review of the evolution of ferritic and austenitic materials for power plants [134]. The alloys with greatest corrosion resistance under alkali sulfate deposits in superheater/reheater environments contained 22-27% chromium. The alloys most resistant to steamside oxidation contained at least 23% chromium. For waterwall corrosion resistance, tubes needed to contain at least 15% chromium. Weldability and fabricability were also evaluated.

A report from the UK's Cleaner Coal Technology Programme [48] provides a UK perspective on the status of materials for advanced power generation, including materials for boilers, steam turbines, gas turbines and gasifiers. With regard to superheaters, the authors conclude that steam side oxidation is likely to restrict the practical use of 8% Cr steels to temperatures below 600°C (1112°F). Although newer ferritic steels with high creep strength may be useful in cooler parts of the steam circuits, boilers operating at 325 bar (4714 psi) and 620°C (1148°F) will have surface temperatures of about 660°C (1220°F) on the final superheater tubes. Austenitic materials such as X8CrNiMoNb1616 (16Cr-16Ni-1.8Mo, 0.5Si, Nb), X8CrNiMoVNb1613 (16Cr-13Ni-1.5Mo, 0.5Si, Nb, V) and X3CrNiMoNb1713 (17Cr-12Ni-2Mo, B) have adequate creep strength 70-80°C (160-175°F) above the temperature limit of the current 12% Cr steels (such as X20CrMoV121). The corrosion resistance

of these austenitic steels rises as their chromium content increases, until the chromium content reaches about 30%. A 20% Cr steel corroded at about one third the rate of a 15% Cr steel under the same conditions. Fine-grained steels 347HFG and Super 304 have adequate creep rupture strength to about 650°C (1202°F), but their corrosion resistance becomes inadequate at temperatures above 615-620°C (1140-1148°F). Alloys NF709 and HR3C show promise, but had creep rupture data for only 30,000 hours at the time the report [48] was written. For superheater tubes operated with metal temperatures approaching 700°C, improved versions of alloys such as NF709, AC66, HR3C and HR6W will be needed to limit the steam side oxide thickness.

Other studies of steamside oxidation were made in Denmark. Hansson, Korcakova, Hald and Montgomery [28] reported the long term steam-side oxidation of Type 347HFG at ultra-supercritical temperatures in a Danish coal-fired power plant. Steam oxidation formed a double-layered oxide. At temperatures below 585°C (1085°F), the inner Cr-containing layer contained regions of mixed $(Fe,Cr,Ni)_3O_4$ spinels in a matrix of mixed $(Fe,Cr)_2O_3$ sesquioxides. At higher temperatures, almost all the inner oxide was the mixed sesquioxide, apparently because increased rates of ionic diffusion increased the availability of Cr to form more protective oxides.

Montgomery and others [29] later applied analytical methods developed to understand corrosion and to project service life in straw-fired boilers to evaluate the performance of test sections of 9-12% Cr martensitic steels welded into coal-fired boilers at Armager 3 and at Avedøre 1 in Denmark. The authors found that their interpretation of field data from test tubes is hindered by a lack of detailed information about the temperature history of the specimens analyzed. Fireside corrosion rates of the new high temperature creep-resistant steels T-92 and HCM12 were comparable with those of T-91. HCM12 showed high oxidation rates after 85,000 hours (nearly 10 years) service.

4.3 EFFECT OF CHLORINE IN COAL ON BOILER CORROSION

Although chlorine has not been shown to cause systematic increases in corrosion in coal-fired boilers in the US, some correlation between coal chlorine and high temperature corrosion rates has been reported in the UK [140] (Figure 3) [147].

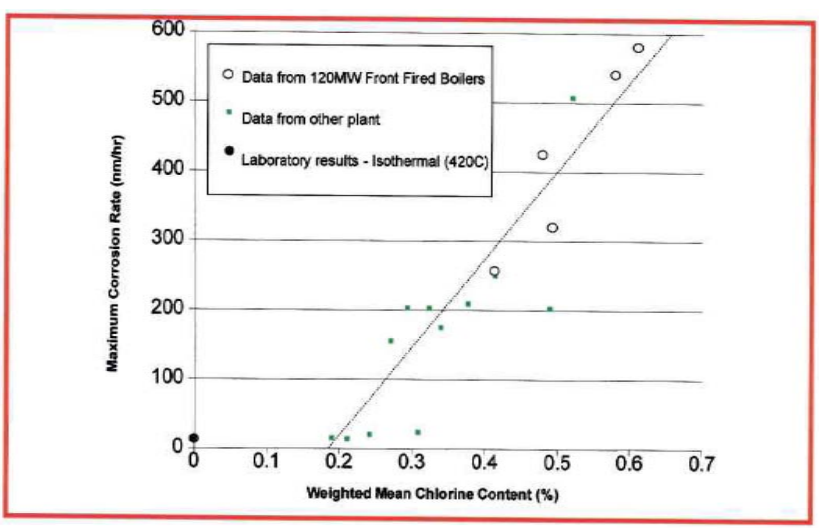

Fig. 3. Empirical relationship between high temperature corrosion rate and coal chlorine.

James and Pinder have reviewed the impact of fuel chlorine on fireside corrosion of boiler tubes [145]. This comprehensive review of several decades of research notes that many of the worsening fireside corrosion problems in UK power stations in the 1960's and 1970's were attributed to changes in coal composition, especially the fuel chlorine content. Chlorine-related corrosion problems reported from the UK encouraged US utilities to enforce a chlorine maximum of 0.25% or 0.3%. Chou and others [124] noted that many US manufacturers recommend maximum coal chlorine concentrations of 0.3%, based on the British correlations, despite the fact that chlorine-related corrosion had not been observed with high-Cl Illinois coals. Chou used corrosion probes and measurements in a pilot burner rig to compare corrosion produced by high-Cl fuels from the UK and Illinois and a low-Cl Illinois coal. However, the corrosion rates were not correlated with the coal chlorine concentrations. Similarly, Plumley and Roczniak's short term corrosion tests in a high chloride coal [53] showed rather slow corrosion rates except on Inconel 617. The best performer was Inconel 690 (Ni -27-31%Cr–7-11%Fe). Chou and others [124] concluded that the different observations in the UK and the US might have arisen from the use of different tube operating temperatures in the two countries.

James and Pinder's tabulation of chlorine and sulfur concentrations in coals delivered to two UK power stations between 1992 and 1994 shows that UK fuels generally have higher Cl (0.2 to 0.5%) and lower S (1.5 to 1.9%) concentrations than fuels burned in other countries. The consequent superheater/reheater corrosion appears as wastage flats at 2 and 10 o'clock related to the gas flow at 12 o'clock. The wasted surfaces have either an "orange-peel" appearance or fine and predominantly transverse "alligator hide" craze cracking, but not as the smooth ash-free surfaces characteristic of erosion damage. Tube attachments and support lugs increase local heat input and therefore serve as preferred sites for ash deposition. Thinning rates of up to about 25nm/h (0.0086" per year) can be tolerated within the design life of the tubing. The scale on corroded tubes is mostly Fe_3O_4, containing "pancakes" of Fe- or Cr-sulfides oriented parallel to the tube surface. The ash layer outside the scale typically appears to have been molten and consists of alkali metal sulfates with a K/Na range between 2/1 and 1/1. The outer layer is mostly Fe_2O_3 mixed with ash deposits. Even when relatively high chlorine fuels are being burned, the scale and deposit contains very little chlorine. Such chlorine as is present is concentrated at the scale/metal interface.

James and Pinder state that fireside corrosion by molten alkali sulfates is accelerated by SO_3 as follows:

$$M_2SO_4 + SO_3 \rightarrow M_2S_2O_7$$

Free SO_2 in this molten pyrosulfate reacts with iron oxides to form alkali metal trisulfates:

$$Fe_2O_3 + 3SO_3 \rightarrow Fe_2(SO_4)_3$$
$$\text{or } Fe_2O_3 + 3M_2SO_4 + 3SO_2 \rightarrow 2M_3Fe(SO_4)_3$$

Alkali metal trisulfates have frequently been found in deposits on corroded superheater tubes. The dissolution of iron sulfates depresses the melting temperature of sodium-potassium sulfates from 823°C (1513°F) to about 550°C (1022°F), which is within the operational range of superheater/reheater tube temperatures of UK pulverized coal boilers that operate with final steam temperatures of 568°C (1054°F).

When superheater tubes are operated at temperatures below 550°C (1022°F), the ash deposits and corrosion products are porous solids that allow flue gases to access the tube metal surface. At higher tube temperatures Na_2SO_4 and K_2SO_4 deposits formed upstream in the boiler accumulate on the windward side of the tubes and condense at the base of the alumino-silicate deposit. If the tube

temperature exceeds the FMT of the deposit, the corrosion rate increases rapidly. At still higher temperatures, the alkali iron trisulfates decompose and the corrosion rate reduces to that caused by the gaseous species in the flue gas. Rates of corrosion produced by these trisulfates show a bell-shaped relationship with the tube temperature.

Associated studies in the UK[14] developed an empirical correlation between the chlorine content of the coal and superheater corrosion rates, as follows:

$$\text{Corrosion Rate (nm/h)} = A \cdot B \cdot \{T_g/1000\}^{\alpha} \cdot \{(T_m - 550)/100\}^{\beta} \cdot \{Cl - 0.06\}$$

Pinder and James observe that the reasons for the correlation between corrosion rate and chlorine content are not well understood. The chlorine does not seem to facilitate alkali metal release or to cause gaseous corrosion directly.

Ferritic superheater materials in UK power station superheaters are limited to temperatures below about 580°C (1076°F) to maintain tolerable corrosion rates. James and Pinder's attempts to correlate corrosion rates with fuel composition in this lower temperature range were not successful [145] possibly because these temperatures produce a combination of gaseous and molten sulfate attack (i.e. parabolic and linear kinetics).

Two other major reviews of corrosion by chlorine in coals should also be mentioned [71, 13]. Wright, Mehta, and Ho [71] and many others agree that the UK data confirm high temperature corrosion as a consequence of chlorine. This conclusion was also reached by Tillman and others [13] who documented the range of chlorine concentrations found in coals mined around the world and reviewed field experience with chlorine corrosion in boilers fired with 100% coal. They concluded that, while high chlorine coals have been shown to cause corrosion, the difference between the US and UK findings has not been resolved.

4.3.1 Effect of Temperature Gradients

James and Pinder [145] have observed that, in the absence of heat flux, molten salts on the surface of a superheater tube quickly become saturated with corrosion products and stifle the corrosion reactions. However, when a temperature gradient exists, the concentration gradient through the molten deposit reduces the solubility of SO_3 in the deposit and reduces the stability of the sulfated corrosion product in the hotter deposit in the more oxidizing environment further from the tube surface. This precipitates a non-protective porous iron oxide in the hottest (outermost) ash layer, releasing alkali metal sulfates and SO_3 that can migrate back to the tube surface to cause more corrosion, without the need for additional alkali metal sulfate deposition from the fuel gases. Essentially this mechanism is active oxidation driven by the temperature gradient. The decomposition of the outermost sulfates also reduces the melt thickness, which speeds the transport of the corrosion products away from the scale/melt interface and increases the corrosion rate.

Effects of heat flux and chlorine content established by E.ON and its predecessor companies Powegen and CEGB, are presented in a single graph in Figure 4 [147]

14 James and Pinder cite the reference for this work as L.W. Pinder, S. Brooks and D.B. Meadowcroft, "Derivation of model equations for the prediction of corrosion rates of austenitic superheater and reheater tubing in coal-fired boilers", MID/SSD/86/0028/n/MT, but I have not yet been able to trace this reference.

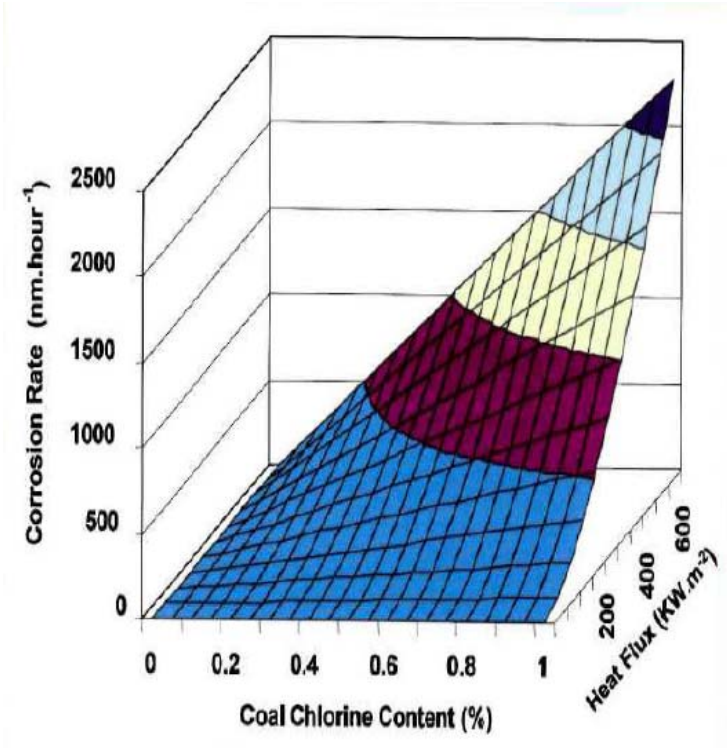

Fig. 4. Effects of coal chlorine content and heat flux on high temperature corrosion rates.

These effects were modeled by Glover using non-equilibrium thermodynamics to develop general flux equations that could be combined with point defect information for specific oxides to predict oxidation rates [144]. In addition to the effects of temperature on diffusion rates in oxides, thermal gradients can affect active oxidation mechanisms, where the chlorides in superheater deposits are concentrated at the metal/scale interface [145]. Because laboratory tests that do not simulate the temperature gradient across the tube wall and deposit hinder the growth of the chlorine-rich inner layer and underestimate the corrosivity of the environment, E.ON uses laboratory tests only for preliminary sorting of candidate alloys and uses corrosion probe tests in a burner rig and in operating boilers to evaluate corrosion mechanisms and rates in operating boilers [147].

Another recent summary of the effects of temperature gradients on corrosion has been published by Covino and others [123]. Their study was to develop a basis for understanding rapid corrosion in Waste-to-Energy (WTE) plants. They note that heat flux can affect:

Oxide scale adhesion, cracking and spalling
Transport and chemical processes within fireside deposits on tubes
Condensation effects, such as chloride deposition
Point defect migration in oxide scales – thermal diffusion[15] and heat of transport effects

Covino and his colleagues point out that WTE plants have more severe corrosion produced by thermal gradients than most coal-fired boilers because the tubes are often covered by molten salt deposits. Substantial temperature gradients exist across the ash deposits and corrosion products in the

15 This is similar to the Ludwig-Soret effect in which applied temperature gradients establish concentration gradients in liquid mixtures.

areas most susceptible to corrosion. The paper [123] then describes laboratory and field tests to investigate the effects of temperature and thermal gradients on the high temperature corrosion of carbon steel and of cobalt. Carbon steel corroded about twice as rapidly under a thermal gradient than under isothermal conditions at 450°C (842°F), although no effects of thermal gradients were detected with cobalt.

Kawahara, Nakagawa and Li [165] reported that apparent galvanic corrosion beside tube welds made with Alloy 625 filler metal in a waste incineration plant was reproduced in the laboratory only when a temperature gradient existed between the alloy substrate and the flue gas. Later work by Kawahara, Kira and Ike [156] found that laboratory tests in simulated environments under-estimate the corrosion rate experienced in the field, and concludes that isothermal tests should be used only for evaluating candidate materials, but may not reproduce the type of corrosion found in operating boilers. This work developed a thermal gradient corrosion test to reproduce the thermal conditions found in WTE boilers. Results obtained with the thermal gradient corrosion test were described in a later publication [165].

Additional evidence for the effects of thermal gradients on superheater tube corrosion rates comes from the work of Montgomery, Jensen, Hansson and Vilhelmsen [30]. These authors found high corrosion rates were associated with areas of high heat flux in the Maribø and Avedøre 2 superheaters, although increasing heat flux produced very little increase in the surface metal temperature. For example, doubling of heat flux from 6,800 to 12,200 w/m^2 in the Maribø superheater 3 produced an estimated temperature increase of only 6°C (11°F) [30]. The authors noted that effects of increased flue gas temperature are complex because they can simultaneously affect the thickness, composition and morphology of the deposit and the degree of deposit sulfation.

4.4 FOULING TENDENCY AND ASH DISPOSAL

Coals from different sources can show significantly different slagging and fouling[16] tendencies. For example Liu, Heinzel, Maier and Hein fired three kinds of lignite coals and their blends [44] and showed that serious slagging and fouling began where local flue gas temperatures exceeded the fly ash melting temperature. The lignite coals with the highest slagging potential contained high concentrations of pyrite (FeS_2) and calcium that produced fly ash with a low melting temperature. A 1% Cr boiler tube material with grain boundary sensitization produced a thick (failed) Fe/Cr oxide layer under these conditions.

In a related paper, Heinzel and his colleagues [43] studied ash formation and corrosion caused by blends of hard coal and lignite with straw, energy crops, wood and sewage sludge in a conventional pulverized fuel test facility. Adding biomass to hard coal reduced the slagging temperature by about 100°C (180°F). 100% straw firing reduced the slagging temperature by about 200°C (360°F). Slag formation in the furnace was not a problem because the high combustion temperatures volatilized alkali salts, producing low silicate concentrations in the bottom ash. However, straw substitution greater than 10 or 20% produced bottom ashes that contained more chlorine than European industry regulations allow for use in the cement industry. The authors also concluded that increases in the alkali and chloride concentration of the flue gases caused by co-firing biomass are likely to cause corrosion under superheater deposits if the Cl to S ratio becomes too high ("too high" was not defined). Potassium in the biomass fuels enriched the filter ash in KCl and K_2SO_4 by condensing sub-micron alkali salt particles on the micron-sized fly ash particles.

16 Slagging is agglomeration in the furnace. Fouling is the growth of accumulation of deposits in the convection passes of the boiler.

The disposal of boiler ash is less regulated in the US than in Europe. However, the disposal of ash produced by US power stations is becoming a focus of environmental concern. Each year the US utility industry generates more than 70 million tons of fly ash, 15 million tons of bottom ash and 2 million tons of boiler slag [164]. All three materials are used in cement manufacture. The highest value of fly ash is as a substitute for Portland cement in concrete. Bottom ash is also used to replace virgin sand and gravel in structural fill and road base. Boiler slag is used as structural fill and blasting grit. In 2008, 42.3 million tons of coal fly ash, 10.4 million tons bottom ash, and 0.34 million tons boiler slag were landfilled, representing roughly 58%, 56%, and 17% of the amount generated, respectively. The American Coal Ash Association (ACAA) estimates that, since the 1920s, when fly ash was first landfilled, between 100 million and 500 million tons of fly ash have accumulated in U.S. landfills [164].

Given the potential problems of disposing of the ash generated by burning biomass fuel in a conventional utility boiler, Heinzel and others at the University of Stuttgart [42] investigated ash formation during the burning of coals, sewage sludges and biomass in a pilot scale vertical cyclone slag tap furnace[17] and in a conventional pulverized fuel boiler [43]. Combustion in a slag tap furnace can be compared to combustion in a black liquor recovery boiler. Fuel particles ignited in suspension fly to the cyclone walls where they burn out completely on top of the slag. The high furnace temperatures, which exceed 1400°C (2552°F), reduce the volume of fly ash and produce a slag from which blasting abrasives can be manufactured. However, volatilized inorganics deposited in the flue gas path produce corrosive alkali chlorides and sulfates when high chlorine, high alkali and low sulfur fuels like straw residues and brown coal[18] are burned. Other particularly corrosive deposits are formed by fuels containing significant amounts of Zn or Pb (e.g. sewage sludge) which form low melting temperature deposits. Heinzel and his co-workers concluded that it would be possible to combust hard coal – sewage sludge in an industrial slag tap furnace, although excessive concentrations of chlorine, sulfur and heavy metals could form corrosive deposits or unacceptable flue gas emissions. Different straw fuels showed very different behaviors in the slag-tap furnace. One produced a foam glass-type slag that would not flow out of the slag tap. Other types of straw produced deposits that flowed normally, but that were correspondingly more corrosive. Co-combusting straw with coal reduced the corrosion tendency by producing alkali sulfate rather than alkali chloride deposits.

4.5 EFFECTS OF OXYFUEL COMBUSTION

Oxyfuel combustion is an attractive firing practice because it reduces the formation of nitrogen oxides and creates a flue gas that is essentially only carbon dioxide, which can therefore be captured at much lower cost than in a conventionally-fired power plant.

Two papers on corrosion effects of oxyfuel combustion were published in 2010. Davis summarized the impact of oxyfuel combustion on corrosion in coal fired plants [128]. He concluded that oxyfuel combustion increases the risk of corrosion in superheater/reheater tubes by surface chromium depletion caused by chromium carbide formation on austenitic alloy tubes. Corrosion could be minimized by using low-sulfur, low-chlorine coals, implementing good combustion control to avoid reducing conditions at the furnace wall, flue gas desulfurization in the recycled gases to reduce the concentrations of SO_2 and Cl species within the furnace, and the use of corrosion-resistant (i.e.

17 A slag-tap boiler burns pulverized coal in a boiler that contains a port from which molten furnace bottom ash can flow out into a quench hopper. The quenching freezes and fractures the ash, which is removed by high pressure water jets for dewatering and screening. The crystallized boiler slag is a coarse, angular, glassy, black material, usually known as "Black Beauty". When pulverized coal is burned in a slag-tap furnace, up to 50% of the ash is retained in the furnace as boiler slag.
18 Brown coal contains relatively high sodium and has a low ash content.

stabilized) tube materials or of coatings. Dew point corrosion caused by flue gas recirculation could also become a problem.

Also in 2010, Tuurna and others at VTT conducted experiments to evaluate the performance of superheater steels in simulated oxyfiring conditions [66]. Combustion in oxygen or oxygen-enriched air tended to increase the conversion of SO_2 to SO_3. The associated use of flue gas recirculation to dissipate the intense heat produced by combustion in oxygen increased the concentration not only of CO_2 in the fuel gases but also that of CO, SO_x, Cl and HCl and H_2O. The concentration of other troublesome flue gas vapors like Hg, As and Se also increased. Samples of alloys T22, X20CrMoV11-1, 347HFG and HR3C were exposed in premixed gases simulating oxy-fired and air-fired coal combustion at temperatures of 580 and 650°C (1076 and 1202°F). The oxy-fuel gas environment contained 3.6% O_2, 60% CO_2, 30% H_2O and 6.4% Ar.

T22 and X20 steels were heavily oxidized at rather similar rates at 580°C (1076°F). Their oxidation rates were slightly lower in oxyfuel combustion conditions than during conventional firing. The corrosion rate of X20 steel was not significantly higher at 650°C (1202°F). Although the higher temperature formed a porous internal layer, no spalling was observed. Type 347HFG was more oxidation-resistant than T22 or X20, and performed slightly better in oxyfuel conditions than in air-fired conditions. The rapid formation of a protective oxide was attributed to the fine grain size of this alloy. The oxidation of HR3C samples was very slow, particularly in oxyfuel conditions. Although the initial indications of this study are that oxy-firing will be no more corrosive than air firing, the authors commented that the addition of impurities such as SO_2 and HCl to the oxy-firing test environment could change the performance of the materials [66].

4.6 EFFECTS ON CORROSION OF CO-FIRING BIOMASS WITH COAL

Tests of candidate alloys at metal temperatures between 640 and 670°C (1184 and 1238°F) in Swedish boilers burning coal- biomass blends and 100% biomass were reported by Henderson and others [38]. Corrosion rates were generally higher when burning 100% biomass than when burning coal-biomass blends. Alloys with the highest chromium content generally showed the lowest corrosion rates, but there were some exceptions. Manganese additions e.g. as in alloy Esshete 1250 (Fe-15Cr-10Ni-6.3Mn-1Mo-0.6Si-NVB) also seemed to be beneficial.

Hansen, Frandsen, Dam-Johansen, Sørenson and Skrifvars [8] analyzed bottom ash, fly ash and superheater deposits in a pulverized coal-fired boiler burning 0%, 10% and 20% (energy basis) straw. Potassium released by firing increased proportions of straw reacted with alumino-silicates from the coal, producing more potassium-alumino-silicates in the fly ash. Ash samples collected on probes contained silicates rich in K, Ca and Fe, but no molten components. Simultaneous thermal analysis measurements (STA) showed that the ash did not melt until the temperature reached the range 1000 to 1390°C (1832 to 2534°F). Despite the mineralogical differences, there was no significant difference between the melting behavior of the fly ashes and the bottom ashes. The FMT of the fly ash was about 150°C (270°F) below the initial deformation temperature[19] (IDT). Sintering experiments showed that all the ashes grew stronger at temperatures below the FMT. During coal combustion, the fly ash grew stronger in the absence of a liquid phase, but during co-combustion with straw, ash strengths remained low unless molten phases were present. Sintering began when the average viscosity of ashes was $(1-3) \times 10^6$ P. Quantification of melting by STA showed that between 1% and 36% of the deposit was molten when at the IDT measured in ash fusion tests. The authors concluded

19 The Initial Deposition Temperature (IDT) is the temperature at which the point of a pressed pyramid of boiler ash begins to round.

that standard ash fusion test data should be used with care when determining melting behavior and fouling tendency.

In laboratory studies simulating superheater corrosion in straw-fired boilers, Nielsen, Frandsen and Dam-Johansen [10] coated boiler tube steels with synthetic (KCl and/or K_2SO_4) and real deposits, and exposed them to a synthetic flue gas at 550 °C for durations between 1 week and 5 months. The corrosion was generally uniform, with corrosion products that were largely Fe and Cr oxides. The authors suggested that KCl forms a eutectic with K_2SO_4 and various iron compounds at the tube surface, and KCl is rapidly converted to K_2SO_4 in this melt whenever the tube surface temperature is high enough to melt it. This sulfation releases Cl_2 and HCl, causing rapid oxidation of the tubes according to the mechanism first called "active oxidation"[20] by Lee and McNallan [146] and later studied in detail by Grabke and co-workers [e.g. 57]. Many types of sulfur compounds can produce the sulfation reaction, although SO_3 appears to be most reactive [13]. Lokare and others have shown that increasing the molar ratio of available sulfur to chlorine can make corrosion very unlikely [139]. After reviewing industry experience with co-firing biomass and coal, Duong and Tillman [108] attribute the rarity of corrosion problems to the sulfation of chlorine-containing deposits by sulfur from the coal component of the fuel.

Salmenoja and Mäkelä concluded [69] that gaseous HCl discharges with the flue gases and does not corrode superheater tubes when the environment is oxidizing and the tube metal temperature below 600°C (1112°F). However, in reducing conditions, corrosion of biomass boiler superheater tubes begins at about 450°C (842°F) with metal chloride formation.

Anderson and others [18] described deposit formation in a 150 megawatt (MW) pulverized coal utility boiler converted to burn 20% straw (on an energy basis). The Fe-rich upstream deposits formed during coal combustion gave way to Ca- and Si-rich deposits during coal-straw co-combustion. Potassium from the biomass formed K-Al silicate deposits that had higher melting temperatures and were not problematic. No chlorine was found in deposits collected during combustion and chlorine was not expected to cause corrosion problems with the fuels used. The formation of stable K-Al silicates was confirmed by thermodynamic calculations. This emphasized the importance of good mixing during combustion so as to form K-Al silicates rather than K_2SO_4.

Wei and others [6] made thermodynamic equilibrium analyses of the effect of other fuel minerals on the release and fate of chlorine and alkali metals during the co-combustion of coal and straw. In a pulverized fuel boiler, very little of the chlorine and sulfur in the fuel is found in furnace bottom ash, air preheater ash or cyclone ash. Instead, the chlorine and sulfur concentrations in the fly ash are relatively high. In the combustion of hard coal with less than 50% straw, most of the potassium is found as potassium aluminosilicates, which have a high melting temperature and inhibit ash deposition on the furnace surface. Sodium forms sodium aluminosilicates, some NaCl(gas) and some NaOH(gas). Increasing the faction of straw in the fuel increases potassium silicate formation. Most of the sodium is released as NaOH(gas), NaCl(gas) and Na_2SO_4(liquid). When the fuel contains less than 50% straw, Na_2SO_4(liquid) is formed at temperatures between 1200 and 1400°K (1700-2060°F). If the fuel is 100% straw, the predominant species are KCl(gas) and $K_2Si_4O_9$(liquid). When the flue gases cool, KCl(gas) and KOH(gas) may react with SO_2(gas) and H_2O(gas) to form K_2SO_4(gas) and other aerosols.

Later work by Wei, Schnell and Hein extended these studies of the thermochemistry of gaseous chlorine and alkali metals to the combustion of Danish straw, Swedish wood and sewage sludge, and in the pressurized pyrolysis of wood and sludge [27]. HCl(g), KCl(g), KOH(g) and NaCl(g) released

20 The term "active oxidation" was chosen because the scale formed on the metal substrate was not protective.

during biomass combustion caused agglomeration, fouling and corrosion. The gas-phase alkaline species are severely corrosive to gas turbines in combined cycle plants[21], consistent with the work of Pettersson, Svensson and Johansson [75]. The equilibrium compounds in each fuel mixture were calculated as a function of temperature. In straw combustion, the predominant alkali species were predicted to be $K_2Si_4O_9$(liq), KCl(gas) and KOH(gas). In wood combustion, KCl(gas), K_2SO_4(gas) and KOH(gas) predominated. NaCl and NaOH(g) predominated in sewage combustion. The release of chlorine and potassium was essentially independent of the amount of excess air used in combustion. However, when straw or sludge is burned, increasing combustion air reduces the release of HCl(gas) and increases the formation of KCl(gas) and NaCl(gas) at high temperatures. Wei notes that HCl emissions are regulated in many jurisdictions.

Additional calculations were made to predict the effects of excess air on emissions of alkali metal gases, chlorine and hydrogen chloride during the pyrolysis of biomass, wood and sewage sludge [27]. During the pyrolysis of wood and sewage, nitrogen[22] forms toxic KCN(gas) and NaCN(gas). The addition of kaolin during straw combustion appeared to increase the formation of potassium aluminosilicates in the ash. These additions also reduced the formation of KCl(gas) and KOH(gas) and increased the formation of HCl(gas).

In 2005, Frandsen summarized 10 years of research at the Technical University of Denmark on deposits and corrosion in boilers firing biomass and waste [82]. This includes ternary diagrams summarizing the composition of fly ash and bottom ash in straw-fired grate boilers and coal/straw fired CFB or pulverized fuel boilers (figure 5). The deposits are characterized by their concentration of three types of material: quartz and aluminum silicates; potassium and calcium silicates; potassium chloride.

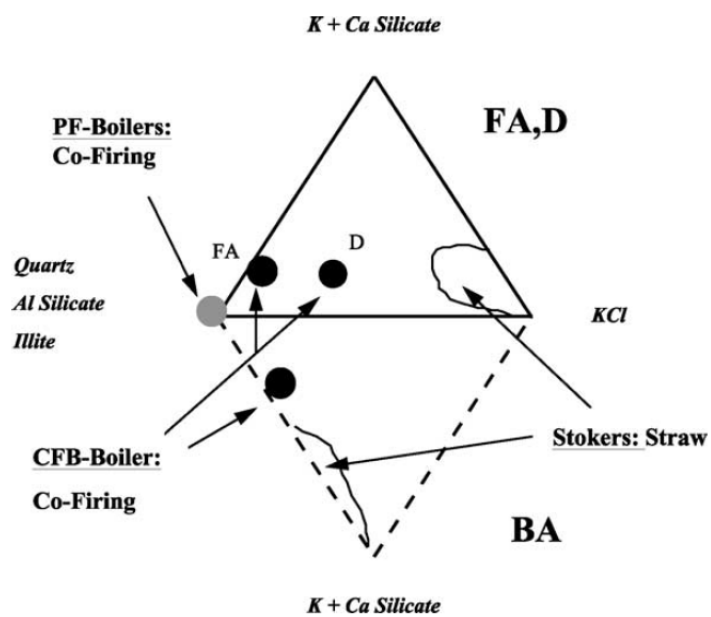

Fig. 5. Composition of fly ash (top triangle) and bottom ash deposits (lower triangle) in deposits from wheat straw-fired grate boilers, a coal-fired CFB boiler and a straw-coal co-fired boiler.

21 References 11-13 in [27].

22 Nitrogen is used in pressurized pyrolysis reactors to heat the biomass and carry the pyrolysis gases forward.

A historical overview by Frandsen [24] summarized progress in the understanding of ash and corrosion research reported at a series of biennial international conferences. A previous review had covered the period 1963 to 1991 and Frandsen's paper extended this through the period 1991 to 2009.

Davidsson and others evaluated the effects of co-firing coal and wood/straw biomass fuels with sewage sludge in a 12MW CFB boiler [26]. The fuels fired were biomass fuel, coal + biomass fuel, coal + biomass fuel + sewage sludge and biomass fuel + sewage sludge. Other experiments included limestone additions and chlorine additions as PVC. The fuel mixture and the addition of limestone had little effect on the alkali fraction in the bed ash. Chlorine additions decreased the alkali fraction in the bed ash. Adding sewage sludge practically eliminated alkali chlorides from the flue gases and from a superheater deposit probe by causing sulfation reactions. Adding enough limestone to coal and sludge to eliminate SO_2 emissions did not affect the behavior of chlorine. PVC additions increased the amount of alkali chlorides in the flue gas. However, when sewage sludge was co-fired, no chlorine was found in the superheater deposit. Firing coal with the wood/straw biomass fuel produced flue gases with 1/3 the alkali chloride concentration of flue gases from firing biomass fuel only, whether or not limestone or PVC was added. Davidsson concluded that the aluminum compounds in coal and sludge are more important than sulfur in reducing the concentration of KCl in tube deposits and flue gases. This is consistent with his finding with kaolin additions in a wood-burning boiler [20].

Theis, Skrifvars, Zevenhoven, Hupa and Tran have studied the rate and composition of deposits formed by the combustion of mixtures of peat with bark or straw as a function of the substrate surface temperature [79-81]. Peat is a clean fuel that contains large amounts of inert compounds such as silica and alumina in its ash. Ash deposition rates were measured in an entrained flow reactor. Fuel particles are fed into the top of this reactor and can be sampled as they de-volatilized, charred and burned to ash while falling through a 6.5 meter tube furnace entrained in flue gases produced by a natural gas burner. A 1" diameter horizontal probe, air-cooled to 550°C, collected deposits at the base of this reactor. The probe diameter was chosen so that the probability of particles colliding with the probe was the same as that of particles colliding with a superheater tube in a bubbling fluidized bed combustor.

Deposition rates from individual fuels were peat: 20 $gm/m^2/h$; bark: 80 $gm/m^2/h$ and straw: 160 $gm/m^2/h$ [79]. These are within the order of magnitude of deposition rates measured in industrial boilers. Deposition rates of mixed fuels were not linear functions of the mixture composition, indicating that the ash components were interacting with one another. Peat appeared to limit deposition when less than 50% bark was added, but increased fouling, probably by becoming incorporated in bark deposits, when more than 50% bark was added. Adding as little as 30% peat to a straw fuel reduced its deposition tendency to that of pure peat, and up to 70% straw could be added before the deposition rate increased. This cleansing effect of peat had been documented previously in a pulverized wood-fired boiler [143]. This study [79] suggested that up to 30 w/o bark or up to 70 w/o straw (renewable biomass fuels) could be co-fired with peat without increased fouling rates.

Ash from peat burning contained mostly insoluble silicates; ash from bark contained some soluble and volatile ash components and ash from straw contained easily volatilized soluble components [80]. When co-firing fuel mixtures, the ash deposition rate did not increase until the Cl/S molar ratio in the feed ash exceeded 0.15. Associated thermodynamic calculations for peat/bark mixtures showed that increased deposition rates occurred when the deposit material contained more than 15% of molten phases. This affirms that sulfur in the fuel suppresses deposition by sulfating Cl compounds, producing deposits containing less Cl and less molten phases. In peat/straw mixtures, increasing Cl/S ratios in the fuel and increased deposition rates did not correlate with the appearance of molten phases

in the deposit. This might indicate that Si-Al compounds in the peat ash were capturing gaseous alkali compounds from the straw ash [8], or that abrasive peat ash was eroding the straw ash deposits [80].

Studies with probe temperatures between 475 and 625°C (887 to 1157°F) [81] showed that the deposition rate was independent of the substrate surface temperature when 100% peat was burned. When fuel mixtures were co-fired, the situation became more complex. Deposition rates when burning bark or peat/bark mixtures decreased with increasing probe temperatures. However, deposition rates when burning straw or straw/peat mixtures increased with increasing probe temperature at temperatures below 550°C (1022°F), but became independent of probe temperature at higher temperatures. Regardless of the fuel being burned, the chlorine content of the deposit decreased with increasing substrate temperature. Deposits from peat/bark fuels contained K as K_2SO_4 when the deposition rate was low and as KCl when the deposition rate was high. However, deposition rates from peat/straw fuels were not correlated with the Cl, S and K content of the deposit, indicating the cleansing effect of the peat mentioned above [143].

Piotrowska and others showed that co-combustion of rapeseed cake with coal [157] was much less problematic than burning the rapeseed cake by itself, because the alkali metals in the rapeseed interacted with aluminum silicates in the coal. Bed agglomeration and upper boiler deposits were not serious. No gaseous alkali metal chlorides were detected in the beginning of the convection pass. Up to 9 w/o of P was present in deposits on the lee side of a probe. Limestone additions increased the rate of deposition on this probe but reduced emissions of HCl and SO_2.

A recent paper by Fuller, Maier and Scheffknecht [50] reviewed the issues faced by large coal-burning power plants planning to convert to biomass firing. They presented a detailed case study of a 250 MW plant that co-fired up to 100% wood pellets without experiencing serious problems either in operation or in emissions. To achieve complete burnout of the particles the fuel milling system needed some modifications and the fuel needed to be introduced where it would achieve the longest possible residence time. Pure wood pellet combustion produced slightly higher CO_2 emissions than pure coal, but the authors expect that this can be reversed by planned modifications to the burner and firing systems. The high alkali content of the fly ash produced by 100% wood firing will have limited potential as an additive for cementitious materials unless firing procedures can be changed to increase the proportion of silica alumina, and iron oxides in the fly ash to the concentrations required by regional regulations.

4.6.1 Effects of Chlorine from Biomass Fuels on Superheater Corrosion in Pulverized Coal Boilers

Tillman, Duong, Figueroa and Miller have written a comprehensive review of sources of chlorine in fuels that might be co-fired in pulverized coal utility boilers and on the consequences of this chlorine on deposition and corrosion [13]. Their survey focuses on coals and woody and herbaceous biomass fuels and excludes municipal waste fuels. A subsequent publication from the same laboratory [108] includes a useful tabulation of typical chlorine and moisture concentrations in 20 biomass materials used as fuels. All the biomass fuels contained more Cl than coal samples from 9 representative US coalfields. The chlorine concentrations of the biomass fuels, expressed as $lb/10^6$ Btu ranged from 0.012 for willow, polar and almond shells to 0.923 for corn stover and 0.894 for rice straw. The chlorine concentration of a given coal depends primarily on the age and rank (maturity) of the deposit from which it was mined [13]. The highest concentrations are found in immature bituminous coal fields. But, with the exception of wood fuels and a few other materials, the biomass used as fuel

contains significantly higher chlorine concentrations than coal. Field crops, with the exception of nut shells, pits and switchgrass, contain more chlorine than woody materials.

Tillman and his co-authors note that the most common corrosion problems caused by the addition of biomass to coal fuels arise because of reactions of chlorine with the alkali metals potassium and sodium. Chlorides are the most stable alkali species in the gas phase. Although alkali chlorides are formed first regardless of the surplus of sulfur in the system, the chlorine in the alkali compounds can be displaced by sulfur. Although the alkali sulfates thus produced are far from inert, they are much less aggressive than alkali chlorides. KCl formation presents the greatest concern during the combustion of biomass fuels, because of its low melting temperature. Alkali chlorides formed in the initial combustion processes can form corrosive deposits on heat transfer surfaces such as superheater tubes. Depending on the tube surface temperature, these deposits can themselves be molten or form low melting temperature eutectics with other materials. The most aggressive corrosion therefore takes place in a narrow temperature band where liquids are present on the tube surface. Note however, that even above the dew point of the deposits, gaseous KCl is corrosive towards superheater alloys [75].

Tillman and his co-authors pointed out [13] that co-firing 10% straw at a Danish power station did not produce any acceleration in corrosion that could be attributed to chlorine release. At 20% co-firing, the corrosion rate increased by a factor of 2 or 3 to a rate typical of the most corrosive coals. Based on these results the authors concluded that the maximum manageable percentage of co-firing straw with coal would be about 20% straw. With very good mixing and careful deposit control, higher substitution might be possible.

4.7 SUMMARY

In today's marketplace of energy fuels, coal offers an abundant, easy-to-burn fuel with manageable corrosion problems at steam temperatures that offer conversion efficiencies up to 50%. In the absence of policies to promote the use of renewable fuels for power generation, coal is likely to retain its position as the primary fuel for US power stations. Coals containing corrosive contaminants such as alkali chlorides and sulfates are diluted with less problematic fuels to avoid corrosion problems. Current research suggests that, as superheater temperatures are increased to maximize energy recovery from coal, materials limitations in high temperature creep resistance may be reached before corrosion limits are reached.

5. CORROSION IN SUPERHEATERS OF BOILERS BURNING MUNICIPAL WASTE AND TIRE-DERIVED FUEL, ESPECIALLY NEAR AND ABOVE THE FMT

5.1 CO-FIRING WASTES WITH FOSSIL FUELS

Coda Zabetta and others have summarized the history and status of biomass and waste combustion in Europe [102]. For many years pulp and paper mills have used wood fuels to generate steam. Boilers used for steam generation and small-scale electricity generation were small (~10 megawatt equivalent (MWe)) partly because of limits imposed by profitability, technology and the limited availability of biomass fuels. Recent environmental legislation to restrict the emission of greenhouse gases has renewed interest in co-combustion in pulverized coal-fired units. In Europe the introduction of circulating fluidized bed boilers has reduced furnace emissions and enabled greater fuel flexibility. The range of fuels co-combusted with fossil fuels such as coal and pet coke includes both biomass fuels such as wood, agricultural wastes and bio sludges, and waste fuels such as contaminated wood, municipal waste and tire-derived fuel (TDF). Biomass and waste fuels contain less energy than fossil fuels and tend to foul and corrode heat exchanger surfaces like superheater tubes. They also increase the risk of bed agglomeration in CFB furnaces, and often show deleterious synergistic effects. However, in some cases, fuels can be mixed so that deleterious effects of one fuel are neutralized by compounds from another fuel.

5.2 EFFECTS OF CHLORINE IN COMBUSTED WASTES

Bender and Schütze have published a systematic review of the role of major alloying elements on the oxidation behavior of commercial alloys in high temperature chlorine-containing environments [68]. Thermodynamic data were used to develop quasi-stability diagrams for M-O-Cl systems at 800°C (1472°F). Protective oxide cannot be expected to form unless the vapor pressure of metal chlorides or oxychlorides is less than 10-4 bar. Higher vapor pressures produce porous and unprotective scales. Theoretical calculations suggest that Al, Cr, Fe and Si will form protective scales in air containing 0.1% Cl_2. Even if the air contained 2% Cl_2, Al and Si would be expected to form protective scales. Preoxidation to form Al_2O_3, Cr_2O_3 and SiO_2 should resist air containing 2% Cl_2 according to these thermodynamic calculations, provided the oxides do not crack or spall. Because of the volatility of molybdenum oxides and oxychlorides, alloys containing tens of percent of Mo suffered severe attack even in 0.1% Cl_2. Because of the volatility of MoO_2Cl_2, even small alloying additions of Mo produced high corrosion rates at 800°C (1472°F). The authors noted that, because the alloys tested did not contain sufficient Si to form a continuous SiO_2 scale, their Si additions were not beneficial. By far the most corrosion-resistant alloy in Bender and Schütze's high temperature tests was Alloy 602CA (Ni-24Cr-2Al-TiYZr).

To better understand the role of chlorine in the corrosion of waste incinerators burning PVC or power plants burning chloride-bearing coals, Zahs, Spieggel and Grabke compared the corrosion resistance of iron, chromium and nickel in chloridizing and oxidizing environments at 400-700°C, using thermogravimetry and metallography [57]. Their report includes a useful review of the Fe-O_2-Cl_2, Cr-O_2-Cl_2 and Ni-O_2-Cl_2 systems. From their laboratory results, they concluded that, at temperatures above 500°C, the predominant corrosion process was "active oxidation", in which metal chlorides form at the alloy/oxide interface. In the active corrosion mechanism, these chlorides volatilize and diffuse outwards though the corrosion scale until the oxygen partial pressure is high enough to convert them into oxides. Iron is corroded most rapidly, partly because iron reacts very strongly with chlorine and partly because iron chloride has a very high vapor pressure. When iron or chromium is exposed, essentially all the metal chlorides are converted to metal oxides. However, because nickel

chloride is thermodynamically more stable than nickel oxide, significant evaporation of unreacted nickel chloride produces mass loss which produces rectilinear corrosion kinetics at high temperatures. Oxides formed on chromium tended to spall much more than oxides formed on iron or nickel. The formation of multilayered, porous and unprotective oxides on iron-chromium alloys was attributed to oxidation of volatilized chloride environments. The results indicate that additional alloying elements are required for resistance in oxidizing environments that contain chlorine. Fe-Cr-Si alloys show promise in this regard. Nickel-based alloys have the advantage that nickel is relatively inert in these environments. As the iron and chromium additions reacted with chlorides, the nickel concentration increased at the alloy/oxide interface. The best performing alloys, in terms of mass change, were Alloys 825 and 600. AES analysis of fractured samples showed that even at 600°C, there is no preferential diffusion of chromium in the alloy grain boundaries.

5.3 EFFECTS OF ZINC AND LEAD IN COMBUSTED WASTES

Spiegel has reviewed corrosion failures in German waste incineration plants [55]. He notes that about 23% of Western Europe's waste is currently burned in about 600 plants. The ash deposits on tubes from waste-fired boilers contained significant quantities of molten phases such as sulfates of calcium, potassium and sodium and/or chlorides of potassium and sodium. These deposits also contained low melting temperature heavy metals such as lead and zinc. The presence of lead and zinc from demolition wood substantially depresses the FMT of the deposits and produces rapid corrosion on low alloy tube materials. Thermodynamic analysis showed that gaseous HCl will convert $ZnSO_4$ and $PbSO_4$ to volatile chlorides at temperatures of 400°C (752°F) and above even in relatively high partial pressures of SO_2. These volatile chlorides condense on fly ash particles and on steam-cooled superheater tubes surfaces, forming molten or sticky deposits such as KCl-$ZnCl_2$ eutectics. Experiments with a T-22 type alloy showed that the heavy metal chlorides fluxed the otherwise protective oxides. The higher chromium content in Alloy AC-66 reduced its corrosion rate at 600°C by forming insoluble $PbCrO_4$ and $ZnCr_2O_4$, accompanied by significant inward growth of spinels and metal chlorides. At 500°C the corrosion rate of AC-66 was much lower – only two or three times higher than in a purely oxidizing environment.

A very different understanding of the corrosion mechanism was proposed by Otero and others [59] after using electrochemical test techniques to study the corrosion of Incoloy 800 in a molten eutectic of 52% $PbCl_2$-48% KCl chosen to simulate a waste incineration environment. The authors detected evidence that molten lead had been present on the alloy surface, and concluded that it had formed at cathodic sites on the alloy surface by the reduction of Pb^{2+} ions in the eutectic. Additions of carbon to the molten salt reduced the corrosion rate. This was attributed to the carbon's role in facilitating the enhanced reduction of Pb^{2+} at the alloy/molten salt interface. Unlike the Incoloy 800, a 12CrMoV alloy studied previously [63] showed a corrosion rate that did not decrease with time, indicating the absence of a thickening barrier film between the alloy and the molten salt. Increases in corrosion rate with temperature were attributed to reduction in the viscosity of the molten salt that reduced the polarization of the anodic and/or cathodic reactions.

Returning to more conventional research, Li, Niu and Wu [60] described laboratory studies of the corrosion of several Fe-based alloys and of pure Fe, Cr and Ni at 450 °C (842°F) beneath $ZnCl_2$-KCl deposits in flowing O_2. Alloys tested included carbon steel, a 5CrMo steel, P91, Type 310 stainless steel and Kubota Alloy HP (Fe-26Cr-35Ni-1Si). 25-hour tests showed very little oxidation in pure oxygen alone. However, adding a 55/45 (mole fraction) mixture of $ZnCl_2$/KCl produced accelerated corrosion on all the alloys, that was associated with the formation of thick and porous oxides. Chlorine was always enriched at the alloy/scale interface. Alloys containing more Ni had greater corrosion resistance, while alloys containing more Cr produced less-adherent corrosion products.

Chromium carbides within the HP alloy were attacked more than the alloy matrix. The melting temperature of the $ZnCl_2$/KCl salt mixture was only 250°C (482°F). The authors suggested that molten salt first fluxed the oxide (i.e. reacted with Cr_2O_3 to form $ZnCr_2O_4$ and $FeCl_2$. The $FeCl_2$ migrated outward towards the higher oxygen partial pressures at the salt/gas interface, where it reacted to form $Fe2O_3$ and to release Cl_2. The Cl_2 could then penetrate back through the porous oxide to form more metal chlorides at the alloy surface, continuing the active oxidation cycle. The authors noted that $ZnCl_2$ was also significantly volatile. Consumption of the $ZnCl_2$ in the molten salt eutectic - either by volatilization or by $ZnCr_2O_4$ formation – could raise the FMT above the experimental temperature. Thus, unless $ZnCl_2$ were continuously resupplied to the tube deposit by zinc-bearing fuels, KCl would gradually replace $ZnCl_2$ in the salt mixture, raise the FMT and slow the corrosion reaction.

Later studies by Li and Spiegel [58] in similar test environments at 400 to 450°C (752 to 842°F) showed that the corrosion resistance of a series of alloys increased with increasing Al content in Fe-10 to 45%Al and in Ni-Al alloys. The alloy that showed the least mass loss was a 50Ni50Al alloy. Al-free materials corroded by an oxide fluxing mechanism. The authors concluded that, in alloys of intermediate Al content, $ZnCl_2$ reacted with Al in the alloy to form volatile $AlCl_3$ (melting temperature 178°C (352°F)) and metallic Zn. In alloys containing 45% Al, the released metallic Zn reacted with Al-rich alloy surface to form an Al-Zn eutectic.

Related corrosion studies by Ruh and Spiegel [54] investigated the corrosion of Fe, Ni and Cr beneath a eutectic mixture of 50% KCl, 50% $ZnCl_2$. Iron chloride is soluble in the eutectic, so $FeCl_2$ diffuses through the molten deposit to be oxidized at the deposit/gas interface in the active oxidation cycle. In contrast, nickel and chromium have very limited solubility in the molten eutectic. Because chromium dissolves in the melt as chromate, additional studies of the effects of gases like HCl and water vapor on the solubility of the metals are under way. It would appear that waterwall tube and superheater tube materials for boilers burning fuels that can contain zinc should not rely on chromium to form protective oxides, but aluminum or silicon instead [54].

Later work by Pan, Zeng and Niu [61] studied the corrosion of 9% and 11% Cr steels and Type 304 stainless steel under $ZnCl_2$-KCl deposits at 400-500°C (752-932°F) in a CO_2-2%H_2-0.5%HCl gas mixture with and without additions of 0.005% H_2S. The addition of H_2S increased the corrosion rate on all three alloys, producing scales that were more porous and less adherent. Sulfides and chlorides tended to accumulate at the metal/scale interface. Although higher chromium contents increased the corrosion resistance of the tested alloys, even Type 304 stainless steel was unable to form a protective layer of Cr_2O_3 in this environment. The failure to form a protective oxide allowed active oxidation to begin. Pan, Zeng and Niu noted that HCl+H_2S environments are more corrosive than the more widely studied HCl + SO_2 environments that convert alkali metal chlorides to higher melting temperature alkali sulfates.

In later work, Lu, Pan, Zhang and Niu [56] studied a wider range of alloys in the same test environment. Although the corrosion resistance generally increased with the Cr content of the alloy, even Type 304 stainless steel did not show acceptable corrosion resistance under a $ZnCl_2$-KCl deposit at temperatures between 400 and 500°C (752 and 932°F). Chlorine-rich species close to the alloy/scale interface indicated the absence of a protective oxide.

Bankiewicz, Yrjas and Hupa studied the performance of T-22, Type 347 stainless steel and Sanicro 28 in synthetic salt mixtures simulating deposits in furnaces burning wastes containing zinc (K_2SO_4, K_2SO_4-KCl and K_2SO_4-$ZnCl_2$). The FMT of the K_2SO_4-$ZnCl_2$ salt mixtures was about 400°C (752°F) and the tests were made at temperatures between 350 and 500°C (662 and 932°F) [15]. Scale

formation on Sanicro 28 was slow except at 600 °C (1112°F). Oxide thicknesses on Type 347 and Sanicro 28 at 600° (1112°F) ranged from about 12-30 µm (0.0005-0.001") after a one-week test. Tests in chloride salts produced an accumulation of chlorine species at the alloy/scale interface, indicating an active oxidation mechanism, and pitting attack on Sanicro 28.

5.4 CORROSION MONITORING IN WASTE-TO-ENERGY PLANTS

Waldmann, and others [64], described an on-line probe used to monitor corrosion rates on superheater tubes in waste-to-energy plants. This probe consists of a water-cooled support lance made from a nickel based superalloy with an air-cooled head. The head is composed of a series of sample rings separated by ceramic washers. The polarization resistance of each sample ring was monitored continuously. After the tests, which could last for several months, the rings were removed for metallographic analysis. Sample temperatures could range from 50°C below the flue gas temperature to several hundred degrees below the flue gas temperature. Electrochemical measurements were calibrated using either tube wall thickness or the weight loss of a special control ring. The data were also plotted as iso-corrosion lines in a three dimensional plot of corrosion rate versus tube surface temperature versus flue gas temperature. Scatter in the data was attributed to variables like fuel composition, combustion control and plant design. Nevertheless, combining the conclusions from the three-dimensional plots with calculated activation energies for the corrosion reactions correctly predicted that increased superheater temperatures would cause more of an increase in corrosion rate in one of the test boilers than in the other.

5.5 EFFECTS ON CORROSION OF CO-FIRING TIRE-DERIVED FUEL WITH COAL

The US discards about 300,000,000 tires (about one per person) each year. About half of them are burned, usually as a shredded or chipped material from which most of the steel belt reinforcing wire has been removed. About half of this Tire-Derived Fuel (TDF) is burned in cement kilns, and the rest is burned at pulp and paper mills, coal-fired power plants and waste incinerators. The energy content of TDF is high and comparable to that of heavy petroleum fuel oil. It begins to burn at about 315°C (600°F) and combustion is rapidly completed at about 650°C (1200°F). Zinc oxide is used in tire manufacture and lead in TDF ash may originate from automobile wheel balance weights included with tire scrap.

The review of chlorine corrosion in boiler fuels by Tillman, Duong, Figueroa and Miller [13] notes that previous DOE-sponsored research reported trials of TDF as an opportunistic fuel at Allegheny Energy Supply's Willow Island Generating Station. Adding TDF to coal increased the heat content of the fuel and reduced its moisture content. The co-fired mixture contained less sulfur than 100% coal, and its ash contained high concentrations of zinc that produced deposits with very low melting temperatures (see Section 5.3 above). Environmentalists have raised concerns about dioxin formation from TDF combustion, but an EPA study of flue gases produced by tire incineration concluded that, with the exception of zinc-based particulates, there were no significant increases in air emissions when tires were substituted for coal and that some other problematic emissions e.g. Hg were reduced when TDF was substituted for coal.

5.6 SUMMARY

In the absence of national policies to burn wastes, fewer than 100 waste-to-energy boilers operate in the US. Research, primarily in Europe, shows that the corrosion issues in waste-fired boilers are similar to those in biofuel boilers. Most corrosion and fouling problems arise from chlorine and

alkali metals in the waste fuel. Particular problems are introduced when burning waste wood, because zinc from galvanized metal and paint primers and lead from old paint form deposits with unusually low melting temperatures. Wastes are often fired with cleaner fuels like coal to minimize corrosion problems. Corrosion control technologies used in waste-fired boilers include the extension of the boiler passage between the furnace and the superheater, a low temperature tube bank of tubes immediately upstream of the superheater to collect chloride deposits at lower temperatures where corrosion rates are manageable, and the use of additives to eliminate problem deposits.

6. CORROSION IN SUPERHEATERS OF BOILERS BURNING AGRICULTURAL BIOMASS, ESPECIALLY NEAR AND ABOVE THE FIRST MELTING TEMPERATURE

6.1 POLICY ISSUES DRIVING THE USE OF BIOMASS FUELS

Europe's adoption of the Kyoto protocol led to the European Union (EU) Biomass Action Plan, published on December 7, 2005. This proposed measures to more than double the EU's biomass use by 2010, while respecting environmental limits. The plan would reduce oil imports by 8%, eliminate greenhouse gas emissions worth 209 million tons of CO_2-equivalent per year and create up to 300,000 new jobs in the agricultural and forestry sector.

Eighteen months later, the EU's energy ministers launched a Biomass Fuels Technology Program to focus on R&D both to support second generation biomass fuels, bio-refineries and efficient boiler technologies and to ensure the smooth operation of European and global energy markets. EU member states choose the sectors in which they will promote biomass combustion (e.g. electricity generation, energy for heating or cooling, or biomass fuels for transportation), and establish incentives and penalties to achieve them.

Coda Zabetta [102] has reviewed the operational challenges of burning biomass fuels ranging from wood pellets to demolition wood, eucalyptus bark, straw, rapeseed residues (with limestone additives), sunflower residues, rice husks, bio-sludge and meat and bone meal. Eucalyptus bark, meat and bone meal and rapeseed residues introduce the highest concentrations of chlorine. Coda Zabetta also described the design of many recent boilers designed to fire biomass.

Denmark has been a leader in the use of biomass to generate power [102]. Montgomery, Sander and Larsen have summarized Danish experience with straw-firing [45]. Three CHP grate-fired plants firing 100% straw were built as early as the late 1980's [102]. To avoid aggressive corrosion, their steam temperatures were limited to 425-450°C (797 to 842°F). In the early 1990's the Danish government pledged to reduce CO_2 emissions by 20% below 1988 concentrations and supported a substantial program of research [45]. The support of this research has gradually been transferred to electricity and heat consumers. These programs optimized the design and materials of grate-fired boilers and promoted additional biomass usage by studying the co-firing of straw with fossil fuels. The boilers co-firing coal and straw did not experience corrosion of Type 347 stainless steel superheater tubes if the straw content of the fuel remained less than 10%. However co-firing wood with coal is more common than co-firing coal with non-woody biomass. Larger substitution of wood pellets for coal is used in older boilers with relatively low steam temperatures and pressures so as to avoid fouling and corrosion in their superheaters [102]. Selective catalyst reduction (SCR) systems were added to reduce NO_x emissions. Additions of ammonia reacted with the NO_x within a catalyst bed to form nitrogen and water. A 1993 Danish law required the larger power plants to burn 1.4 million tons of biomass per year, including at least a million tons of straw. By 2009, 8 straw-fired and one wood-fired boiler were operating in Denmark [30]. Denmark operates one of the most efficient power plants in the world at Avedøre, south of Copenhagen. While Avedøre Unit 1 primarily burns coal, its Unit 2 can burn natural gas, oil, straw and wood pellets. By simultaneously generating heat and electricity, Unit 2 extracts as much as 94% of the energy in the fuels with an electrical efficiency of 49%, making it one of the most efficient in the world. We will discuss other aspects of this unit in sections 6.4.2 and 6.7.

Swedish regulations governing the emission of NO_x and NH_3 are some of the strictest in the world. To meet these regulations, a 59 MWe boiler at Västerås injects limestone in the furnace to limit SO_x, injects ammonia in the separator to reduce NO_x emissions and uses a catalyst in the back pass to limit

NH_3 emissions [102]. At Södertälje, a 73 MWe boiler, which also provides 219MW of district heating, operates at 90 bars (1305 psi) and 540°C (1004°F). This unit is designed to fire up to 70% demolition wood with clean wood residues and REF pellets[23]. To avoid fouling and corrosion the unit has:

- Its final superheater located in the recirculated fluidizing medium, rather than in the flue gas environment of the convective pass.
- Easily replaceable superheaters
- An empty pass to increase residence time for the flue gases to cool and clean themselves before reaching the convective superheaters
- Water cannons to clean deposits from the empty pass and spring hammers to remove deposits from the convective superheaters
- Use of a stoker grate for more reliable and stable feeding of inhomogeneous fuels
- Systems to add sulfur granules to raise the FMT of the superheater ash

One major UK utility (E.ON) stated its intention to reduce its CO_2 emissions by 50% from 1990 levels by 2030 [127]. Diverting wood waste from landfills to power stations would have a substantial impact on greenhouse gases, particularly by reducing methane generation.

6.2 CHARACTERISTICS OF BIOMASS FUELS

Most biomass fuels have a high volatility, a heating value about one third that of coal and a relatively low sulfur content [69]. Hiltunen, Barišić and Coda Zabetta [103] suggested that, in order to understand the issues arising from their combustion, potential biomass fuels should be classified into one of three categories on the basis of the ash they form. These categories are:

Group 1: Biomass rich in Ca and K but lean in Si
Group 2: Biomass rich in Si but lean in Ca and K
Group 3: Biomass rich in Ca, K and P

Most woody fuels belong to Group 1. Examples of Group 2 fuels include herbaceous and agricultural fuels like rice husk, bagasse and spring-harvested reed canary grass. Group 3 fuels include sunflower seed and rapeseed cakes.

Wood ash (Group 1) starts to agglomerate and sinter at temperatures between 900 and 1000°C (1652 and 1832°F). Coal and peat ashes are generally trouble-free at these temperatures, even if their FMT is as low as that of biomass fuels. Although the coal ashes are typically high in Al, Ca, alkali silicates and iron oxides, their Ca and alkali content is not in a reactive from. Because woody biomass fuels produce much more reactive ashes, Hiltunen, Barišić and Coda Zabetta recommend that the hottest superheater tubes in biomass boilers should be removed from the corrosive environment into the milder environment of the loop seal.

23 REF (recovered fuel usually refers to the segregated high calorific fraction of processed municipal solid waste (MSW). Other terms used for MSW derived fuels include Solid Recovered Fuel, (SRF), formerly called Refuse Derived Fuel (RDF), Packaging Derived Fuel (PDF) and Paper and Plastic Fraction (PPF).

Group 2 fuels show diverse combustion properties and chemical compositions. Some, like straws or cereals, have high K and Cl contents that can be reduced by washing the fuel (see Section 6.6). Ashes from rice husk or bagasse combustion contain high concentrations of SiO_2. Ash from straw or cereal combustion softens at temperatures below 1000°C (1832°F) and may be completely molten at 1200°C (2192°F). This produced bed agglomeration and causes corrosion in conventional superheaters[24].

Ash produced by the combustion of Type 3 fuels melts at temperatures between 700 and 1200°C (1292 and 2192°F), so these fuels cause severe fouling. However, moderate concentrations can be co-fired with coal in CFB boilers and there are indications that they can be burned in CFB boilers with Ca-rich additives such as limestone [103].

Johansson and others [70] agree that the corrosivity of the fireside environment arises from the release of HCl, alkali salts and water vapor with high concentrations of water vapor and oxygen (table 1). They summarized the concentrations of these aggressive components in coal, biomass and municipal wastes in the table reproduced below. Most corrosion problems arise from the release of alkali salts and chlorine-containing gases during combustion processes. The high concentrations of low melting temperature alkali salts in biomass and waste-fired boilers force operators to reduce the maximum steam temperature in the units in order to prevent unacceptable rates of corrosion.

Table 1. Fireside environments and steam temperatures in modern boilers burning biomass, coal and municipal waste

Condition	Biomass	Coal	Municipal waste
$[O_2]$	~5%	~1%	~5%
$[H_2O]$	20-25%	~10%	20-25%
Reactive alkali	High	Low	High
p_{SO2}	Low	High	Low
P_{HCl}	Low	High	High
Maximum steam temperature	~500°C (~932°F)	550-600°C (1022-1112°F)	400-450°C (752-842°F)

6.3 EVALUATING BIOMATERIALS AS BOILER FUELS

6.3.1 Wood Products as Biomass Fuels

Test by Henderson and others [91] in the 540°C (1004°F) CHP unit that fires demolition wood and forest residues in Nyköping and the 98MW, 480°C (896°F) steam, bark-fired boiler at Munksund have concluded that conventional superheater steels must be replaced after about four years' service when burning 100% wood fuels with steam temperatures above 480°C (896°F).

Wood products are some of the most attractive biomass fuels because their combustion produces less fouling and corrosion and generates less ash than most other biomass. However, because they take longer to grow, wood fuels may be more expensive than Group 2 energy crops (grasses and straw). Valmari and others [5] have studied ash deposits formed during the combustion of forest residues and willow in a 35 MW CFB co-generation plant. They analyzed ash deposits collected downstream of the cyclone that removes the fluidizing medium and collected inorganic vapors and fly ash particles

24 i.e. superheaters located in the convective path and exposed to the flue gases.

on filters [5]. When forest wastes were being burned, 80% of the sulfur had already reacted with ash particles larger than 1 micron in diameter by the time the flue gases left the cyclone at 810−850 °C. As a consequence, alkali sulfate particles were not produced in significant quantities during the combustion of forest residues. However, when willow was burned, about half the sulfur was still unreacted SO_2 and half was in alkali sulfate particles when the gasses left the cyclone. Sampling of flue gases at 810-850°C (1,490-1,562°F) showed that chlorine was present as gaseous species (presumed by the authors to be KCl and HCl) with both fuels.

The second part of Valmari's study [129] studied the fate of the fly ash particles. Between soot blowing operations, 70 +/-10% of the fly ash deposited on the heat exchanger surfaces in the convective back pass (i.e. on the superheater tubes). Almost all the particles larger than 10µm were deposited on the tubes, but almost all the particles smaller than 3µm passed through the superheater without depositing. This is consistent with the observations of Backman, Hupa and Skrifvars [116]. The probability of deposition was independent of the particle composition. About half the alkali chloride vapors (KCl + NaCl) condensed onto fly ash particles smaller than 0.6µm and about half condensed onto larger particles. Alkali chloride concentrations in the largest fly ash particles (>10µm) were lower, suggesting that rates of penetration were relatively slow.

6.3.2 Straw as a Biomass Fuel

Early work in Denmark [14] showed that rates of ash deposition when burning wheat and barley straws correlated with the potassium concentration in the straws. However, Jensen, Stenholm and Hald observed that deposition rates on both furnace tubes and superheater tubes changed substantially as individual straw bales were combusted in 23 and 31 MW straw-fired power plants.

Nielsen, Frandsen and Dam-Johansen [10] described more detailed laboratory tests simulating superheater conditions in straw-fired boilers. A 12% Cr boiler tube steel (X-20) and Type 347HFG stainless steel were covered with synthetic (KCl-K_2SO_4) or boiler deposits and exposed to a synthetic fuel gas (N_2-6%O_2-12%CO_2-400ppmHCl-60ppmSO_2) at 550°C (1,022°F). The dense outer layer of the deposit consisted of threads of iron oxide in a potassium sulfate matrix. The corrosion products consisted mainly of iron and chromium oxides. All test specimens covered with KCl suffered minor internal corrosion and some had chloride-filled pits. The corrosion mechanism proposed by Nielsen, Frandsen and Dam-Johansen [10] involves attack by gaseous chlorine coupled with rapid sulfation of KCl to K_2SO_4 in a melt of KCl, K_2SO_4 and iron compounds adjacent to the metal. Chlorine corrosion mechanisms in biofuel combustion will be discussed in more detail in Section 6.5.

Montgomery, Carlsen, Biede and Larsen [49] installed three test loops in the superheaters of the Masnedø straw-fired CHP plant to investigate the corrosion resistance of candidate alloys at higher temperatures than those experienced in the boiler. The steam flow in the test loops was controlled independently of that in the main superheaters to obtain an outlet temperature of 585°C (1,085°F). The alloys in the test loops (fine- and coarse-grained Type 347 stainless steel and an Fe-17Cr-13Ni alloy) had chromium contents ranging from 12% to 22%. All three alloys showed similar corrosion rates. Corrosion began at surface grain boundaries and continued as internal oxidation of Cr at the grain boundaries and within the grains. Where the chromium-rich oxide failed, the remaining alloying elements appeared in the scale. The authors attribute the corrosion primarily to active oxidation caused by chlorine-containing species.

Tubes adjacent to the welds joining the test sections of tubes showed apparent galvanic corrosion. This corrosion was beside welds made with Alloy 625 filler and was more severe on Type 347H stainless steel than on 18/8-type alloys. Montgomery noted that Kawahara had found similar

corrosion adjacent to Alloy 625 welds only when a temperature gradient existed between the alloy substrate and the flue gas[25]. Montgomery concluded that the electrolyte supporting this galvanic corrosion could have been a eutectic mixture of potassium chloride and iron chloride, possibly also containing nickel chloride [49].

Montgomery and others published a series of seven reports about the corrosion studies at Masnedø [97]. Corrosion profiles around the circumference of tube samples cut out of the test superheaters were evaluated using data collected by automated image analysis. Variations in these corrosion profiles were interpreted in terms of variations in flue gas flow and deposition patterns. Because rates of oxide formation on the inside (steam side) of Type 347H stainless steel tubes followed a parabolic rate law, steam side oxide thicknesses were used to estimate the local tube temperature and therefore the heat-flux distribution along test tubes.

Later studies by Jensen and others [9] noted that straw burned in small-scale CHP grate boilers in Denmark produces more rapid deposition and more severe corrosion than coal combustion. Jensen collected superheater deposits from straw-fired boilers at Masnedø and Ensted. The Masnedø unit had a relatively large superheater with a final steam temperature of 520°C (968°F) but did not use soot blowing in this superheater. Ensted had a final steam temperature of 470°C (878°F) but used an external wood-fired superheater to obtain a final steam temperature of 542°C (1008°F). Mature superheater deposits from Masnedø were from 2 to 15 centimeter (cm) (3/4" to 6") thick and consisted of three layers. The innermost layer contained iron oxide, KCl, and K_2SO_4. The intermediate layer was depleted in chlorine but rich in Si, K, and Ca. The authors concluded that this was formed by reactions between KCl and silica-rich particles that released chlorine-containing gases. The Ensted deposits had a maximum thickness of a few centimeters. The intermediate layer consisted of melted KCl with Ca- and Si-rich inclusions over an inner layer of iron oxides and a potassium sulfate layer. The inner layers of pure KCl and K_2SO_4 in mature deposits were thicker and denser than samples collected during brief exposures of deposit probes. The authors concluded that the innermost layer of the deposit expanded by accumulation of KCl (producing active corrosion), even when the deposit had a thickness of several centimeters.

Frandsen [82] described full-scale analysis campaigns to understand the combustion chemistry in different types of boilers. Laboratory studies were used to clarify mechanisms of deposit sulfation and tube corrosion. Deposit formation reactions were studied in the Sandia multi-fuel combustor. Straw firing produced bottom ash deposits of K and K-Ca silicates. In the superheater area K deposited primarily as KCl unless the fuel contained large quantities of sulfur that increased the fraction of K_2SO_4 in the deposits. Superheater deposits contained an inner layer of KCl or K_2SO_4, under iron oxide. The appearance of the innermost KCl deposits suggested they had been molten. Frandsen suggested that the sulfation reactions accelerated when these deposits melted. The release of Cl_2/HCl could then cause active oxidation. Deposits formed when co-combusting 20% straw (energy basis) in coal did not contain Cl.

Related later work from Frandsen's group [23] reported the melting properties of ash fractions collected from a pilot-scale pulverized fuel boiler operated with a range of coal/straw fuel blends. Increased fractions of straw reduced the viscosity of the ash (presumably because of KCl accumulation), increasing the stickiness of the ash at low temperatures and increasing its tendency to cause corrosion.

Paul Kilgallon, Nigel Simms and John Oakey collected data on composition ranges measured in

25 Montgomery cited this work as: Y. Kawahara, M. Kira and M. Ike, Science Reviews: High temperature corrosion and protection 2000, p627, but I have not been able to find the complete reference.

wheat straw and in British coal [109]. They showed that mixing 20% straw with wood or with coal produced gas compositions well within the ranges predicted for firing different coals. Corrosion rates anticipated for these dilute mixtures of biomass in coal were therefore expected to be similar to those observed for firing 100% coal or 100% wood.

Later tests in Danish plants reported by Montgomery, Jensen, Hansson, Biede and Vilhelmsen [30] were made by installing test sections of tubes in the superheaters of the straw-fired CHP boilers at Maribo Saskøbing and Avedøre 2. Their installation was similar to that of the test superheaters at Masnedø described above [49]. Detailed information about temperatures in both the test sections and other parts of the superheater was collected using thermocouples. Tube samples removed from the boilers were covered with deposits of KCl, K_2SO_4 and some iron oxide. Such oxides as remained on the tube surfaces were porous and spalled easily. The outer portion was an iron-rich oxide. The inner portion was an iron-chromium-rich oxide. Chromium was preferentially attacked where it was accessible at grain boundaries in the tube surface. The authors concluded that the overall corrosion reaction was active oxidation. Welds made with matching filler showed some selective attack of chromium and some preferential attack adjacent to welds that was attributed to galvanic corrosion in a low melting temperature mixture of alkali chlorides with metal chlorides or oxychlorides (as in [49]). Tube thickness data were used to project the average worst case tube thickness loss after 100,000 hours (11.5 years) service in the No. 3 and No. 2 superheaters at Maribø as about 3.9 mm and 1.25 mm (0.15" and 0.05") respectively. The higher of these thickness losses represents an annualized thinning rate of Type 347H tubes of 0.34mm per year (0.013" per year). Montgomery, Jensen, Hansson, Biede and Vilhelmsen concluded that such corrosion rates would be tolerable.

Thermography [30] at Maribø showed that superheater tube surface temperatures increased substantially when the tubes were covered with deposits. Deposits with surface temperatures above 950°C (1,742°F) were seen to have molten deposits running off them. Similar observations have been made in the Avedøre 2 unit.

Because the insulating deposits made it difficult to clarify relationships between tube temperature, flue gas temperature and corrosion rate, calculations were made to estimate the increase of tube temperature produced by increasing heat flux [30]. These showed that increasing heat flux due to locally high flue gas temperatures produced very little increase in the surface metal temperature. For example, in the Maribø superheater 3, a doubling of heat flux from 6,800 to 12,200 w/m^2 produced an estimated temperature increase of only 6°C (11°F). However, both the Maribø and Avedøre superheaters showed high corrosion rates where there was the highest heat flux. The authors noted that effects of increased flue gas temperature are complex, because they can simultaneously affect the thickness, composition and morphology of the deposit and the degree of deposit sulfation. This is consistent with results from several other research groups who have shown that temperature gradients increase corrosion rates at constant tube temperature, as discussed in Section 4.3.1.

As in the earlier studies at Masnedø [97] the steam side oxidation at Maribø followed a parabolic growth curve, so the steam side oxide thickness provided an in-place estimate of the tube temperature [30]. However, extrapolations of these thicknesses indicate that steam side oxides could be thick enough to spall before a 100,000 hour service life is reached. Spalled oxides can block tubes and damage turbines.

6.3.3 Rice Husk as a Biomass Fuel

Skrifvars and others have reported the fouling behavior of rice husk fuels in fluidized bed combustion in a series of two papers [77, 17]. Rice husk can be considered an opportunity fuel, but is rarely used

as a primary fuel. It produces millimeter-sized ash particles that are almost pure silica with a few percent of potassium. The FMT of this ash is very high. Short term (3-10 hour) exposures of deposit probes were made in the superheater of a large (157MW) fluidized bed BFB burning rice husks and eucalyptus bark and systematic studies of the relationship between the fuel mixture ratio and the fouling tendency of the fly ash were made in an entrained flow reactor. Burning only rice husks produced no fouling in either the boiler or the entrained flow reactor. Burning eucalyptus bark alone caused significant fouling. The fouling tendency of mixtures of the two fuels showed a non-linear dependence on the mixture ratio, suggesting that the rice ash had an erosive, cleaning action on the fly ash mix.

6.3.4 Salix as a Biomass Fuel

Skrifvars and others [25] reported a detailed study of the potential for agglomeration, fouling and slagging problems that might arise if Swedish willow (*Salix viminalis*), a fast-growing energy crop, was burned in a 12MW circulating fluidized bed boiler. Bed agglomeration and fouling documented during the full-scale testing were interpreted in light of thermodynamic equilibrium calculations of stable species and melting temperatures.

6.3.5 Rapeseed as a Biomass Fuel

Studies of the fate of alkali metals and phosphorus during the co-combustion of Group 3 fuel rapeseed cake were recently described by Piotrowska and others [130,157]. When co-combusted with wood chips and pellets in a 12 MW boiler [130], the rapeseed fuel caused agglomeration of the fluidizing material and fouling of the superheaters. These problems were attributed to the high concentration of P-rich phytic acid and alkali salts in the fuel. Gaseous K vapors attacked silicate bed particles on the bed surface, and the sticky silicates attracted ash particles rich in P. Deposits enriched in K, Na and P also built up on the windward side of a test probe. When limestone was added to the boiler, calcium silicate formation was suppressed but P was retained in the bed, probably because it formed high melting temperature $Ca_3(PO_4)_2$. Limestone additions also increased the KCl concentration upstream of the convection pass and decreased the P concentration in the fly ash.

6.3.6 Uncommon Biomass Fuels

Capablo [4] compared ash deposits produced by firing uncommon biomass wastes such as pectin waste, mash from a beer brewery and waste from cigarette production with ash deposits from wood and straw firing. Ash behavior was studied during suspension firing in an entrained flow reactor and in a burner rig. Results were interpreted using thermodynamic equilibrium calculations and the ash properties were classified according to a sequential analysis. The fuels were divided into three groups according to the content of silica, alkali metals and calcium and magnesium in their ash (comparable to the classification in Section 6.2). The classification was refined by measuring the molar ratio of Cl, S and P to alkali. The influence of the fuel ash composition on ash transformation rates, ash deposit flux and deposit chlorine content can be gauged from these classifications.

6.4 CO-FIRING BIOMASS WITH OTHER FUELS

Co-firing biomass fuels with coal can reduce the fouling problems associated with biomass burning. Pilot studies by Robinson, Junker and Baxter [19] showed that co-firing biomass with coal reduced the ash deposition rates from the high values characteristic of biomass fuels towards those of coal. The primary interaction between the biomass and the coal was the sulfation of alkali species released by the biomass by sulfur released by the coal. This had two consequences. The sulfation reduced ash

deposition rates by raising the melting temperature of the ash deposits and making them less sticky. Sulfation also reduced the chlorine content of the deposits, again making make them less corrosive. Krause and others concluded in 1979 [149] that corrosion rates increase significantly when the S/Cl ratio in a boiler fuel falls below 2 and that corrosion was not problematic when the S/Cl ratio exceeded 4. In 2000, Salmenoja and Mäkelä [69] stated that the best way to avoid corrosion when firing biomass was to keep the S/Cl ratio in the fuel greater than 2 and, preferably, greater than 4. In 2002, Robinson, Junker and Baxter [19] concluded that to completely eliminate chlorine from ash deposits, the ratio of sulfur to alkali in the fuel should exceed 5 times the sulfur-to-alkali stoichiometric ratio. Salmenoja and Mäkelä presented the table reproduced as Figure 6 to compare the S/Cl molar ratio in dry biomass fuels with those of coal and wastes.

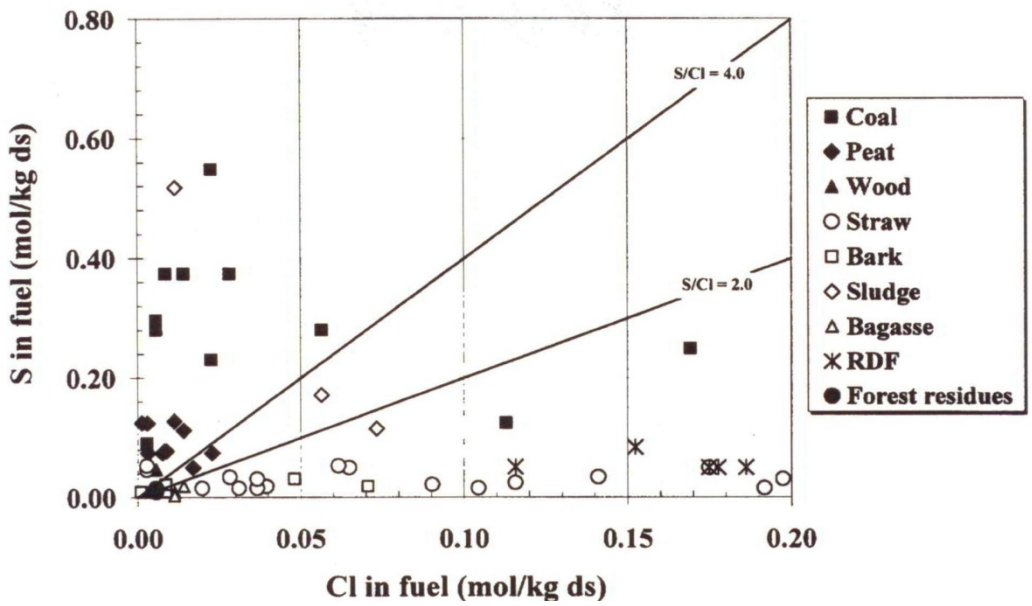

Fig. 6. Sulfur/chlorine ratios in boiler fuels.

The easiest way to achieve this sulfation of low melting temperature chlorides is to blend high sulfur fuels such as oil, peat and coal with the high chloride biomass fuel. Co-firing biomass fuels with coal was reviewed in Section 4.6, above and will not be discussed further here.

6.5 EVALUATING MATERIALS PERFORMANCE IN BIOMASS BOILER SUPERHEATERS

Backman, Hupa and Skrifvars [116] noted that ash deposits formed on biomass boiler superheaters consist mainly of carbonates, sulfates and/or chlorides of calcium, magnesium, potassium and sodium, derived from the fuel. The authors concluded that fouling tendency cannot be estimated from studies of the fuel ash alone. Instead the actual deposits formed during biomass combustion must be studied. Deposit compositions varied with distance from the tube surface. Na and K were concentrated near the tube surface, while calcium concentrations were higher at the outer surface of the deposit. The concentration of chlorides at the tube surface was taken to indicate that they were involved in the early stages of deposit formation.

Backman and his co-authors also studied the large inorganic ash particles that impact boiler tubes in the convective section after being swept along by the flue gases. Unlike these large particles,

submicron particles are transported by diffusion or thermophoresis. In addition, volatile compounds in the flue gas (like alkali chlorides) can condense onto the relatively cool surface of superheater tubes. Backman, Hupa and Skrifvars noted that these processes tend to produce deposits of differing thickness and composition of the windward and leeward sides of superheater tubes.

Salmenoja and Mäkelä published an overview of superheater corrosion in biomass boilers [69]. They identified Cl_2, HCl and alkali chlorides as the most important corrosives. HCl is mainly of concern on furnace wall tubes where the environment can be reducing. The FMTs of superheater tube deposits in the boilers studied ranged as low as 530°C (986°F) and the authors commented that molten phase formation can produce superheater corrosion rates exceeding 10mm/year (nearly 0.4" per year) [150].

Mäkipää, Baxter, Sroda and Oksa have described laboratory methods for evaluating candidate materials for biomass boiler superheaters [78]. Field tests carried out in many operating boilers showed that whenever corrosion occurred, sulfation of the deposits was observed. In short-term tests the Cl/(Na+K) ratio was very high, indicating that most of the alkali salts were chlorides. James and Pinder [148] have also suggested that Cl accumulation at the alloy/scale interface may weaken the scale/alloy bond. In long-term tests, however, this ratio was very small on both the windward and leeward sides of the tubes, indicating that the alkali chloride deposits had reacted to form sulfates. The HCl released in the sulfation reactions was thought to have caused active oxidation [146]. In light of work by Folkeson, Johansson and Svensson [35] showing that corrosion by HCl in the absence of alkali metal chlorides produced metal chlorides throughout the scale but did not show the concentration of chlorides at the scale/metal interface that is characteristic of active oxidation, Mäkipää's conclusion seems doubtful.

Coleman, Simms, Kilgallon and Oakey [96] reported laboratory procedures to assess the corrosion of high temperature tube materials during the combustion of potential biomass fuels. Their study focused on the effects of high K and Cl concentrations released by fast-growing energy crops. 1000-hour tests were carried out at 450-600°C (842-1112°F) with gas compositions and deposits (refreshed by re-coating) selected to simulate biomass combustion. Six alloys were studied: 1% Cr steel, 2.25% Cr steel (T23), 9% Cr steel (T91), 12% Cr steel (X20CrMoV121), Type 347HFG stainless steel and Alloy 625. Corrosion was assessed by thermogravimetry and by dimensional metrology before and after exposure. This experimental approach, also used at Åbo Akademi, E.ON Engineering and elsewhere, involves using automated image analysis to robotically scan the circumference of a tube sample and make statistical analyses of the depth of penetration and the corrosion product thickness. Pre-exposure measurements were made using a micrometer and post-exposure damage was assessed with an automated image analyzer system. The original dimensions of the tube can be measured by sectioning an electroless-nickel-plated ring around the tube sample [147].

Hiltunen, Barišić and Coda Zabetta [103] emphasized that alkali salts, in particularly alkali chlorides, cause superheater corrosion both by lowering the FMT of superheater ash and by releasing chlorine when they are converted to sulfates by reaction with sulfur compounds. The release of chlorine can cause active corrosion on the tubes. Boiler operators typically keep tube temperatures below the FMT of the deposits to avoid the rapid wastage caused by molten deposits.

In 2008, Pinder summarized materials challenges in biomass combustion identified in the MatUK Strategic Research Agenda [127]. This agenda noted the importance of achieving good energy efficiency in biomass combustion. Except in Denmark, conversion efficiencies are generally low and steam temperatures are limited because of fouling and corrosion risks. For example, Pinder pointed out that even the most energy efficient straw-burning plants in Sweden achieve conversion

efficiencies of only about 29% and are restricted to superheater temperatures of 540°C (1004°F) and pressures of 92 bar (1334 psi), compared with current targets for coal-fired plant of 650°C/300bar (1,202°F/4,350psi). He anticipates that Type 347H superheater tubes in a UK straw-fired power station will need to be replaced every 5 years. Reducing the steam temperature by 10°C (18°F) would nearly triple the life of these tubes. Other options being explored are the application of Alloy 625 weld overlay or of other protective coatings to the tubes and the use of anti-corrosion additives containing calcium/phosphorus or sulfur.

6.6 EFFECTS OF BIOMASS CHLORINE ON SUPERHEATER CORROSION MECHANISMS

Ten years of research at Chalmers University of Technology on superheater corrosion caused by chlorine species in biomass-and waste-fired boilers, summarized by Johansson, Skog and others [70, 84], identified two mechanisms as critical to the corrosion of Cr_2O_3-forming alloys. These involve vaporization and fluxing, respectively. High temperatures and rapid gas flow increase rates of evaporation of chromium from the chromium-rich protective oxide on alloy surfaces:

$$Cr_2O_3(solid) + 2H_2O(gas) + 3/2\ O_2(gas) \rightarrow 2CrO_2(OH)_2(gas)$$

The lost chromium may be replenished from the alloy, but if the rate of evaporation exceeds the rate of supply, the Cr_2O_3 scale gives way to an unprotective M_3O_4 spinel beneath an outer layer of Fe_2O_3.

The formation of alkali metal chromates fluxes away the Cr_2O_3 from the oxide surface:

$$Cr_2O_3(s) + 4KCl(s) + 2H_2O(g) + 3/2\ O_2(g) \rightarrow 2K_2CrO_4(s) + 4HCl(g)$$

As with the volatilization of $CrO_2(OH)_2$, the fluxing of Cr_2O_3 by alkali salts leads to the formation of an unprotective $(Fe,Cr)_3O_4$ spinel beneath an outer layer of Fe_2O_3. This allows inward penetration of chlorine-containing gases and accelerated active oxidation of the alloy that forms a sub-scale of $FeCl_2$.

At boiler temperatures even small concentrations of KCl and K_2CO_3 are much more damaging than the oxygen and water vapor environments that promote scale volatilization. Note that K_2SO_4 is much less corrosive than KCl because it does not react with Cr_2O_3 to form K_2CrO_4. This difference in reactivity between KCl and K_2SO_4 forms the basis of many approaches to controlling superheater corrosion by sulfation, i.e. by adding sulfur compounds to convert corrosive potassium chloride to less reactive potassium sulfate:

$$2KCl(solid) + SO_2(gas) + 1/2O_2(gas) + H_2O(gas) \rightarrow K_2SO_4 + 2HCl(gas)$$

Liu, Maier and Hein [1] studied the fireside corrosion kinetics in ashes formed from the combustion of straw, wood or lignite coals in a 0.5 MW pulverized fuel boiler. The test gas environment contained HCl, H_2O, SO_2, O_2 and N_2. Alloys T-24 (: ferritic 2¼Cr), HCM12A (ferritic-martensitic, 12Cr) and NF709 (austenitic 20Cr-25Ni) all showed "active oxidation" beginning as pitting corrosion. Detailed analyses of the corrosion morphologies produced on ferritic, martensitic and austenitic boiler steels were described in a second paper by the same authors [110]. The Cr content of the ferritic steel was too low to offer much protection and the corrosion product was thick and porous. Martensitic steels suffered isolated corrosion that was within alloy grains, while austenitic steels suffered deep grain boundary attack. The authors related this corrosion morphology to the carbide attack. Carbides in the martensitic steel were finely-dispersed, while carbides in the austenitic steel

were segregated to the grain boundaries. Severe grain boundary attack occurred under chlorine-rich deposits at 650°C (1202°F).

Pettersson, Flyg and Viklund [83] describe 960-hour laboratory exposures at 550 and 700°C (1022 and 1292°F) under KCl-K_2SO_4 deposits in synthetic gas mixtures designed to simulate biomass boiler superheaters. The gas environment contained 13% CO_2, 5% O_2, 15% H_2O, 0.02% HCl with the balance nitrogen, as established by the PREWIN European network on performance, reliability and emissions reduction in waste incinerators. The eutectic temperature of the salt mixture was 690°C (1274°F). 2% and 9% Cr steels, Type 304 stainless steel and Alloy 253MA (Fe-21Cr-11Ni-1.6Si-Ce) were evaluated. Alloy 253MA was the best performer, apparently because of the 1.5% Si it contained. Limited formation of metal chloride reaction products was ascribed to the accumulation of SiO_2 in a partial internally-oxidized layer under the corrosion product.

The effects of alkali salt deposits on the initial stages of high temperature corrosion of Type 304L stainless steel in a 12MW CFB research boiler were reported by Pettersson and others at Chalmers University [36]. The base fuel was a mixture of 2/3 wood chips and 1/3 pellets. Superheater deposits formed on a superheater probe during the combustion of this fuel were almost entirely K_2SO_4. When HCl was added to the fuel, KCl deposits were formed and when both HCl and SO_2 were added, a mixture of KCl and K_2SO_4 was formed, simulating the deposits formed by burning biomass. As ash accumulated on the probe surface, the outer surface of the Cr_2O_3 became enriched in potassium (possibly as K_2CrO_4). Although this oxide remained protective and did not contain chlorine, the authors suggested that during longer exposures the protective Cr_2O_3 would react with the KCl deposits to form unprotective K_2CrO_4 and allow active oxidation to begin [36].

Davidsson and others continued this work with a study of the effects of HCl and SO_2 added to a CFB combustor on the composition of deposits, fly ash and flue gas composition [21]. Adding gaseous SO_2 and an aqueous solution of HCl increased both the formation of submicron particles and the rate of deposition of K_2SO_4 and KCl on a deposit probe.

Folkeson, Johansson and Svensson [35] studied the initial effects of adding HCl vapor on the corrosion on Type 310 stainless steel in nitrogen environments containing O_2 and 10 ppm H_2O at 500°C (932°F). This paper is important because it shows that active oxidation, cited as the cause of most biomass superheater corrosion under chloride ash deposits, is not caused by HCl in the absence of alkali salt deposits. Folkeson's addition of 500 ppm of HCl accelerated the oxidation of Type 310 stainless steel. However, the corrosion products formed in these environments that did not contain alkali salts did not show the concentration of chlorides at the scale/metal interface that is characteristic of active oxidation. Instead, metal chlorides were present throughout the scale. Iron chloride was present even at the scale/gas interface, while in active oxidation, chlorides dissociate to oxides at the higher oxygen partial pressures in the outer portion of the scale. In the test environment (5% O_2, 10 ppm H_2O, 500 ppm HCl at 1 bar and 500°C (932°F), the equilibrium partial pressure of Cl_2 would have been 150 x 10^{-6} bar. The formation of elemental chlorine in this environment:

$$2HCl(gas) + \frac{1}{2}O_2(gas) \rightarrow Cl_2(gas) + H_2O(gas)$$

would be slow in the absence of a catalyst. Without a source of chlorine gas to diffuse through the scale and produce conventional active oxidation, the authors proposed other ways in which chloride ions could be produced at the scale/gas interface. Chlorine molecules could dissociate at the scale surface to be reduced to chloride ions by electrons generated by corrosion at the scale/metal interface.

$$Cl_2 + 2e^- \rightarrow 2Cl^-(adsorbed)$$

Alternatively, HCl could be reduced to chloride ions in the presence of oxygen

$$2HCl(adsorbed) + ½\ O_2(adsorbed) + 2e- \rightarrow 2Cl^-(adsorbed) + H_2O(gas)$$

Chloride is not expected to substitute for oxide ions in an iron oxide lattice and chloride ions have limited solubility in iron oxides. Therefore the iron chloride scales are thought to have formed by reaction between inwardly diffusing chloride ions that penetrate the scale by grain boundary diffusion and outwardly diffusing ferrous ions. As the proportion of iron chloride in the scale increases, diffusion rates through it (and hence corrosion rates) would increase. The fact that iron chlorides remain at the scale/gas interface is ascribed to the slow rate of iron chloride decomposition. Iron chlorides have a significant vapor pressure, so vaporization losses make mass change an unreliable measure of corrosion rate.

Thin portions of the scale were mainly chromium oxide. Chromium chlorides were not present because of reaction with hematite:

$$2CrCl_2(solid) + Fe_2O_3 \rightarrow 2FeCl_2(solid) + Cr_2O_3(solid)$$

Above the grain boundaries in the alloy, where the imperfect lattice structure allows more rapid delivery of chromium from the alloy, the $FeCl_2 + Cr_2O_3$ scale forms a healing subscale that is relatively pure Cr_2O_3 under an outer layer of FeCl2 that is being thinned by volatilization.

$$2FeCl_2(gas) + 3/2\ O_2(gas) \rightarrow Fe_2O_3 + 2Cl(gas)$$

J. Pettersson, J-E. Svensson and L-G Johansson [131] showed that the KCl-induced corrosion of Type 304 stainless steel in an O_2-H_2O environment increased rapidly with temperature within the range 400-600°C (752-1112°F). At 600°C (1112°F) the addition of KCl increased the oxide thickness by up to two orders of magnitude [34]. The same authors made a detailed comparison of the corrosion of Type 304 stainless steel by KCl, K_2CO_3 and K_2SO_4 [32]. Short-term thermogravimetric tests in O_2 + H_2O at 600°C (1112°F) showed that KCl and K_2CO_3 both reacted with Cr_2O_3 on the alloy surface to form K_2CrO_4, as follows:

$$½\ Cr_2O_3(solid) + 2KCl(solid) + H_2O(gas) + ¾\ O_2(gas) \rightarrow K_2CrO_4(solid) + 2HCl(gas)$$
$$½\ Cr_2O_3(solid) + K_2CO_3(solid) + ¾\ O_2(gas) \rightarrow K_2CrO_4(solid) + CO_2(gas)$$

The presence of water vapor accelerated the volatilization of Cr_2O_3 as follows:

$$½Cr_2O_3(solid) + H_2O(gas) + ¾O_2(gas) \rightarrow CrO_2(OH)_2(gas)$$

The HCl and $CrO_2(OH)_2$ released by these reactions have significant equilibrium vapor pressures so their removal by flowing gases increases the corrosion rate. Paul, Clark and Eckhardt reported a similar corrosion rate increase when adding 2 v/o of water vapor to a coal-fired combustion environment [121].

After the depletion of Cr_2O_3 by chromate formation or chromic acid volatilization exceeds a critical amount, the protective scale gives way to a thick layer of Fe_2O_3 over an unprotective $(FeCrNi)_3O_4$ spinel. This non-protective oxide can be penetrated by chlorine species that cause further acceleration of the corrosion rate by active oxidation [32].

The formation of K_2CrO_4 did not account for all the chloride and carbonate that was present. The authors attribute the difference to the vaporization of KCl and K_2CO_3. The vaporization of K_2CO_3 produces KOH, which may itself cause corrosion.

$$K_2CO_3(solid) + H_2O(gas) \rightarrow 2KOH(gas) + CO_2(gas)$$

In contrast, K_2SO_4 deposits did not produce K_2CrO_4 and did not significantly accelerate the corrosion of Type 304 stainless steel in $O_2 + H_2O$ at 600°C (1112°F). This is consistent with thermodynamic data showing that the reaction of K_2SO_4 with Cr_2O_3 is not favored.

The authors also noted that K_2SO_4 deposits can contribute to corrosion by forming eutectics. In the systems KCl-K_2SO_4 and K_2CO_3-K_2SO_4 eutectics form at temperatures as low as 658 and 788°C (1216 and 1450°F), respectively.

Later studies with Sandvik 28 [37] showed that like Type 304 stainless steel [32], it formed a protective, chromium-rich oxide in dry oxygen at 600°C (1112°F). However, while the addition of water vapor to the oxygen caused rapid oxidation on Type 304, associated with the vaporization of $CrO_2(OH)_2$, the $O_2 + H_2O$ environment did not accelerate oxidation on Alloy 28. This was attributed to the greater availability of chromium in Sanicro 28. The addition of KCl to this environment by spraying KCl droplets on the alloy surface caused rapid attack on both alloys. Most of the KCl had reacted within the first 24h exposure, after which the corrosion rate was much lower. The corrosion products were outward-growing sesquioxides – Fe-rich $(Fe_{0.9},Cr_{0.1})_2O_3$ on Type 304 and mixed $(Fe_{0.5},Cr_{0.5})_2O_3$ on Sanicro 28 - over inward-growing $(Fe,Cr,Ni)_3O_4$ spinels. These scales also contained K_2CrO_4, especially near the surface. Preferential corrosion took place far from the surface grain boundaries in Type 304 stainless steel, where evaporated $CrO_2(OH)_2$ could not easily be replaced. The preferential formation of K_2CrO_4 above surface grain boundaries in Sanicro 28 was attributed to the increased availability of chromium at these locations. Although Sanicro 28 contained a sufficient reserve of chromium to form a healing Cr_2O_3 layer in these experiments where small KCl deposits were applied at the beginning of the experiment, the authors pointed out that continuous supply of KCl in an operating biomass boiler would present much more of a challenge to this alloy [37].

Field tests by Pettersson and others in the superheater of a 75MW waste-fired CFB boiler at Händelö, Sweden, showed that adding an amount of sulfur calculated to convert all the alkali chlorides in the fuel to sulfates suppressed the deposition of alkali chlorides and eliminated the formation of K_2CrO_4 [33]. This affirms Petterson's laboratory work showing that alkali sulfates do not react with the protective Cr_2O_3 [32].

6.7 FUEL TREATMENTS TO REDUCE CORROSION

6.7.1 Introduction

Because alkali sulfates have higher melting temperatures and are much less corrosive than alkali chlorides, great efforts have been made to develop methods for converting alkali chlorides (and carbonates) into alkali sulfates by reaction with sulfur compounds. This conversion has been achieved both by blending high chloride fuels with high sulfur fuels and by using additives to raise the concentration of SO_2 or SO_3 in the flue gas.

6.7.2 Sulfation Additives

6.7.2.1 Co-firing with high-sulfur fuels

Co-firing biomass with other fuels is the most widely practiced method of corrosion control. In countries where biofuel combustion is mandated, other fuels may be added simply to dilute the biofuel. However co-firing with high sulfur fuels has the added benefit of converting corrosive low melting temperature alkali chlorides into much less corrosive and higher melting temperature alkali sulfates. For example, Johansson, Leckner, Tullin, Åmand and Davidsson [16] found that fine (<1 μm) fly ash particles produced during combustion in a biomass boiler were largely KCl. However, when a sulfur-bearing additive was introduced, the fine particles were mostly K_2SO_4. Replacing part of the biomass fuel with sludge, or adding kaolin, reduced the deposition rate because of the sulfation of alkali chlorides by sulfur from the sludge.

Aho and others [72] noted that preventing Cl deposition by mixing Cl-rich fuels with S-rich fuels, i.e.

$$2MCl + SO_2 + ½\ O_2 + H_2O \rightarrow M_2SO_4 + 2HCl$$

(where M is an alkali metal) is not effective unless the Ca/S ratio is low. The sulfation reactions will be accelerated if some of the sulfur addition is converted from SO_2 to SO_3.

6.7.2.2 Sulfur dioxide

Skog and others [84] report the addition of SO_2 to the fuel in a 75MW waste-fired boiler at Händelö (near Norrköping, Sweden) to produce the reaction:

$$2KCl(s) + SO_2(g) + ½\ O_2(g) + H_2O \rightarrow K_2SO_4(s) + 2HCl(g)$$

The amount of SO_2 added was controlled to be sufficient to react with the measured content of alkali salts. The SO_2 completely suppressed chromate formation on the boiler tubes but did not entirely prevent the deposition of alkali chlorides. Evidently the HCl vapor is less damaging than molten KCl.

6.7.2.3 Ammonium sulfate

In 2002 Vattenfall AB patented the use of reagents such as $(NH_4)_2SO_4$, NH_4HSO_4, H_2SO_4 and $FeSO_4$ [105] for avoiding problems when burning chlorine-containing fuels. Most of this company's subsequent publications describe the use of ammonium sulfate. The technology is marketed as ChlorOut® [76]. This system uses a previously developed in-situ alkali chloride on-line monitor [7] to control the addition of ammonium sulfate according to the concentration of alkali in the flue gas stream. This uses a surface ionization technique. It can detect concentrations as low as about 1ppb and as high as about 10ppm. The measured alkali concentration corresponds to the sum of the concentration of alkali vapors and fine particles. Coarse particles can also be analyzed using a pulse counting method.

The decomposition of ammonium sulfate to form SO_3 can be written:

$$(NH_4)_2SO_4 \rightarrow SO_3 + 2NH_3 + H_2O$$

The actual situation is much more complex [72]. Water-soluble sulfates can decompose at widely different temperatures; their decomposition rates can be catalyzed or inhibited and some sulfates produce alkali capture reactions. Finally, CaO can react with the SO_3 to form calcium sulfate and alkali hydroxides can consume SO_3 and convert HCl back to alkali chlorides.

Henderson and others [91] exposed a range of alloys in long-term superheater probe tests in two wood-fired boilers with and without additives. One test boiler was the 540°C (1004°F) steam CHP unit in Nyköping and the other was a 98MW, 480°C (896°F) steam, bark-fired boiler at Munksund, also in Sweden. The paper, which included two co-authors from Vattenfall, concluded that ammonium sulfate additions reduced the KCl levels in the flue gases, removed the chlorides from both tube deposits and the tube/scale interface. The additives greatly reduced the deposition rates and halved the corrosion rates of superheater materials.

An independent field evaluation of the ChlorOut® technology was performed by Broström and others [46]. The tests were performed in a 96MW(thermal)/25MW(electricity) circulating fluidized bed (CFB) boiler burning bark with and a chlorine-containing waste. Spraying ammonium sulfate into the flue gases reduced the KCl concentration from more than 15 ppm to about 2 ppm. Test probes showed that the additive decreased both deposition rates and corrosion rates. When ammonium chloride was added, the deposit contained more sulfur and almost no chlorine. Other data confirmed that the additive was sulfating KCl to K_2SO_4.

6.7.2.4 Aluminum and ferric sulfates

Aho and others [72] have evaluated the effectiveness of aluminum and ferric sulfate additives to produce SO_3 and convert alkali chlorides to sulfates. The authors sprayed controlled dosages of aqueous solutions of Al_2SO_4 and $Fe_2(SO_4)_3$ into a pilot-scale fluidized biomass reactor. Both additives removed the chlorides from the fine ash particles at dosages with a S(additive)/Cl(fuel) ratio of 1.5. With aluminum sulfate a dose of S/Cl_2 of 0.45 was sufficient to sulfate almost all the chloride in the finest fly ash (0.03 to 0.1μm; 300 to 1000Å). The authors noted that selecting the correct dosage is not an exact calculation because SO_3 reacts with calcium and magnesium oxides as well as with the troublesome alkali salts. Sulfation requires more ferric sulfate than aluminum sulfate, but ferric sulfate is less expensive and is more soluble in water than aluminum sulfate. The use of these additives was patented in 2006 [99].

Becidan, Serum, Frandsen and Pedersen studied effects of aluminum sulfate additives on corrosion by alkalis and Na, K, Pb and Zn salts in MSW incinerators using thermodynamic equilibrium calculations [159]. A factorial experiment was used to determine the direct and interactive effects of alkali (Na and K) species and of trace metals (Pb and Zn).

6.7.2.5 Aluminum-containing additives and silicates

Coda, Aho, Berger and Hein [2] studied the vaporization of chlorine species and the formation of alkali deposits during combustion of biomass and waste - with and without aluminum-containing additives. Flue gases were analyzed and fly ash particles were analyzed in pilot-scale BFB reactors that simulated the particle residence times in full-scale plants. The fuels burned (softwood and bark, paper mill sludge, and blends of wood with agricultural waste or plastic waste) had low sulfur concentrations (i.e. <0.5 wt. %), but their alkali concentrations ranged widely (0.02−3.2 w/o for Cl and 0.07−3.1 w/o for K). Cl was found in the fly ash samples but appeared to have completely volatilized from the bed ash. Al-containing additives (kaolin, bauxite and fly ash from a pulverized coal plant) increased HCl formation and decreased the concentration of Cl in the fly ash. Al−Si-based

additives reacted with alkali chlorides to form alkali aluminum silicates in coarse fly ash particles. In contrast, limestone additions promoted reactions between Cl in the flue gas and coarse flue gas particles.

Henriksen, Blum and Larsen studied superheater corrosion in the external ash cooler of a CFB co-firing straw and coal [160]. Probes installed in the loop seal, which has a similar environment to an ash cooler, showed that this corrosion was caused by chlorine. Corrosion rates were lower in the ash cooler than in the convective pass, probably because most of the corrosives in the ash particles had been removed in the cyclone. However experiments in a pilot plant indicated that the chlorine concentration could be reduced by silica or kaolinite additions. The authors concluded that increasing residence time and using additives could reduce the concentration of KCl in the upper furnace by a factor of 100.

In related work, Davidsson, Steenart and Eskilsson studied the addition of kaolin to the loop seal of a 35MW CFB boiler fired with forest residues [20]. Almost all the kaolin ended up in the electrostatic precipitator. A small fraction of the kaolin remained in the furnace bed as a thin layer on the sand particles. As the kaolin passed through the boiler, it removed alkali and raised the agglomeration temperature of the bed material. This increased the alkali concentration of the fly ash but decreased the solubility of alkali in the fly ash, suggesting that alkali aluminum silicates had formed. The high melting temperature of silicates would make them unlikely to form sticky deposits on superheater tubes. The authors concluded that kaolin additions can reduce superheater deposition and corrosion and reduce bed agglomeration in biomass fuel boilers.

Additional studies on the effects of silica additives on corrosion by alkalis and trace metals in MSW incinerators have been made, using thermodynamic equilibrium calculations, by Becidan and others [159].

6.7.3 Leaching

Leaching biomass with water reduces or eliminates the release of corrosive alkali metal vapors during combustion.

Dayton and others [3] have shown that leaching biomass fuels with water reduces or eliminates the release of alkali metal vapors when these fuels are subsequently burned. Leaching typically removes >80% of the potassium and sodium and >90% of the chlorine. It also removes smaller fractions of sulfur and phosphorus. Dayton compared the volatile inorganic species evolved in bench-scale combustion tests by leached and un-leached biomass fuels: rice straw, wheat straw, switchgrass, power plant wood fuel, fuel crop banagrass and sugarcane bagasse. The fuels that contained more alkali and chlorine evolved more HCl, KCl, and NaCl when they were combusted.

Jensen, Sander and Dam-Johansen reported that when co-firing straw (up to 20% on a thermal basis) with coal in existing pulverized coal-fired boilers, [141] the most serious problems are deactivation of SCR catalysts applied for NO_x reduction and accumulation of potassium in the fly ash. Pretreatments to avoid these problems should maintain the heating value of the straw without introducing potassium into the furnace. A pretreatment process was evaluated in which pyrolysis of the straw at a moderate temperature left the potassium in the char. Potassium and residual chlorine were extracted from the char by water, and the char and pyrolysis gases were co-fired with coal. The investigations indicated that the low temperature pyrolysis of straw can be performed in a circulating fluid bed reactor applying only straw and straw char as bed material. A pyrolysis bed temperature of approximately 550°C released no significant concentrations of potassium into the gas phase. The authors concluded

that extracting the potassium and chlorine in a counter-current moving bed would probably be advantageous. In related laboratory work [142], the same authors studied the extraction of potassium and chlorine while the pyrolysis char was being washed with water. Three fractions of potassium in the straw reacted differently: 35–58% of the char potassium was dissolved very rapidly, followed by a slow release that was strongly influenced by particle size, water temperature, char type and water KCl content. The last 5–10% of the char potassium remained in the char and could not be removed by extraction with pure water.

6.8 OPERATIONAL MODIFICATIONS TO REDUCE CORROSION

6.8.1 Slagging Superheater

Operating a boiler with a slagging superheater (i.e. at temperatures where the outer layer of tube deposits are molten and flow off can be regarded as a design modification to reduce corrosion because Vattenfall's experience with the "chlorine trap" in the Schweinfurt waste boiler suggests that superheater deposits that grow thick enough to be molten at the ash/flue gas interface appear to provide protection to the underlying tube because they slow the delivery of corrosive species to the tube surface [167].

Žbogar, Frandsen and others studied the shedding of fireside ash deposits from superheater tubes in a straw-fired grate boiler at Avedøre in Denmark [11]. The investigation used video recording, measurements of probe heat uptake and probe mass gain. The Avedøre 2 unit, which can burn natural gas, oil, straw and wood pellets, operates with a high flue gas temperature (900-1100°C) and a low deposit melting temperature. The authors noted that the main shedding mechanism in this boiler is the flow of molten material off the outer surface of the deposit. The rate at which these deposits are shed depends on the percentage of molten material in the deposit and therefore on the flue gas temperature.

Thermographic measurements by Montgomery, Jensen, Hansson, Biede and Vilhelmsen [30] in the Maribø Sakskøbing boiler confirmed the insulating properties of biomass ash deposits by showing that the superheater surface temperatures increased substantially when the tubes were covered with deposits. Deposits with surface temperatures above 950°C (1,742°F) were seen to have molten deposits running off them. Tube thickness data were used to project the average worst case tube thickness loss after 100,000 hours (11.5 years) service in the hottest superheater bank as about 3.9 mm (0.15"). This represents an annualized thinning rate of Type 347H tubes of only 0.34 mm per year (0.013" per year). Montgomery, Jensen, Hansson, Biede and Vilhelmsen concluded that such corrosion rates would be tolerable.

The results from Maribø and Avedøre show that the presence of molten phases on the fireside surface of a superheater deposit does not in itself cause a major corrosion problem. Corrosion is controlled by the environment and temperature at the tube surface.

6.9 DESIGN MODIFICATIONS TO REDUCE CORROSION

6.9.1 "Chorine Trap"

Anders Hjörnhede (Vattenfall) [167] described an interesting approach to chlorine removal used in a waste-fired boiler in Schweinfurt, Germany. Cool furnace screen tubes were installed upstream of the superheater in the convection pass of a waste-fired boiler. Dr. Ragnar Warnecke, MD of the GKS Company that operates the Schweinfurt boiler, added this low temperature heat exchanger as a

"chlorine trap" following an empty downward flue gas pass between the furnace and the first superheater section. The WTE plant has steam parameters of 65 bars and 435°C (943 psi and 815°F). The "chlorine trap" tubes operate at temperatures between 300 and 400°C (572 to 752°F). Alkali metal chlorides condense on these tubes forming massive deposits that are removed only once each day. It seems that a molten layer on the fireside of the deposits on these tubes may block the inward diffusion of chlorine-containing gases and thus reduce the corrosion rate of the underlying tubes [167].
A similar empty "radiation pass" between the furnace and the superheater, designed into a WTE energy plant at Norrköping, Sweden was described by Enestam, Lehtonen and Heinke [126].

A similar shield installed to protect the superheater of a CFB firing straw was described by Henriksen, Blum and Larsen [160]. Co-firing the straw fuel with coal reduced corrosion to manageable rates except in the external ash cooler, which received recycled ash from the cyclones and contained the hottest superheaters. This recycled ash included unburned particles that contained enough chlorine to initiate corrosion of the superheaters. Design changes included keeping metal temperatures in the convective pass below about 450°C (842°F). As at Schweinfurt, this was achieved by increasing the residence time between the furnace and the first superheater and by installing an additional evaporator tube bundle immediately ahead of the first superheater to act as a shield. This evaporator section also compensated for lower evaporation in the waterwalls because their thick refractories restricted heat transfer.

6.9.2 Easily Replaced Superheater Tubes

Henriksen, Blum and Larsen [160] described a boiler suffering superheater corrosion in an external ash cooler environment in which the heat exchange units that formed the final superheater in the final ash cooler were designed for easy replacement. An example of what can be achieved in rapid superheater replacement is that the City of Amsterdam achieved a 48-hour fire-to-fire superheater replacement in a WTE boiler [166].

Rapidly changeable superheater tube banks were also incorporated in the design of a WTE energy plant at Norrköping, Sweden, according to Enestam, Lehtonen and Heinke [126].

6.9.3 Remove Superheater from Corrosive Flue Gas Environment

6.9.3.1 External superheater using a less-corrosive fuel

A straw-fired boiler at Ensted in Denmark avoids excessive superheater corrosion from flue gas products of straw combustion by adding an external superheater that burns a cleaner fuel. An external wood-fired superheater produces a final steam temperature of 542°C (1008°F), while the steam exit temperature from the straw-fired boiler itself is 470°C (878°F) [9].

6.9.3.2 Relocate CFB superheater to loop seal

In a CFB boiler, the fluidizing medium (sand) is separated from the flue gases by a cyclone and recirculated through a loop seal to the bottom of the boiler where it flows upward with the combustion air to form the fluidized bed. Skog and others [84] have described the relocation of superheaters in biomass boilers from the flue gas stream into the recirculated fluidizing medium between the loop seal and the bottom of the boiler. Immersed in the hot sand, the superheater has much less exposure to alkali metal salts and corrosive gases than in the flue gases. In addition the heat transfer per unit area is 5 to 10 times better than in a conventional superheater [155]. This design

modification to move the superheater to the loop seal has been commercialized in Foster Wheeler's INTREX design and in Metso's CYMIC design.

Erosion damage in these relocated superheaters is not rapid because the sand velocities are low. Nafari and Nylund [98] measured erosion-corrosion of steel tubes installed in the loop seal of a 30MW CFB boiler. The tubes were in service for either about 7 months or about 16 months in a co-generating plant fired with coal and forest residues[26] at Nässjö, Sweden. Tubes exposed for the longer period showed no more wastage than tubes exposed for the shorter period. Thinning rates increased with tube temperature. The steam inlet and outlet temperatures were 470 and 540°C (878 and 1004°F), and the authors suggested that the tube surface temperatures would be 50 to 100°C (90 to 180°F) higher than these values. The corrosion products consisted of an inner layer of Cr and Fe oxides beneath an outer Fe-rich oxide. Chloride was present at the alloy/scale interface and was associated with K and S. Average material losses on Esshete 1250 (Fe-15Cr-9Ni-1Si-6Mn-MoVNbB) and Type 347H were comparable and just slightly greater than on AC66 (Fe-27Cr-32Ni-AlMnSiNbCe). However, AC66 showed the most severe internal oxidation.

Later work by the same authors [132] tested the same alloys and various coatings in the loop seal of a wood-fired CFB at Nässjö. Tube temperatures ranged from 510 to 550°C (950 to 1022°F). The loop seal ash contained 13% Ca, 9% K, 0.9% Na, 800 ppm sulfate and 100 ppm chloride. Even the uncoated alloys suffered little corrosion during boiler operation. The fact that the degradation was no worse after two firing seasons than after one indicated that corrosion, rather than erosion, is the dominant deterioration mechanism. The thickest oxides, on a 9% Cr alloy, were only about 150µm (0.006") thick after about seven months in service. Austenitic steels suffered some internal oxidation and grain boundary attack. Although some coatings delaminated, 8 of the 17 coatings tested were unaffected by the exposure.

6.9.4 Add an Insulating Layer to Raise the Surface Temperature of Superheater Tubes Above the Dew Point of Alkali Chlorides

Enestam, Lehtonen and Heinke [126] have described a series of changes that were incorporated in the design of a WTE energy plant at Norrköping, Sweden. In addition to locating the superheater in the loop seal (referred to as a novel fluidized bed heat exchanger - FBHE in this paper) the boiler added the following design features:

- Directional primary air nozzles to aid bottom ash removal
- Fuel residence time of 2 seconds at 850°C (1562°F)
- Auxiliary burners that start automatically if the combustion temperature falls below 850°C (1562°F)
- Flue gases cool in an empty "radiation pass" before the lower temperature superheater sections
- Tube banks were designed to allow rapid changing

Despite these precautions, the boiler experienced deposit formation and rapid corrosion of the tubes in the final (loop seal) superheater. This corrosion was attributed to the condensation of alkali chloride deposits, mainly NaCl, on these tubes. To prevent this condensation Metso developed a new type of composite tube with an internal insulating layer (Patent pending [126]) to raise the surface temperature above the dew point temperature of NaCl. Figure 7, below, shows the three layers in the tube [154].

26 The fly ash is returned to the forest [132].

Although the higher surface temperature of the new tubes will reduce the heat transfer per unit area, this can be compensated for by adding additional heating surface in the loop seal superheater.

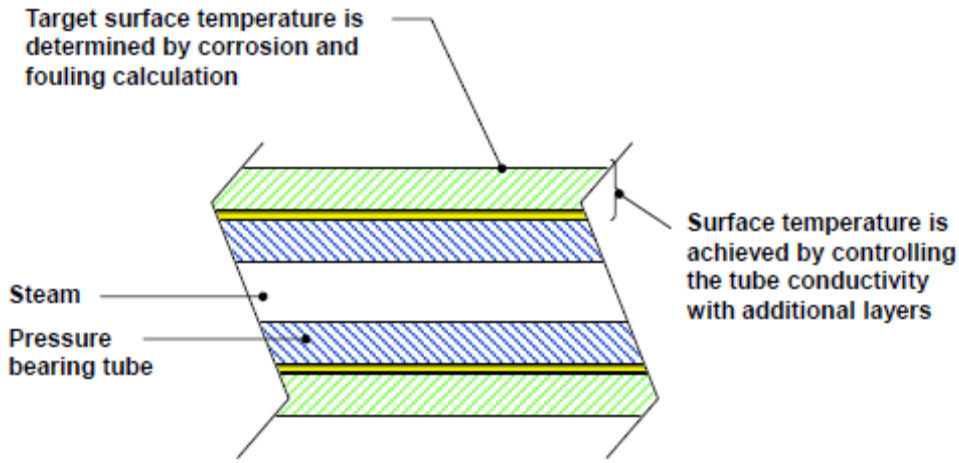

Fig. 7. Metso tube containing a thermally-insulating layer to raise its surface temperature above the dew point of NaCl vapor

Enestam, Lehtonen and Heinke [126] noted that fouling of superheater surfaces has been clearly reduced by installing the insulating tubes except in a few areas where the fluidization pattern was not ideal. Adding the insulating layer changed the composition of loop seal superheater tube deposits from NaCl, KCl, small amounts of Ca and SiO_2 and only about 1% S (as SO_3) to SiO_2, Ca, S (probably as $CaSO_4$), alumina, with some Na and Mg. The chlorine content of the deposits fell to about 1% (with a maximum value of 4.5 w/o in a single sample).

Skog and others [84] plotted the effects of increasing superheater tube surface temperatures on the concentrations of potentially corrosive species, as shown in Figure 8 [84].

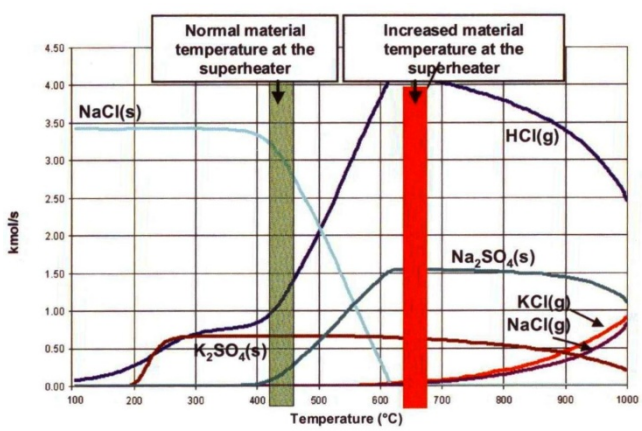

Fig. 8. Effects of increasing superheater tube temperature on concentrations of potential corrosives

Although the data shown in Figure 8 indicate that KCl is not expected to condense as a liquid on the surface of these new three-layer composite tubes, it cannot be assumed that alkali chlorides are not corrosive above their dew point temperatures. Segerdahl and others showed that the KCl vapors in

the flue gas can react with the Cr_2O_3 on the tube surface to form K_2CrO_4. This caused local oxide failure on an 11% Cr martensitic steel which led to the formation of non-protective Fe_2O_3 [92]. Petterson, Svensson and Johansson [75] investigated the corrosivity toward a highly-resistant superheater alloy of gaseous KCl at temperatures above its dew point. They studied the corrosion resistance of Sanicro 28 at 600°C under conditions where the dew point temperature of KCl was 590°C. KCl gas additions reacted with the protective Cr_2O_3 on Sanicro 28 to form K_2CrO_4. Although this increased the oxidation rate, it did not cause a sudden failure (breakaway oxidation). The distribution of K_2CrO_4 on the alloy surface depended on the gas flow rate, indicating that the rate of chromate formation was limited by the rate of arrival of KCl at the surface. No chlorides were found on the alloy surface.

6.10 COATINGS TO REDUCE CORROSION

Lee, Themelis and Castaldi [158] have reviewed corrosion prevention technologies in WTE boilers, focusing on the use of Alloy 625 weld overlay cladding, thermal spray coatings, combustion fluid dynamics and soot blowing.

Uuistalo and others have compared the corrosion resistance of a 0.17%C superheater tube steel (Grade 35.8; DIN 17175) with that of diffusion coated and thermally sprayed materials in 5-hour tests in an erosion-corrosion test rig simulating a CFB combustor [95]. The test specimen was cooled to 550°C. The erosive material was SiO_2 and the particle velocity averaged 28 m/s (92 fps). The authors found that even 0.1% of KCl substantially accelerated the thickness loss of the specimens. However, a nickel-based HVOF coating with high chromium content (Ni-57CrMoBSi) showed good resistance to erosion-corrosion even when chloride was added. Chromized coatings and chromium carbide coatings did not survive the tests. Because large platelets in thermal spray coatings are difficult to dislodge by erosive particles, the authors concluded that HVOF thermal spray coatings should be dense with a large splat size in order to perform well in this type of environment.

Tuurna and a large group of co-workers [65] recently evaluated the use of corrosion-resistant coatings to control corrosion in a biomass boiler. Their tests evaluated the corrosion resistance of thermally sprayed HVOF coatings and related materials both on superheater tubes (high temperature fireside corrosion) and on economizer tubes (low temperature fireside dew point corrosion) in three biomass boilers. The first test site was in a fluidized bed unit burning peat and wood-based fuels in an economizer location that had experienced pluggage. The tubes were coated with about 200µm (0.008") of a Ni-20Cr coating containing 75% Cr_3C_2. The second boiler also had a fluidized bed and burned wood-based fuels with small amounts of peat. The test sites were located at the hot and cold ends of the economizer, where tube failures had been experienced. A 300µm (0.012") HVOF coating and a 400µm (0.016") arc spray coating were tested. The chromium contents of the two coatings were either 46% or 20%. The third boiler was a waste-fired grate boiler. Here the test area was in the superheater. HVOF (16%, 25% and 27% Cr) and spray-and-fused coatings (16% Cr) were applied. The coatings were evaluated after one year's service [65]. The coatings performed well in the first boiler, but the adjacent tubing showed little attack and it was concluded that coatings were not really needed. In the second boiler the HVOF tubes showed no appreciable corrosion where uncoated P235 and P265 tubes had thinned at rates of up to millimeters per year. The superheater tube coatings in the third boiler performed well, with no visible corrosion. Quality of application, adhesion and high density seem to be the critical factors in determining the performance of these coatings. Amorphous coatings and the spray-and-fuse coatings cracked before the test was complete.

6.11 PREDICTION OF CORROSION IN CFBS

Boiler manufacturers and other consortia have developed models to predict fouling and corrosion in biomass boilers in order to specify tube materials for particular operating conditions. Foster Wheeler's model predicts the tendency of fuels to cause agglomeration, fouling and corrosion in CFB boilers and the corrosion produced by a specified fuel on a specified alloy under specified operating conditions [104]. Its data base draws on 10,000 fuel sample analyses and over 1,000 tests in about 150 CFB boilers. The fuel model combines empirical results with theoretical calculations concerning agglomeration, fouling and corrosion [107]. The agglomeration module is based on the formation of low melting temperature compounds by alkali elements (Na, K and P) from the fuel and by silica from the fluidized bed. It is assumed that only materials that are soluble at pH 3 will be involved in agglomeration reactions and that the likelihood of agglomeration is reduced when aluminosilcates are present, particularly from kaolinite minerals. The fouling module is based on the hypothesis that fouling is promoted by alkali (Na and K) compounds and alkaline earth (Ca and Mg) and reduced by compounds of aluminum and silicon. Alkalis soluble at pH 3 are particularly likely to deposit on convective heat exchangers. The corrosion module assumes that chlorine from the fuel is the primary corrosive. If the fouling tendency is low, then corrosion rates will be low and if the fouling tendency is high, corrosion rates can be either high or low depending on the concentration of chlorine contributed by the fuel. The presence of sulfur oxides and the addition of kaolinite minerals reduce the availability of chlorine to cause corrosion. The authors hope to extend the corrosion module to include effects of zinc, lead and metallic aluminum, which can be introduced by demolition wood and which produce deposits with extremely low melting temperatures. The output of the fuel model is expressed on a ten-point scale as the probability that the fuel or fuel mixture will cause agglomeration.

The corrosion model estimates the corrosion rate produced by a particular fuel on a particular alloy at a particular temperature. It was developed using fuzzy logic to be used as an advisory tool for experts. Recent upgrades of this model have included re-training with a broader range of field data, addition of newer austenitic and nickel-based tube materials and extension to supercritical and ultra-supercritical steam conditions. An example of the use of this model cited by Coda Zabetta and others [104, 107] refers to a boiler operated on random mixtures of coal, rice husks and eucalyptus bark. Corrosion rates estimated for two extreme fuel mixtures (low rice husks and high eucalyptus bark and the reverse) correlated reasonably well with tube thinning rates measured in the operating boiler.

Metso Power has developed its own predictive model for the same purpose. Enestam, Niemi and Mäkelä describe the Metso tool which is called STEAMAX [125]. This estimates the corrosivity of a given fuel mixture and recommends maximum steam temperatures for candidate tube materials. Given the analysis of a proposed fuel or fuel mix, the program uses multiphase, multi-component thermochemical equilibrium calculations to predict the melting behavior of the fuel ash as a function of temperature. Elements considered include C, H, N, O, S, Cl, Ca, Mg, Na, K, Al, Si, Fe, P, Pb and Zn, 12 solid compounds, 2 solid solutions, 2 liquid solutions and 1 gas phase. As in the Foster Wheeler program, the corrosivity is measured by the amount of chlorine in the flue gas at different temperatures and boiler locations. The maximum allowable temperature for given tube alloys is estimated from an empirical database based on data from 20 biomass-fuelled and black liquor recovery boilers in which the superheater conditions have been well characterized. The risk of corrosion by a molten deposit is assessed by determining whether the tube surface temperature exceeds the FMT of the deposit. The output of the program is a maximum operating temperature for candidate alloys, considering solid chlorine-induced corrosion, gas phase chlorine-induced corrosion and molten phase corrosion. This type of program is useful not only for designing new boilers but also for determining where corrosion is likely to appear first in a given boiler where a new type of fuel mixture is being considered.

UK models of fireside corrosion in coal-fired boilers have been extended by Kilgallon, Simms and Oakey at Cranfield University to predict rates of fireside corrosion in biomass-fired boilers [109]. Their model applies to the corrosion of 1% Cr steel for evaporator conditions, of a 2¼% Cr steel for low temperature superheater conditions, of X20CrMoV121 and Type 347HFG for superheater conditions and of Alloy 625 for superheater and evaporator repair conditions. The fuel is coal with up to 20% biomass. Data from a matrix of 1000 hour laboratory tests were used to develop empirical models of corrosion under these test conditions. These corrosion tests were made in various mixtures of KCl, K_2SO_4 and pulverized coal fly ash based on deposit analysis from Danish biomass fuel and co-fired boilers. The deposits were applied to the coupons and re-applied every 100 hours. The gas atmospheres consisted of more and less oxidizing mixtures of O_2, CO_2, H_2O, CO, SO_2 and HCl. A model was developed based on these data to simulate the effect of the deposit composition (w/o of K^+, Cl^- and SO_4^- in the deposits), the gas composition (vpm of SO_x and HCl at 560 and 600°C (1040 and 1112°F) and p_{O2} at 425°C (797°F), and the test temperature was developed. The model fitted the medial metal loss measurements fairly well, although it was not verified using a data set different to those on which it had been trained.

As part of the UK research effort, Plaza, Griffiths, Syred and Rees-Gralton developed a model to predict slagging and fouling during the co-firing of biomass fuels with coal [12]. This model was applied to a 618MW pulverized coal boiler burning volatile bituminous coal with sewage sludge and sawdust. Adding sewage sludge increased slagging and high temperature firing and adding sawdust had the reverse effect.

It would be of great interest to compare the results of the three prediction models of biomass corrosion developed independently by Foster Wheeler, Metso and Cranfield.

6.12 SUMMARY

Setting the steam temperature of a biomass boiler is compromise between wasting fuel energy, risking pluggage that will shut the unit down and creating conditions that will produce rapid corrosion on the superheater tubes and force replacement expenses. For example the life of Type 347H superheater tubes in a UK straw-fired power station could be extended from 5 years to 15 years by reducing the steam temperature by 10°C (18°F). Where such data are available a boiler operator can make an informed decision about the most economic combinations of particular biomass fuels and steam temperatures in combination with, boiler design and operation modifications, high alloy tubes and the cost of fuel treatments to remove corrosives.

Generally, the most corrosion resistant alloys in biomass superheater environments are FeCrNi alloys containing at least 25%Cr. The critical issue in the corrosion resistance of superheater alloys in biomass boilers is their ability to maintain a protective surface oxide despite the tendency for such oxides to react with alkali chloride deposits and sulfur oxides to form alkali metal chromates. If the supply of chromium from the bulk of the alloy cannot resist this fluxing and the high temperature volatilization of chromic acid, the resulting non-protective oxide can be penetrated by chlorine species that cause further acceleration of the corrosion rate by active oxidation.

The most widely used fuel treatments to reduce corrosion in biomass boiler are co-firing biofuels with high sulfur fuels, and using additives such as aluminum sulfate that raise the concentration of SO_2 or SO_3 in the flue gas. Firing biomass with coal has proved successful in situations where sulfur from the coal increases the FMT of superheater ash by reacting with KCl to form K_2SO_4, and where aluminosilcates from the coal react with otherwise corrosive alkali metal salts.

Design modifications that have been shown to control biomass superheater corrosion include adding a radiant pass (empty chamber) between the furnace and the superheater, installing cool tubes like a furnace screen immediately upstream of the superheater to trap high chloride deposits, designing superheater banks for quick replacement (one European municipal waste boiler recently replaced its superheater in 48 hours fire-to-fire), using an external superheater that burns a less corrosive biomass fuel and moving CFB superheaters from the convective pass into the hot recirculated fluidizing medium and adding an insulating layer to superheater tubes to raise their surface temperature above the dew point temperature of alkali chlorides. All these design modifications offer advantages but bring disadvantages.

Danish experience shows that boilers can be operated with molten materials on the surface of superheater deposits, if the boiler can operate with insulating deposits on the tubes. The chlorine trap in the Schweinfurt waste boiler suggests that superheater deposits that grow thick enough to be molten at the ash/flue gas interface appear to provide protection to the underlying tube because transport rates through the molten deposits are slow.

Boiler manufacturers and other consortia have developed models to predict fouling and corrosion in biomass boilers in order to specify tube materials for particular operating conditions. It would be very useful to analyze the conditions in the boiler environments where field tests will be performed in the current program using the models developed by Foster Wheeler, Metso and the UK consortium at Cranfield University.

7. DISCUSSION AND CONCLUSIONS

7.1 STATUS OF SCIENCE AND TECHNOLOGY OF OPERATING BIOMASS BOILERS AT OR ABOVE THE MELTING TEMPERATURE OF ASH DEPOSITS

Although the prevailing opinion is that superheater tube alloys cannot survive in contact with any molten deposits, we have not found any basis for this opinion in systematic studies of corrosion rates in biomass boiler superheater environments where the tube temperatures exceed the FMT of the fly ash. However, we have identified several biomass boilers that successfully operate with superheater deposits so thick that the fireside surface of their deposits is molten.

It is important to remember that, the fact that the flue gases contain species that would be molten at the tube surface temperature does not indicate that molten deposits are in contact with the tube surface. The suitability of an alloy for superheater service depends on its ability to maintain its protective oxide in the environment produced by the mix of particles that adhere to its surface and the gaseous species in the combustion gases. Mechanisms of oxide failure have been studied in some detail. These typically involve reactions between chlorine species and chromium oxide. If the protective chromium oxide fails (either by forming alkali metal chromates or by physically fracturing, direct access of chlorine species to the tube surface will cause active oxidation that will proceed at higher corrosion rates than are manageable.

Major suppliers of biomass boilers have selected the following as the lowest-cost approach to generating energy from biofuels: (a) use a boiler design optimized for biomass fuels[27], (b) reduce the corrosivity of the biomass to an acceptable level by co-firing it either with a less corrosive fuel or with a high sulfur fuel that will convert alkali chloride deposits to alkali sulfates, (c) add sulfur or silicate chemicals as required to prevent the formation of alkali metal chloride deposits, and (d) having taken these precautions, choose the maximum steam temperature to achieve the lowest total cost of energy plus maintenance. Future work in this project will study the economics of these optimization processes in model systems.

7.2 FINDINGS APPLICABLE THE LABORATORY AND FIELD TESTING IN THIS PROJECT OR FUTURE PROJECTS

The current survey of biomass boiler corrosion research findings revealed several laboratory approaches that could be used either in the current project or in future projects. For example several laboratories have shown that increases in temperature gradient increase corrosion rates at a given tube temperature[28]. Although most of these studies were in coal fired or in WTE boilers, they were confirmed in biomass boilers at Maribø and Avedøre 2. While constant temperature laboratory tests may be useful to identify candidate alloys, field or laboratory testing under a thermal gradient appears necessary to simulate the conditions in an operating boiler.

Simultaneous Thermal Analysis measurements by Hansen and others to quantify the melting of fly ash produced when co-firing coal and straw [8] showed that the proportion of molten material at the first melting temperature measured by standard ash fusion test ranged from 1% to 36%. In related work, Salmenoja and Turiemo [136, 115] concluded that conventional deposit sampling procedures

---

27 Features of such boilers typically include an empty radiation pass to ensure that flue gas reactions go to completion, a superheater removed from the convection pass, easily-replaced tube banks and other features such as a chlorine trap or tubes with an insulating layer so that their fireside temperature exceeds the salt dew point.
28 See references 30, 123, 144, 145, 147, 156, 165.

can allow sulfides to become oxidized to sulfates and that this would overestimate the FMT. These findings cast doubt on the reliability not only of FMT measurements using the standard ash fusion test but also of thermochemical equilibrium calculations based on the analysis of deposit samples.

Dimensional metrology techniques developed in a number of European laboratories robotically scan the circumference of a tube sample and use automated image analysis to make statistical analyses of the depth of penetration and the corrosion product thickness. Using this type of standard method for evaluating damage on irregularly corroded surfaces would be useful in the laboratory evaluation of test materials in this project.

A very powerful method for evaluating the corrosion resistance of candidate alloys in operating boilers has been developed in Denmark. These involve the installation of individual test loops in operating superheaters. The steam flow in each loop is controlled independently of that in the main superheater to control its tube temperature. Detailed thickness measurements can be made before the tube is installed and after it is replaced at a routine shutdown [49].

8. REFERENCES

1. Xiaoyang Liu, Joerg Maier and Klaus R.G. Hein, "The kinetics of fireside corrosion in biomass combustion system and the influence from gas and deposit ash chemistry", Electrochemical Society 201st Meeting - Philadelphia, PA, May 16, 2002. Abstract available at http://www.electrochem.org/dl/ma/201/pdfs/0328.pdf.
2. Beatrice Coda, Martti Aho, Roland Berger and Klaus R.G. Hein, "Behavior of chlorine and enrichment of risky elements in bubbling fluidized bed combustion of biomass and waste assisted by additives", Energy Fuels, 15 (3), 680-690, 2001.
3. D.C. Dayton, B.M.Jenkins, S.Q. Turn, R.R. Baker, R.B. Williams, D. Belle-Oudry and L.M.Hill, "Release of inorganic constituents from leached biomass during thermal conversion", Energy Fuels, 13 (4), 860-870, 1999.
4. Joaquin Capablo, Peter A. Jensen, Kim H. Pedersen, Klaus Hjuler, Lars Nikolaisen, Rainer Backman and Flemming Frandsen, "Ash properties of alternative biomass", Energy Fuels, 23 (4), 1965-1976, 2009.
5. T. Valmari, T.M. Lind and E. Kauppinen, G. Sfiris, K. Nilsson and W. Maenhaut, "Field study of ash behavior during circulating fluidized bed combustion of biomass. 1. Ash Formation", Energy Fuels, 13 (2), 379-389, 1999.
6. Xiaolin Wei, Christian Lopez, Thore von Puttkamer, Uwe Schnell, Sven Unterberger and Klaus R.G. Hein, "Assessment of chlorine-alkali-mineral interactions during co-combustion of coal and straw", Energy Fuels, 16 (5) 1095-1108, 2002.
7. Kent O. Davidsson, Klass Engvall, Magnus Hagström, John G. Korsgren, Benny Lönn and Jan B.C. Pettersson, "A surface ionization instrument for on-line measurements of alkali metal components in combustion: instrument description and applications", Energy Fuels, 16 (6), 1369-1377, 2002.
8. Lone A. Hansen, Flemming J. Frandsen, Kim Dam-Johansen, Henning S. Sørenson and Bengt-Johan Skrifvars, "Characterization of ashes and deposits from high temperature coal-straw co-firing", Energy Fuels, 13 (4), 803-816, 1999.
9. Peter A. Jensen, Flemming J. Frandsen, Jern Hansen, Kim-Dam-Johansen, Niels Henriksenand Stefan Hörlyck, "SEM investigation of Superheater deposits from biomass-fired boilers", Energy Fuels, 18 (2), 378-384, 2004.
10. Hanne-P. Nielsen, Flemming J. Frandsen and Kim Dam-Johansen, "Lab-scale investigation of high temperature corrosion phenomena in straw-fired boilers", Energy Fuels, 13 (6), 1114-1121, 1999.
11. Ana Žbogar, Peter A. Jensen, Flemming J. Frandsen, Jern Hansen and Peter Glarborg, "Experimental investigation of ash deposit shedding in a straw-fired boiler", Energy Fuels, 20 (2), 512-519, 2006.
12. Piotr Plaza, Anthony J. Griffiths, Nick Syred and Thomas Rees-Gralton, "Use of a predictive model for the impact of cofiring coal/biomass blends on slagging and fouling propensity", Energy Fuels, 23 (7), 3437-3445, 2009.
13. David A. Tillman, Dao Duong, Sheila Figueroa and Bruce Miller, "Chlorine in solid fuels fired in pulverized coal boilers – sources, forms, reactions and consequences: a literature review", Fuel Conference, Banff, Canada, September 28 – October 3, 2008. Energy Fuels, 23 (7), 3379-3391, 2009. Available at http://www.fwc.com/publications/tech_papers/files/TP_METAL_08_02.pdf
14. P.A. Jensen, M Stenholm and P. Hald, "Deposition investigation in straw-fired boilers", Energy Fuels, 11 (5), 1048-1055, 1997.
15. Dorota Bankiewicz, Patrik Yrjas and Mikko Hupa, "High temperature corrosion of superheater tube materials exposed to zinc salts", Energy Fuels, 23 (7), 3469-3474, 2009.

16. Linda S. Johansson, Bo Leckner, Claes Tullin, Lars-Erik Åmand and Kent Davidsson Tech Res Inst of Sweden), "Properties of particles in the fly ash of a biofuel-fired circulating fluidized bed (CFB) boiler", Energy Fuels, 22 (5), 3005-3015, 2008.
17. Bengt-Johan Skrifvars, Partik Yrjas, Tor Laurén, Jouni Kinni, Honghi Tran and Mikko Hupa, "The fouling behavior of rice husk ash in fluidized bed combustion. 2: Pilot-scale and full-scale measurements", Energy Fuels 19 (4), 1512-1519, 2005.
18. Karin H. Andersen, Flemming J. Frandsen, Peter F.B. Hansen, Kate Wieck-Hansen, Ingvar Rasmussen, Peter Overgaard and Kim Dam-Johansen, "Deposit formation in a 150MWe utility PF boiler during co-combustion of coal and straw", Energy Fuels 14 (4), 765-780, 2000.
19. Allen L. Robinson, Helle Junker and Larry L. Baxter, "Pilot-scale investigation of the influence of coal-biomassco-firing on ash deposition", Energy Fuels, 16 (2), 343-355, 2002.
20. K.O. Davidsson, B-M. Steenari and D. Eskilsson, "Kaolin addition during biomass combustion in a 35MW circulating fluidized bed boiler", Energy Fuels, 21 (4), 1959-1966, 2007.
21. Kent O. Davidsson, Lars-Erik Åmand, Bo Leckner, Borka Kovacerik, Maria Svane, Magnus Hagström, Jan B.C. Pettersson, Jasper Pettersson, Henrik Asteman, Jan-Erik Svensson and Lars-Gunnar Johansson, "Potassium, chlorine and sulfur in ash, particles, deposits and corrosion during wood combustion in a circulating fluidized bed boiler", Energy Fuels, 21 (1), 71-81, 2007.
22. Shrinivas S. Lokare, J. David Dunaway, David Moulton, Douglas Rogers, Dale R. Tree and Larry L. Baxter, "Investigation of ash deposition rates for a suite of biomass fuels and fuel blends", Energy Fuels 20 (3), 1008-1014, 2006.
23. S. Arvelakis and F. J. Frandsen, "Melting behavior of ashes from co-combustion of coal and straw", Energy Fuels, 21 (5), 3004-3009, 2007.
24. Fleming J. Frandsen, "Ash research from Palm Coast, Florida to Banff, Canada: Entry of biomass in modern power boilers", Energy Fuels 23 (7), 3347-3378, 2009.
25. B-J. Skrifvars, G. Sfiris, R. Backman, K. Widegren-Dafgård and M. Hupa, "Ash behavior in a CFB boiler during combustion of *Salix*", Energy Fuels 11(4), 843-848, 1997.
26. K.O. Davidsson, L-E. Åmand, A-L. Eiled and B. Leckner, "Effect of co-firing coal and biofuel with sewage sludge on alkali problems in a circulating fluidized bed boiler", Energy Fuels 21 (6), 3180-3188, 2007.
27. Xiaolin Wei, Uwe Schnell and Klaus R.G. Hein, "Behavior of gaseous chlorine and alkali metals during biomass thermal utilization", Fuel 84 (7-8), 841-848, 2005.
28. A.N. Hansson, L. Korcakova, J. Hald and M. Montgomery, "Long term steam oxidation of TP 347H FG in power plants", Materials at high temperatures, 22 (3-4), 263-267, 2005.
29. M. Montgomery, S.A. Jensen, F. Rasmussen and T. Vilhelmsen, "Fireside corrosion and steamside oxidation of 9-12% martensitic steels exposed for long term testing", Corrosion Engineering, Science and Technology, 44 (3), 196-210, 2009.
30. M. Montgomery, Søren A. Jensen, Annette Hansson, Ole Biede and Tommy Vilhelmsen, "High temperature corrosion testing at Maribo Sakskøbing and Avedøre straw firing power plants", Manuscript associated with poster SS 2-P-7984 at EUROCORR European Corrosion Congress, Nice, France, 6-10 September, 2009.
31. James R. Keiser, Joseph. R. Kish, Gorti R. Sarma, Jerry Yuan, J. Peter Gorog, Laurie A. Frederick, Francois R. Jetté, Roberta A. Meisner, Douglas L. Singbeil, Final Technical Report: Materials for Industrial Heat Recovery Systems, Project period 04/01/2004 to 03/30/2007, December 31, 2007.
32. J. Pettersson, J-E. Svensson and L-G. Johansson, "Alkali-induced corrosion of 304-type austenitic stainless steel at 600°C; comparison between KCl, K_2CO_3 and K_2SO_4", Materials Science Forum, 595-598, 367-375, 2008.

33. J. Pettersson, C. Pettersson, N. Folkeson, L-G. Johansson, E. Skog and J-E. Svensson, "The influence of sulphur additions on the corrosive environment in a waste-fired CFB boiler", Materials Science Forum, 522-523, 563-570, 2006.
34. J Pettersson, H. Asteman, J-E. Svensson and L-G. Johansson, "KCl-induced corrosion of a 304-type austenitic stainless steel at 600°C; the role of potassium", Oxidation of Metals 64 (1-2), 23-41, 2005.
35. N. Folkeson, L-G. Johansson and J-E. Svensson, "Initial stages of the HCl-induced high-temperature corrosion of Alloy 310", J. Electrochem. Soc., 154 (9), C515-C521, 2007.
36. J. Petterson, C. Petterson, H. Asteman, J-E. Svensson and L-G. Johansson, "A pilot plant study of the effect of alkali salts on initial stages of the high temperature corrosion of Alloy 304L", Materials Science Forum, 461-464, 965-972, 2004.
37. C. Pettersson, J. Pettersson, H. Asteman, J-E. Svensson and L-G. Johansson, "KCl-induced high temperature corrosion of the austenitic Fe-Cr-Ni alloys 304L and Sanicro 28 at 600°C", Corrosion Science, 48 (6), 1368-1378, 2006.
38. P.J. Henderson, T. Eriksson, J. Tollin and T. Abyhammar, "Corrosion testing of superheater steels for 600°C steam in biomass/co-fired boilers", Proceedings of conference on advanced heat resistant steels for power generation, San Sebastian, Spain, April 27, 1998, published Maney Publishing, Leeds, UK, 1999.
39. M. Hupa, R. Backman and B.J. Skrifvars, "The influence of chlorides on the fireside behavior in the recovery boiler", TAPPI J., 73 (6), 153-158, 1990.
40. H.N. Tran, D.C. Pryke, D. Barham and D.W. Reeve, "Local reducing atmosphere – a cause of superheater corrosion in kraft recovery units", TAPPI J. 68 (6), 102-106, 1985.
41. Thomas R. Miles, Thomas R. Miles, Jr., Larry L. Baxter, Richard W. Byers, Bryan M Jenkins and Laurance L. Oden, "Alkali deposits found in biomass power plants: a preliminary investigation of their extent and nature", summary report for NREL, 1995, available at http://www.trmiles.com/alkali/Alkali_Report.pdf
42. T. Heinzel, W. Scheurer, J. Baum, J. Maier and K.R.G. Hein, "Combustion performance and residue analysis of trial burns in a pilot scale slag tap furnace with coals and waste fuels", Proceedings IT-3 2000, Portland, OR, 2000. Proceedings of the International Conference on Incineration and Thermal Treatment Technologies, ed. Cohen, Lori B., pp. 791-796. University of California, Irvine, CA.
43. T. Heinzel, C. Lopez, J. Maier, H. Spliethoff, K.R.G. Hein, "Ash deposit and corrosion characteristics of coal-biomass blends in a 0.5 MW pulverized fuel test facility", Conference on effects of coal quality on power plant management: ash problems, management and solutions, May 8 to 11, Park City, Utah, 2000, published EPRI, Palo Alto, CA, 2000.
44. Xiaoyang Liu, T. Heinzel, J. Maier and K.R.G. Hein, "Fireside slagging and corrosion by firing lignite coals and coal blends in a PF boiler", 6th International Conference on Clean Air, Porto, Portugal, 2002.
45. M. Montgomery, B. Sander and O.H. Larsen, "Biomass firing: Danish experiences", Energy Materials, 1 (1), 17-19, 2006.
46. Markus Broström, Håkan Kasseman, Anna Helgesson, Magnus Berg, Christer Andersson, Rainer Backman and Anders Nordin, "Sulfation of corrosive alkali chlorides by ammonium sulfate in a biomass fired CFB boiler", Fuel Processing Technology, 88 (11-12), 1171-1177, 2007
47. Greg F. Weber and Christopher J. Zygarlicke, "Barrier issues to the utilization of biomass", Semiannual Technical Progress Report on US DOE Contract DE-FC26-00NT41014.
48. UK Department of Trade and Industry, "Review of status of advanced materials for power generation", Technology Status Report 018, Publication URN 02/1267, published Cleaner Coal Program, DTI, London, UK, 2002.
49. M. Montgomery, B. Carlsen, O. Biede and O.H. Larsen, "Superheater corrosion in biomass-

fired power plants: investigation of welds", Paper 02379 at NACE International CORROSION/2002 conference, April 7-12, Denver CO, published NACE, Houston, 2002.
50. Aaron Fuller, Jörg Maier and G. Scheffknecht, "Impact of co-combustion on emission behavior and ash quality by co-firing high shares of biomass and residues", 35th International Technical Conference on Clean Coal and Fuel Systems", June 6-10, 2010, Clearwater, FL, published Coal Technology Association, Gaithersburg, MD, 2010.
51. K. L. Luthra and D.A. Shores, "Mechanism of Na_2SO_4 induced corrosion at 600-900°C", J. Electrochem Soc., 127 (10), 2202-2210, 1980.
52. A.M. Beltran and F. Saegusa, "Behavior of superalloys in low temperature fused salt corrosion", Paper 292 at NACE International CORROSION/82 conference, March 22-26, 1982, Houston, TX, published NACE, Houston, 1982
53. A.L. Plumley and W.R. Roczniak, "Naturally occurring high chloride coal and superheater corrosion in a laboratory study", Paper 293 at NACE International CORROSION/82 conference, March 22-26, 1982, Houston, TX, published NACE, Houston, 1982.
54. Andreas Ruh and Michael Spiegel, "Thermodynamic and kinetic consideration on the corrosion of Fe, Ni and Cr beneath a molten KCl-$ZnCl_2$ mixture", Corrosion Science 48, 679-695, 2006.
55. M. Spiegel, "Salt melt induced corrosion of metallic materials in waste incineration plants", Materials and Corrosion, 50, 373-393, 1999.
56. W.M. Lu, T.J. Pan, K. Zhang and Y. Niu, "Accelerated corrosion of five commercial steels under a $ZnCl_2$-KCl deposit in a reducing environment typical of waste gasification at 673-773°K", Corrosion Science 50, 1900-1906, 2008.
57. Armin Zahs, Michael Spiegel and Hans J. Grabke, "Chloridation and oxidation of iron, chromium, nickel and their alloys in chloridizing and oxidizing atmospheres at 400-700°C", Corrosion Science 42, 1093-1122, 2000.
58. Y.S. Li and M. Spiegel, "Models describing the degradation of FeAl and NiAl alloys induced by $ZnCl_2$-KCl melt at 400-450°C", Corrosion Science 46, 2009-2023, 2004.
59. E. Otero, A. Pardo, M.C. Merino, M.V. Utrilla, M.D. Lopez and J.L. dePeso, "Corrosion behavior of IN-600 superalloy in waste-incineration environments: hot corrosion by molten chlorides", Oxidation of metals, 31 (516), 507-525, 1999.
60. Y.S. Li, Y. Niu and W.T. Wu, "Accelerated corrosion of pure Fe, Ni, Cr and several Fe-based alloys induced by $ZnCl_2$-KCl at 450°C in oxidizing environment", Materials Science and Engineering A345, 64-71, 2003.
61. T.J. Pan, C.L. Zeng and Y. Niu, "Corrosion of three commercial steels under $ZnCl_2$-KCl deposits in a reducing atmosphere containing HCl and H_2S at 400-500°C", Oxidation of Metals, 67 (1/2), 107-127, 2007.
62. S.C. Stultz and J.B. Kitto, Eds., "Steam – its generation and use", published Babcock and Wilcox, 1982. Available at http://www.gutenberg.org/etext/22657.
63. E. Otero, A. Pardo, F.J. Pérez, M.V. Utrilla and T. Levi, "Corrosion behavior of 12CrMoV steel in waste incineration environments: hot corrosion by molten chlorides", Oxidation of Metals 49 (516), 467-484, 1998.
64. Barbara Waldman, D. Schrupp-Heidelberger, B. Stöcker, Ferdinand Haider, Siegfried Horn and Ragnar Warnecke, "Corrosion monitoring in waste-to-energy plants", EUROCORR 2008, 7-11 September, Edinburgh, UK, published European Federation of Corrosion, published IOM^3, London, UK.
65. Satu Tuurna, Tommi Varis, Kimmo Ruusuvuori, Stefan Holmström, Jorma Salonen, Pertti Auerkari, Tuomo Kinnunen, Partik Yrjas, Risto Finne, Matti Nupponen, Ulla McNiven, Hannu Ahonen and Ari Kapulainen, "Managing corrosion in biomass boilers: benefits and limitations of coatings", Baltica VIII Conference on Life Management and Maintenance for Power Plants, Vol. 2, pages 22-36, published VTT, Espoo, Finland, 2010.

66. Satu Tuurna, Pekka Pohjanne, Sanni Yli-Olli, Tuomo Kinnunen and Petra Jauhianen, "Oxyfuel combustion: oxidation performance of steels in simulated oxyfuel condidions", Baltica VIII Conference on Life Management and Maintenance for Power Plants, Vol. 2, pages 52-62, published VTT, Espoo, Finland, 2010.
67. Esa K. Vakkilainen and Pekka Pohjanne, "Selecting the right material for recovery boiler superheaters", Baltica VIII Conference on Life Management and Maintenance for Power Plants, Vol. 2, pages 37-51, published VTT, Espoo, Finland, 2010.
68. R. Bender and M. Schütze, "Oxidation behavior of several commercial alloys in chlorine-containing high temperature environments", Paper 00239 at NACE International CORROSION/2000 conference, published NACE, Houston, 2000.
69. K. Salmenoja and K. Mäkela, "Prevention of superheater corrosion in the combustion of biofuels", Paper 00238 at NACE International CORROSION/2000 conference, published NACE, Houston, 2000.
70. Lars-Gunnar Johansson, Jan-Erik Svensson, Erik Skog, Jasper Pettersson, Carolina Pettersson, Nicklas Folkeson, Henrik Asteman, Torbjörn Jonsson and Mats Halvarsson, "Critical corrosion phenomena on superheaters in biomass and waste-fired boilers", Proceedings of the Sino-Swedish Structural Materials Symposium, 2007, pages 35-39.
71. I.G. Wright, A.K. Mehta, and K.K. Ho, "Survey of the Effects of Coal Chlorine Levels on Fireside Corrosion in Pulverized Coal Boilers". Proc. The Effects of Coal Quality on Power Plants: Fourth International Conference, Charleston, SC, August 17 – 19, 1994, published Electric Power Research Institute, Palo Alto, CA.
72. Martti Aho, Pasi Vainkka, Raili Taipale and Partik Yrjas, "Effective new chemicals to prevent corrosion due to chlorine in power plant superheaters", Fuel 87, 647-654, 2008.
73. B-J. Skrifvars, R. Backman, M. Hupa, K. Salmenoja and E. Vakkilianen, "Corrosion of superheater steel materials under alkali salt deposits Part 1: The effect of salt deposit composition and temperature", Corrosion Science 50, 1274-1282, 2008.
74. B-J. Skrifvars, M. Westén-Karlsson, M. Hupa and K. Salmenoja, "Corrosion of super-heater materials under alkali salt deposits. Part 2: SEM analyses of different steel materials", Corrosion Science 52, 1011-1019, 2010.
75. C. Pettersson, J-E. Svensson and L-G. Johansson, "Corrosivity of KCl(g) at temperatures above its dew point – initial stages of the high temperature corrosion of Alloy Sanicro 28 at 600°C", Materials Science Forum, 522-523, 539-546, 2006.
76. "Chlorout", published Vattenfall Business Services Nordic AB, August, 2005. Available as www.vattenfall.com/en/file/chlorout_8459980.pdf.
77. Bengt-Johan Skrifvars, Partik Yrjas, Tor Laurén, Jouni Kinni, Peter Siefen and Mikko Hupa, "The fouling behavior of rice husk ash in fluidized bed combustion. 1: Fuel characteristics", Energy Fuels 19 (4), 1503-1511, 2005.
78. Pierre Steinmetz, Ian G. Wright, Gerry Meier, Alan Galerie Bernard Pieraggi and Renaud Podor, "Laboratory testing for evaluation of steels and alloys used in superheater area of boiler for biomass-based fuels", Materials Science Forum, 461-464, 989-998, 2004.
79. Mischa Theis, Bengt-Johan Skrifvars, Mikko Hupa and Honghi Tran, "Fouling tendency of ash resulting from burning mixtures of biofuels. Part 1: Deposition rates", Fuel 85, 1125-1130, 2006.
80. Mischa Theis, Bengt-Johan Skrifvars, Maria Zevenhoven, Mikko Hupa and Honghi Tran, "Fouling tendency of ash resulting from burning mixtures of biofuels. Part 2: Deposit chemistry", Fuel 85, 1992-2001, 2006.
81. Mischa Theis, Bengt-Johan Skrifvars, Maria Zevenhoven, Mikko Hupa and Honghi Tran, "Fouling tendency of ash resulting from burning mixtures of biofuels. Part 3: Influence of probe surface temperature", Fuel 85, 2002-2011, 2006.
82. Flemming J. Frandsen, "Utilizing biomass and waste for power production – a decade of

contributing to the understanding, interpretation and analysis of deposits and corrosion processes", Fuel 84, 1277-1294, 2005.
83. Rachel Pettersson, Jasper Flyg and Peter Viklund, "High temperature corrosion under simulated biomass deposit conditions", Paper 09168 at NACE International CORROSION/2009 conference, March 22-26, 2009, Atlanta, GA, published NACE, Houston, 2009.
84. Erik Skog, Lars-Gunnar Johansson, Jan-Erik Svensson, Jesper Pettersson, Carolina Pettersson, and Nicklas Folkeson, "Why does bio-mass and waste cause severe corrosion of superheater tubes?", 33rd International Technical Conference on Clean Coal and Fuel Systems", Clearwater, FL, June 1-5, 2008, published Coal Technology Association, Gaithersburg, MD, 2008.
85. F.H. Stott, "Influences of alloy additions on oxidation", Materials Science and Technology, August 1989, 5, pages 734-740.
86. Robert A. Rapp, "Hot corrosion of materials", Pure and Applied Chemistry 62 (1), 113-122, 1990.
87. W.B.A. Sharp, "Incorporation of divalent cations in Cr_2O_3 during the oxidation of Fe-18%Cr-Ni alloys at 1123°K", Corrosion Science, 10, 283-295, 1970.
88. J.L. Blough and W.W. Seitz, "Fireside corrosion testing of candidate superheater tube alloys, coatings and claddings – Phase III", 15th Annual Conference on Fossil Energy Materials, April 30 – May 2, 2001, Knoxville, TN, published US Office of Scientific and Technical Information, 2001. Available as http://www.netl.doe.gov/publications/proceedings/02/materials/blough02.pdf
89. K. Natesan, A. Purohit and D.L. Rink, "Coal-ash corrosion of alloys for combustion power plants", 17th Annual Conference on Fossil Energy Materials, Baltimore, MD, April 22-24, 2003, published US National Energy Technology Laboratory.
90. John P. Shingledecker and Ian G. Wright, "Evaluation of the materials technology required for a 760°C power steam boiler", 8th Liege Conference on Materials for Advanced Power Engineering, Liege, Belgium, 18-20 September, 2006, Materials for Advanced Power Engineering, pages 107-119, published Grafische Medien, Belgium, 2006.
91. P. Henderson, P. Szákalos, R. Pettersson, C. Andersson, J. Hogberg, "Reducing superheater corrosion in wood-fired boilers", Werkstoffe, und Korrosion – Weinheim, 57 (2), 128-134, 2006.
92. K. Segerdahl, J. Pettersson, J-E. Svensson and L-G. Johansson, "Is KCl(g) corrosive at temperatures above its dew point? Influence of KCl(g) on initial stages of high temperature corrosion of 11% Cr Steel at 600°C", Materials Science Forum, 461-464, 109-116, 2004.
93. Brian A. Baker and Gaylord D. Smith, "Corrosion resistance of Alloy 740 as superheater tubing in coal-fired ultra-supercritical boilers", Paper 04526 at NACE International CORROSION/2004 conference, March 28 - April 1, 2004 , New Orleans, LA, published NACE, Houston, 2004.
94. Horst Hack and Greg Stanko, "Fireside corrosion resistance of advanced materials for ultra-supercritical coal-fired power plants", 22nd Annual International Pittsburgh Coal Conference, Pittsburgh, PA, September 12-15, 2005, published University of Pittsburgh, 2005.
95. M. Uusitalo, M. Kaipiainen, P. Vuoristo and T. Mäntylä, "High temperature erosion-corrosion of superheater materials and coatings in chlorine-containing environments", Materials Science Forum, 369-372, 475-482, 2001.
96. K.E. Coleman, N.J.Simms, P.J. Kilgallon and J.E. Oakley, "Corrosion in biomass combustion systems", Materials Science Forum, 595-598, 377-386, 2008.
97. Melanie Montgomery, Ole Biede and Ole H. Larsen, "Corrosion investigations at Masnedø combined heat and power plant", Part VII, published as Technical University of Denmark report, 2002.

98. Anna Nafari and Anders Nylund, "Erosion corrosion of tubes in the loop seal of a biofuel boiler fired CFB plant", 7th Liege Conference on Materials for Advanced Power Engineering, Liege, Belgium, September 30 – October 2, 2002, published as Materials for advanced power engineering 2002 Schriften des Forschungszentrum, Jülich, Germany, 2002.
99. M. Aho, "Method for preventing chlorine deposition on the heat transferring surface of a boiler", Finnish Patent FI117631B, December 29, 2006.
100. R. Viswanathan, J.F. Henry, J. Tanzosh. G. Stanko, J. Shingledecker, B. Vitalis and R. Purgert, "U.S. Program on materials technology for ultrasupercritical power plants", J. Materials Engineering and Performance, 14 (3), 281-292, 2005.
101. U.S. Energy Information Administration, "Renewable energy consumption and electricity: preliminary statistics 2009", Office of Coal, Nuclear, Electric and Alternative Fuels, U.S. Department of Energy, Washington D.C., published August, 2010. Available at http://www.eia.gov/fuelrenewable.html.
102. Edgardo Coda Zabetta, Arto Hotta, Brad Moulton and Matti Hiltunen, "Biomass and waste co-combustion – European experience", 11th annual Electric Power conference, Rosemont, IL, May 12-14, 2009. Available at http://www.fwc.com/publications/tech_papers/files/TP_FIRSYS_09_01.pdf
103. Matti Hiltunen, Vesna Barišić and Edgardo Coda Zabetta, "Combustion of different types of biomass in CFB boilers", 16th European Biomass Conference, Valencia, Spain, June 2-6, 2008. Available at http://www.fwc.com/publications/tech_papers/files/TP_CFB_08_05.pdf
104. Edgardo Coda Zabetta, Vesna Barišić and Brad Moulton, "Foster Wheeler references and tools for Biomass- and waste-fired CFBs", 34th International Technical Conference on Coal Utilization and Fuel Systems, Clearwater FL, May 31 – June 4, 2009, published Coal Technology Association, Gaithersburg, MD, 2009. Available at http://www.fwc.com/publications/tech_papers/files/TP_CFB_09_06.pdf
105. C. Andersson, "A method for operating a heat-producing plant for burning chlorine-containing fuels", Patent WO 02059526, August 1, 2002.
106. Michael Gagliano, Gregory Stanko, Horst Hack, "Materials overview and fireside corrosion considerations for advanced steam cycles", Power-Gen International, Orlando, FL, December 2-4, 2008, Available at http://www.fwc.com/publications/tech_papers/files/TP_METAL_08_03.pdf
107. Vesna Barišić, Edgardo Coda Zabetta and Juha Sarkki, "Prediction of agglomeration, fouling and corrosion tendency of fuels in CFB co-combustion", 20th International conference on Fluidized Bed Combustion, Xi'an, China, May 18-20, 2009. Available at http://www.fwc.com/publications/tech_papers/files/TP_CFB_09_04.pdf
108. Dao N.B. Duong and David A. Tillman, "Chlorine issues with biomass co-firing in pulverized coal boilers: sources, reactions and consequences – a literature review", 34th International Technical Conference on Coal Utilization and Fuel Systems, Clearwater FL, May 31 – June 4, 2009. Available at http://www.fwc.com/publications/tech_papers/files/TP_PC_09_01.pdf
109. Paul Kilgallon, Nigel Simms and John Oakey, "Modeling corrosion in biomass-fired power plants", Paper 05318 at NACE International CORROSION/2005 conference, April 3-7, Houston, TX, published NACE, Houston, TX, 2005.
110. Xiaoyang Liu, Joerg Maier, Klaus R.G. Hein, "The kinetics and influence factors on chlorine-induced fireside corrosion in biomass combustion system. Part 3: Corrosion morphology of chlorine corrosion", *This is not the same as reference [1]. Aaron Fuller Stuttgart University has promised to send the citation.*
111. T.N.Adams, W.J. Frederick, T.M. Grace, M. Hupa, K. Iisa, A.K. Jones and H.N. Tran, editors, "Kraft Recovery Boilers", TAPPI Press, Atlanta, GA, 1997.

112. D.C. Crowe, W.C. Youngblood, "Recovery Boiler Superheater Corrosion," Preprints of 9th International Symposium on Corrosion in the Pulp and Paper Industry, CPPA, Montreal, PQ, pages 225-230, 1998.
113. F. Bruno, "Thermochemical Aspects on Chloride Corrosion in Kraft Recovery Boilers", Paper No. 01426 at NACE International CORROSION/2001 conference, Houston, TX, published NACE, Houston, 2001.
114. M.Mäkipää, E, Kauppinen, T. Lind, J. Pyykönen, J. Jokiniemi, P. McKeough, M. Oksa, Th. Malkow, R.J. Fordham, D. Baxter, L. Koivisto, K. Saviharju, E. Vakkilainen, "Superheater tube corrosion in recovery boilers," 10th International Symposium on Corrosion in the Pulp and Paper Industry, Volume 1, published VTT, Espoo, Finland: 157-180, 2001.
115. J. Tuiremo, K. Salmenoja, "Control of superheater corrosion in black liquor recovery boilers" 10th International Symposium on Corrosion in the Pulp and Paper Industry, Volume 1, published VTT, Espoo, Finland: 181-200, 2001.
116. Rainer Backman, Mikko Hupa and Bengt-Johan Skrifvars, "Predicting superheater deposit formation in boilers burning biomasses", Impact of Mineral Impurities in Solid Fuel Combustion, edited by R. Gupta, T. Wall and L. Baxter 3, 405-416, published Kluwer/Plenum Publishers, NY, 2002. (Proceedings of an Engineering Foundation conference on mineral matter in fuels, Kona, Hawaii, November 2-7, 1997).
117. H. N. Tran, X. Mao, D.C.S. Kuhn, R. Backman and M. Hupa, "The sticky temperature of recovery boiler fireside deposits", Pulp & Paper Canada, 103 (9), 29-33, 2002.
118. Matthew J. Estes, Institute of Paper Chemistry, Atlanta, GA, Private communication, 1989.
119. P-E. Ahlers, A. Jaakola, "Experiences of austenitic superheater tube bends in Finnish recovery boilers, Black Liquor Recovery Boiler Symposium 1982, Ekono Oy/Finnish Recovery Boiler Committee/Finnish Energy Economy Association, Helsinki, Finland: D7-1, (1982).
120. H. Tran, Y. Arakawa, "Recovery Boiler Technology in Japan," Paper 12-6 at TAPPI 2001 Engineering/Finishing and Converting Conference, Published TAPPI Press, Atlanta, GA, pages 49-62, 2001.
121. L. Paul, G. Clark and M. Eckhardt, "Laboratory and Field Corrosion Performance of a High Chromium Alloy for Protection of Waterwall Tubes from Corrosion in Low NOx Coal Fired Boilers," Paper No. 06473 at NACE International CORROSION/2006 conference, published NACE, Houston, TX, 2006.
122. S.D. Kiser, E.B. Hinshaw and T. Orsini, "Extending the life of fossil fired boiler tubing with cladding of nickel based alloy materials," Paper No. 06474 at NACE International CORROSION/2006 conference, published NACE, Houston, TX, 2006.
123. Bernard S. Covino, Jr., Gordon R. Holcomb, Stephen D. Cramer, Sophie J. Bullard and Margaret Ziomek-Moroz and Mark L. White, "Corrosion in a temperature gradient", 17th Annual Conference on Fossil Energy Materials, Baltimore, MD, April 22-24, 2003 Available at www.netl.doe.gov/publications/proceedings/03/materials/manuscripts/Holcomb_m.pdf.
124. M-I. M. Chou, J.M. Lytle, S.C. Kung and K.K. Ho, "Effects of chlorine in coal on boiler superheater/reheater corrosion", 1999 Spring Meeting of ACS Division of Fuel Chemistry, 44 (1), 167-171, 1999. Available at http://www.anl.gov/PCS/acsfuel/preprint%20archive/Files/44_1_ANAHEIM_03-99_0167.pdf.
125. S. Enestam, J. Niemi and K. Mäkelä, "STEAMAX – a novel approach for corrosion prediction, materials selection and optimization of steam parameters for boilers firing fuel and fuel mixtures derives from biomass and waste", 33rd International Technical Conference on Clean Coal and Fuel Systems", Clearwater, FL, June 6-10, 2008, published Coal

Technology Association, Gaithersburg, MD, 2010.
126. Sonja Enestam, Pekka Lehtonen and Bengt Heikne, "Operating experience of the novel FBHE superheater at Norrköping Energy from waste facility, 9th International Conference on Circulating Fluidized Beds, May 13-16, 2008, Hamburg, Germany (In conjunction with 4th International VGB Workshop "Operating experience with fluidized bed firing systems", published TuTech Innovation, Hamburg, Germany, 2008.
127. Len Pinder, "Materials challenges in biomass combustion", MATUK Energy Materials Working Group Conference, Loughborough UK, 09-10/10/2008, available as http://www.matuk.co.uk/docs/Len%20Pinder%20Biomass%20combustion.pdf.
128. Colin Davis, "Impact of oxy-fuel operation on corrosion in coal-fired power plant", Carbon capture and Storage opportunities, Harrogate, UK, May 25, 2010, published National Metals Technology Centre, Rotherham, UK, 2010. Available as http://www.specialmetalsforum.com/uploads/docs/12754067434.EONEngineeringOxyfuelCorrosion.pdf.
129. T. Valmari, T.M.Lind, E. Kauppinen, G. Sfiris, K. Nilsson and W. Maenhaut, "Field study on ash behavior during circulating fluidized bed combustion of biomass. 2: Ash deposition and alkali vapor condensation", Energy Fuels, 13 (2), 390-395, 1999.
130. Patrycja Piotrowska, Maria Zevenhoven, Kent Davidsson, Mikko Hupa, Laars-Erik Åmand, Vesna Barišić and Edgardo Coda Zabetta, "Fate of alkali metals and phosphorus of rapeseed cake in circulating fluidized bed boiler Part 1: Co-combustion with wood", Energy Fuels, 24 (1), 333-345, 2010.
131. J. Pettersson, J-E. Svensson and L-G Johansson, "KCl-induces corrosion of a 304-type austenitic stainless steel in O_2 and in $O_2 + H_2O$ environment: The influence of temperature", Oxidation of Metals, 72 (3-4), 159-177, 2009.
132. Anna Nafari and Anders Nylund, "Field study on superheater tubes in the loop seal of a wood-fired CFB plant", Materials and Corrosion, 55 (12), 909-920, 2004.
133. M. K. Mann and P. L. Spath, "Net CO_2 emissions and energy balances of biomass and coal-fired power systems", in Biomass: A Growth Opportunity in Green Energy and Value-Added Products; Proceedings of the Fourth Biomass Conference of the Americas, 29 August - 2 September 1999, Oakland, CA, R.P. Overend and E. Chornet, Editors, Volume 1, pp. 379-385, published Elsevier Sceince, UK, 1999. NREL Report No. 27280.
134. F. Masuyama, "Alloy development and materials issues with increasing steam temperature", in Proceedings of 4th International Conference on Advances in Materials Technology for Fossil Power Plants, Hilton Head Island, October 25-28, 2004, Edited R. Viswanathan, D. Gandy, and K. Coleman published ASM International, Metals Park, OH, 2005. Available as www.asminternational.org/content/ASM/StoreFiles/05226G_Sample.pdf - 2008-08-12 -
135. E.K.Vakkilainen, "Future of recovery boiler technology", in 40th Anniversary International Recovery Conference, , Porvoo, Finland, May 12-15, 2004, pages 51-58, published Finnish Recovery Boiler Committee, 2004.
136. K. Salmenoja and J. Turiemo, "Achievements in the control of superheater corrosion in black liquor recovery boilers", Proceedings of TAPPI Engineering, Finishing and Converting Conference, Atlanta, pages 9-18, published TAPPI Press, Atlanta, 2001.
137. John L. Clement and Thomas M. Grace, "Investigation of superheater design and performance - Part 1, TAPPI Engineering, Pulping and Environmental Conference, October 11-14, 2009, Memphis, TN, 27 pages, published TAPPI Press, Atlanta, GA, 2009.
138. Thomas. M. Grace and John L. Clement, "Investigation of superheater design and performance, Part 2, TAPPI Engineering, Pulping and Environmental Conference, October 11-14, 2009, Memphis, TN, 14 pages, published TAPPI Press, Atlanta, GA, 2009.
139. S. Lokare, D. Dunaway, D. Rogers, M. Anderson, L. Baxter, D. Tree and H. Junker,

"Effects of fuel ash composition on corrosion deposits", Proceedings of 28th International Technical conference on Coal Utilization and Fuel Deposits, Clearwater, FL, March 9-13, 2003, published Coal Technology Association, Gaithersburg, MD, 2003.
140. E. Latham, D.B. Meadowcroft and L. Pinder, "The effects of coal chlorine on fireside corrosion", in Chlorine in Coal, Edited by J.Stringer and D.D. Banerjee, published Elsevier, Amsterdam, 1991.
141. P.A. Jensen, B. Sander and K. Dam-Johansen, "Pretreatment of straw for power production by pyrolysis and char wash", Biomass and Bioenergy, 20 (6), 431-446, 2001.
142. P.A. Jensen, B. Sander and K. Dam-Johansen, "Removal of K and Cl by leaching of straw char", Biomass Bioenergy, 20 (6), 447-457, 2001.
143. B-J. Skrifvars, T. Laurén, M. Hupa, R. Korbee and P. Ljung, "Ash behaviour in a pulverized wood fired boiler – a case study", Fuel, 83, 1371-1379, 2004.
144. D.M. Glover, "Heat Flux Effects on Oxidation Rates and Kinetics," Corrosion Science 20 (1980) pp. 1185-1193.
145. P.J. James and L.W. Pinder, "The impact of fuel chlorine on the fireside corrosion behavior of boiler tubing: A UK Perspective", NACE International COROSION/97 conference, New Orleans, LA, March 1997, published NACE, Houston, TX, 1997.
146. Y.Y.Lee and M.J. McNallan, "Ignition of nickel in environments containing oxygen and chlorine", Metallurgical Trans. A, 18 (6), 1099-1107, 1987.
147. Paul J. James, E.ON Engineering Group, Ratcliffe-on-Soar, UK, Private Communication, August 18, 2010.
148. P.J. James and L.W. Pinder, "Effect of coal chlorine on the fireside corrosion of boiler furnace wall and superheater/reheater tubing", Materials at High Temperatures, 14 (3), 187-196, 1997.
149. H.H. Krause, D.A. Vaughan, P.W. Cover, W.K. Boyd and R.A. Olexsey, "Corrosion and deposits from combustion of solid waste, Part VI: Processed refuse as a supplementary fuel in a stoker-fired boiler", Trans. ASME Journal of Engineering for Power, 101 (10), 592-597, 1979.
150. K. Salmenoja, K. Mäkelä, M. Hupa and R. Backman, "Superheater corrosion in environments containing potassium and chlorine", Journal of the Institute of Energy, 69 (480). 155-162, 1996.
151. David J. Young, High Temperature Corrosion and Oxidation of Metals, page 391, published Elsevier, 2008.
152. George Y. Lai, High-Temperature Corrosion of Engineering Alloys, page 145-149, published ASM International, Materials Park, OH, 1990.
153. Neil Birks, Gerald H. Meier and Fred S. Pettit, Introduction to the High Temperature Oxidation of Metals, 2nd Edition, pages 230-237, published Cambridge University Press, 2006.
154. Marko Palonen, Pekka Lehtonen and Tero Luomaharju, "Increase of steam data with challenging fuels", October 8, 2009. Available as www.processeng.biz/iea-fbc.org/upload/59_3_Palonen.pdf.
155. P.J. Henderson, P. Ljung, P. Kallner and J. Tollin, "Fireside corrosion of superheaters in a wood-fired circulating fluidized bed boiler", EUROCORR 2000 conference, September 10-14, 2000, London, U.K., published Institute of Materials, Minerals and Mining, London, 2000.
156. Y. Kawahara, M. Kira and M. Ike, "Effect of gas temperature and its fluctuation on the high temperature corrosion of WTE boiler materials", Paper 01159 at NACE International CORROSION 2001 Conference, March 11-16, Houston, published NACE, Houston, TX, 2001.
157. Patrycja Piotrowska, Maria Zevenhoven, Kent Davidsson, Mikko Hupa, Laars-Erik

Åmand, Vesna Barišić and Edgardo Coda Zabetta, "Fate of alkali metals and phosphorus of rapeseed cake in circulating fluidized bed boiler Part 2: Co-combustion with coal", Energy Fuels, 24 (8), 4193-4205, 2010.

158. Shang-Hsiu Lee, Nickolas J. Themelis and Marco J. Castaldi, "High temperature corrosion in waste-to-energy boilers", Journal of Thermal Spray Technology, 16 (1), 1-7, 2007.

159. Michaël Becidan, Lars Serum, Flemming Frandsen and Anne Juul Pedersen, "Corrosion in waste-fired boilers: a thermodynamic study", Fuel, 88 (4), 595-604, 2009.

160. Niels Henriksen, Rudolf Blum and Ole Hede Larsen, "Investigations of the possibilities of influencing the corrosive environment in an external ash cooler", International Flame Research Foundation TOTeM 24 meeting, "Challenges in the development of high efficiency combustion - The Excess Enthalpy Combustion Project", March 19, 2003, Velsen Noord, The Netherlands, pages 271-294. Available at: ftp://www.ifrf.net/pub/pdf/JOF3-CT95-0024-pdf-files/JOF3-CT95-0024-06-Henriksen-ElsamP.pdf

161. N.B. Pilling and R.E. Bedworth, Journal of the Institute of Metals 29, 529-591, 1923.

162. Carl Wagner, "Beitrag zur Theorie des Anlaufvorgangs (On the Theory of Scaling Reactions)", Z. Phys. Chem. B, 21, 25-41, 1933.

163. Stanislaw Mrowec and Teodor Werber, Gas Corrosion of Metals (translated from "Korozja Gazowa Metali" – published by Wyndawnictwo "Slqsk", 1975 by Waldemar Bartoszewski), published for the NBS and NSF by Foreign Scientific Publications Department of the National Center for Scientific, Technical and Economic Information, Warsaw, Poland, 1978 (TT 76-54038) and available from NTIS, Springfield VA.

164. US Environmental Protection Administration, "Materials characterization paper in support of the proposed rulemaking – Identification of nonhazardous secondary materials that are solid waste coal combustion residuals - coal fly ash, bottom ash, and boiler slag", published April 5, 2010 and available at http://www.epa.gov/wastes1994./nonhaz/define/pdfs/coal-combust.pdf

165. Y. Kawahara, "Evaluation of high temperature corrosion life using temperature gradient corrosion test with thermal cycling component in waste combustion environments", Werkstoffe und Korrosion (Materials and Corrosion) 57 (1), 60-72, 2006.

166. Ragnar Warnecke, Bernd Benker, Christian Deuerling, Ferdinand Haider, Siegried Horn, Jürgen Maguhn, Volker Müller, Hermann Nordsieck, Barbara Waldmann, Ralf Zimmermann, "The mechanisms of corrosion and how to avoid them", 5th ISWA Beacon conference on Waste-to-Energy, October 25, 2007, Malmo, Sweden. Available at http://www.beacon-wte.org/index.php?id=30

167. Anders Hjörnhede, Vattenfall Power Consultant, Racksta, Sweden, Private communication, June 28, 2010.

APPENDIX A
SUPERHEATER CORROSION AND ALLOY PERFORMANCE IN CURRENT GENERATION HIGH PRESSURE RECOVERY BOILERS
(pages 53 to 59 of reference [31])

APPENDIX A. SUPERHEATER CORROSION AND ALLOY PERFORMANCE IN CURRENT GENERATION HIGH PRESSURE RECOVERY BOILERS (pages 53 to 59 of reference [31])

Corrosion of superheaters is generally not an issue in recovery boilers that are operated at a steam temperature below 450°C [32]. In current generation high pressure (HP) boilers, steam temperatures are somewhat higher, usually ranging from 480°C to 500°C. It is generally accepted that accelerated corrosion of superheaters in a HP recovery boiler is mainly caused by molten salt attack [32-36]. Molten salts are generally a good fluxing agent, effectively removing protective metal oxide scale from an alloy surface. Accelerated corrosion proceeds primarily by oxidation, which is then followed by dissolution of metal oxides in the melt.

Superheater deposits consist mainly of sodium sulfate (Na_2SO_4) and sodium carbonate (Na_2CO_3) with small amounts of sodium sulfide (Na_2S), sodium chloride (NaCl) and similar potassium (K) salts [32, 37]. The first melting temperature (FMT) of the deposit depends on the concentration of potassium, carbonate (CO_3^{2-}) and sulfide (S_2-) in the deposit, typically ranging from 520°C to 580°C [37]. Another critical factor is the proportion of liquid phase present at the first melting temperature (FMT) which strongly depends on the chloride concentration [38]. Reported field studies and operating experience consistently show that the corrosion rate of superheater tubes increases rapidly when the first melting point of the deposit is exceeded, and more so if the molten deposit contains sulfide or reduced sulfur compounds [33,39-44]. In the past, many superheater corrosion problems were often caused by molten acidic sulfate deposits containing sodium and potassium bisulphate [$(Na,K)HSO_4$] and pyrosulfate [$(Na,K)S_2O_7$] salts, which are stable at elevated concentrations of acidic sulfur gases (SO_x) [39]. However, as recently discussed, typical SO_x levels produced with current operating practices are not, under almost any circumstances, high enough to promote corrosion by the formation of these molten acidic sulfate salts [34].

Superheater design for low pressure (<6,000 kPa), (LP) recovery boilers traditionally has been governed by the need to achieve a balance between performance (steam temperature and pressure) and plugging. Relative to other boilers, recovery boilers have a much higher particulate flux through the superheater section, and, consequently tend to plug more easily [45]. Side-to-side spacing (across the bank), tube size and mechanical design (including support) has varied throughout the decades to accommodate overall boiler design [46, 47]. Low alloy steels have been commonly used for superheater tubes in LP boilers, with the selection generally governed by similar design constraints as for other types of boilers, namely high temperature strength, creep resistance, oxidation resistance and economics. Table 2 identifies the low alloy steels most commonly used along with the recommended maximum allowable tube temperature.

Table 2. Typical superheater tube materials in LP/HP kraft recovery boilers

Specification		Nominal Composition (wt.%)						Max. T[1]
ASME	UNS	Fe	Cr	Ni	Mo	Cu	C	(°C)
SA-209T1A	K12023	Bal.	- - -	- - -	0.44-0.65	- - -	0.15-0.25	524
SA-213T11	K11597	Bal.	1.0-1.5	- - -	0.44-0.65	- - -	0.05-0.15	566
SA-213T22	K21590	Bal.	1.9-2.6	- - -	0.87-1.13	- - -	0.05-0.15	602
SA-213T91	K90901	Bal.	8.5-9.5	- - -	0.85-1.05	- - -	0.08-0.12	649
SA-213T304	S30400	Bal.	18.0-20.0	8.0-11.0	- - -	- - -	0.08 Max.	760
SA-213TP347H[2]	S34709	Bal.	17.0-20.0	9.0-13.0	- - -	- - -	0.04-0.10	760
SA-213TP310H[3]	S31009	Bal.	24.0-26.0	19.0-22.0	- - -	- - -	0.04-0.10	816
SB-407-800H	N08810	Bal.	19.0-23.0	30.0-35.0	- - -	0.75 Max	0.10 Max.	816
Sanicro™ 28[3]	N08028	Bal.	27.0	31.0	3.5	1.0	0.02 Max.	N/S[4]

[1] Recommended maximum use temperature for superheater tube use in fossil-fired boilers [48].
[2] Nb/Ta content of not less than eight times the carbon content and not more than 1.0 wt.%.
[3] Fabricated as a co-extruded composite tube; exterior layer over a SA-213T22 core.
[4] N/S = Not Specified

For superheaters in HP recovery boilers, a balance between performance, plugging and corrosion is required. With respect to corrosion, a key superheater design constraint is to maintain tube temperatures below the first melting point of the deposits. Temperatures are reduced by ensuring relatively low flue gas velocity, ensuring relatively high steam flow through each tube, arranging for the coolest steam to flow through tubes exposed to hottest flue gas, and locating the majority of the superheater sections behind the bull nose (furnace arch), shielded from radiation [46,47].

This design philosophy has permitted the widespread use of the less-expensive low alloy steels as superheater tube materials. However, such application has not been without problems. Reported experience with HP superheaters fabricated entirely of low alloy steel, revealed rapid corrosion at the bottom bends, with measured rates ranging from 0.3-0.6 mm/y [33,39,44] to as high as 2.4 mm/yr [49]. The cause in each case was attributed to elevated temperatures of the lower bends. Based on the various resistances to heat transfer, the surface temperature of a superheater tube is expected to be about 30 to 50C° hotter, or higher if affected by direct radiation, than the steam temperature inside the tube [50, 51]. In addition, the tube temperature may be 20C° hotter on the windward side than on the leeward side [43]. Note also that the individual tube steam temperature can vary ± 23C° from the average across the steam manifold [52]. The resultant combined increase may be beyond the FMT of the deposit depending upon the composition.

Replacing the low alloy steel lower tube bends with higher chromium-containing, more corrosion-resistant alloys has been one approach used to address the accelerated corrosion observed. A listing of the more typical alloys used is also provided in Table 3. The selection of these alloys was based largely on prior field testing using air-cooled probes [33, 39-44]. Reported experiences of using these upgrades have been positive for the most part. A summary of preliminary experience (no more than seven years' service) of austenitic stainless steel lower tube bends installed in Finnish HP recovery boilers (480°C/8,000 kPa superheater units) was published some time ago [53]. As reported, the corrosion rate of the installed tube bends, fabricated from Type 304, 304L, 321 and 347 stainless steel, was around 0.1 mm/yr, with no significant differences found between the various grades of stainless steel used. There are also limited reports of low corrosion rates observed on Alloy 800H lower tube bends installed in Canadian HP recovery boilers (482°C/6,200 kPa superheater units); one based on a little more than two years of service [40], and the other based on about twenty years of service [54].

However, there have been reported cases in which these alternatives have experienced accelerated corrosion. A summary of these cases is provided in Table 4. A reported case of accelerated corrosion exists for each of the major alloys used as replacement upgrades, with the exception of Alloy 28 for lower superheater tube bends. Alloy 28 tube bends have been installed in Swedish, Brazilian and Finnish HP recovery boiler since 1994 [55]. An elevated tube temperature was identified as the root cause of the accelerated corrosion in each of the reported cases. This conclusion is consistent with the findings of the air-cooled probe studies, which show corrosion of these alternative alloys increases rapidly when the first melting point of the deposit is exceeded [33, 39-44].

In addition to the fireside corrosion issues noted above, the reliability of superheaters in recovery boilers is also strongly affected by stress-related problems. Given that the superheaters are suspended through the roof and hang freely in the flue gas environment, they are susceptible to a combination of mechanical and thermal static and/or cyclic stresses, during start-ups, operation and shut-downs. As recently discussed, these problems can results in distortion (in-plane and out-of-plane) of the assembly, cracks at attachments, or crack-induced tube leaks [57]. Another cause for concern is waterside stress corrosion cracking. As reported in the literature, the monolithic authentic stainless steel tube bends are likely more susceptible [58].

Table 3. Reported cases of accelerated lower tube bend corrosion of replacement alloys

Tube Alloy	Design Steam T (°C)	Design Steam P (kPa)	Tube T (°C)	Deposit FMT (°C)	Corrosion Rate (mm/yr)	Ref.
SA-213T304	480	8,000	N/R	N/R	N/R	[42]
SA-213T304	480	6,500	N/R	N/R	N/R	[42]
SA-213TP347H	480	8,000	N/R	N/R	2.4-3.6	[49]
SA-213TP347H	480	8,000	N/R	N/R	0.3-1.6	[49]
SA-213TP347H	480	8,000	N/R	N/R	1.5	[49]
SA-213TP347H	482	8,620	> 590	520	1.0-2.0	[43]
SA-213TP310H/SA-213T22	454	6,200	> 590	560	1.0-2.0	[56]
SB-407-800H	482	6,200	N/R	N/R	0-1.4	[54]

*N/R = Not Reported.

Superheater Corrosion and Control in Next Generation HT/HP Recovery Boilers

Next generation HT/HP recovery boilers, which are operated at a steam temperature of 500 to 515°C and a steam pressure of 9,900 to 10,900 kPa, already exist in Japan [59-62]. Key design features implemented that help control superheater tube corrosion are reported by the boiler manufacturer to include the installation of non-process element (NPE), namely potassium and chlorine, removal equipment downstream of the recovery boiler, use special austenitic (25Cr-14Ni) stainless steels, and a large number of soot blowers. Reducing the potassium and chlorine content in the liquor cycle helps to control corrosion by lowering the potassium and chlorine content in the deposits that form on the superheater tubes, which in turn increases the FMT [37] and decreases the proportion of the liquid phase present [38], respectively. The special stainless steels were developed with input from laboratory studies, as well as from operating experience [59, 63, 64]. Table 5 documents the nominal compositions of the three grades developed. The original grade YUS170 was used in early HT/HP recovery boilers. The latest grade MN25R was developed to improve the strength at high temperatures and to increase the (intergranular) corrosion resistance. Experience reported has been positive with these alloys, except when there has been contact with a high sulfur dioxide (SO_2)

concentration in the flue gas, and with deposits enriched in chlorine (as chloride) [61]. There was no mention of a waterside stress corrosion cracking concern. It is noted that no independent confirmation of boiler operation and/or superheater tube performance has been reported in the public domain.

The recent interest in implementing the next generation HT/HP recovery boilers in Finland has also initiated laboratory-based research and development programs designed to identify more corrosion resistant alloys from which to fabricate superheater tubes [35,65-67], in addition to those conducted in Japan [59,63,64]. An overview of the alloys and testing conditions studied is provided in Table 5. As the summary shows, a wide range of alloys have been tested in a wide range of salt mixtures, exposed to a wide range of cover gas mixtures, for a wide range of times. In spite of the many inconsistencies among the testing parameters, these studies have generated a reasonably consistent set of results, and thus conclusions regarding corrosion above the FMT.

Major findings are summarized as follows.
• Corrosion increases significantly at temperatures above the FMT, the extent of which increases with the amount of molten phase present at a given temperature.
• The corrosion mode is mostly localized (pitting and intergranular attack), consistent with a mechanism involving attack by a molten chloride-containing salt, and does not require an interaction with SO_2 or HCl in an O_2-containing gas phase.
• Alloys with higher chromium contents have a higher corrosion resistance, more so, if molybdenum and nitrogen are present as additional alloying elements.
• Finally, the removal of non-process elements (NPE) (potassium and chlorine) from the chemical recovery process is a critical part of corrosion control.

In contrast, the conclusions drawn from these studies regarding the corrosion of alloys below the FMT are less consistent. There is a consensus that the risk of corrosion below the FMT by the so-called "active-oxidation" mechanism [68, 69] is low for the set of alloys studied, with the exception of the low alloy steel grade SA-213T22. Active oxidation involves the formation of Cl_2/HCl gas within a chloride-containing deposit, which then migrates to the alloy/scale interface, where the partial pressure of oxygen is low, and then reacts to form volatile metallic chlorides. As the vapor pressure of the metallic chloride products is considerable at the typical heat transfer surface temperatures involved, continuous sublimation occurs, and the gaseous metallic chlorides diffuse towards the scale/flue gas interface. Upon reaching regions with high oxygen (O_2) partial pressures, the gaseous metallic chlorides react with O_2/water vapor (H_2O) to form solid oxides, releasing Cl_2/HCl. The resulting scale is almost detached from the substrate and offers little protection.

Table 4. Superheater tube materials in HT/HP recovery boilers in Japan

Grade	Nominal Composition (wt.%)							
	Fe	Cr	Ni	Mo	Mn	Si	N	C
YUS170	Bal.	23.0-26.0	12.0-16.0	0.5-1.2	< 2.0	< 1.5	0.25-0.40	< 0.06
HR-2EL	Bal.	21.0-23.0	12.5-15.5	1.0-2.0	2.5-3.5	< 0.5	0.10-0.25	< 0.02
MN25R	Bal.	23.0-26.0	13.0-16.0	0.5-1.2	< 2.0	< 0.7	0.25-0.40	< 0.025

Several studies [65, 70] conclude that, below the FMT, KCl-containing recovery boiler deposits are more corrosive than NaCl-containing ones, whereas others report the opposite [71, 72]. Another controversy involves the critical temperature at which active oxidation initiates for stainless steel alloys. Based on a laboratory test, corrosion of stainless steel by active oxidation was found to be moderately dependent on temperature in a range from 550 to 650°C, and strongly dependent on

temperatures at temperatures in excess of 650°C [73]. However, a recent study documenting the corrosion of high alloy superheater tubes in a waste-wood fluidized-bed boiler shows the critical temperature may be as low as 500°C for stainless steel [74].

Table 5. Laboratory superheater tube corrosion testing for HT/HP recovery boilers

Alloys	Deposit Composition				FMT	Environment	Ref.
	NaCl	K	Cl	S			
316, 321, 347	10%	5%	N/R	N/R	N/R	Gas: Not Reported	[59]
YUS170	5%	10%	N/R	N/R	N/R	Temperature: 480-520 °C	
	10%	10%	N/R	N/R	N/R	Time: Not Reported	
	NaCl	K	Cl	S			
321	N/R	5%	3%	N/R	550 °C	Gas: 0.005-1%SO_2-5%O_2-10%CO_2-N_2	[63]
YUS170,MN25R	[56%(Na,K)SO_4-6.5%NaCl]					Temperature : 500-600 °C	
						Time: Not Reported	
304, 316, 316L, 321,	Na	K	Cl	S		Gas: 0.25-1%SO_2-1%O_2-15%CO_2-N_2	
347, 310,170, N71,	34.3%	16.2%	3.9%	12.7%	523 °C	Temperature: 450-650 °C	[64]
HR3CL,A600, A800						Time: 20 Hours	
T22, 304L,HR3C,	Na_2SO_4	Na_2CO_3	NaCl	KCl		Gas: Air; Air + HCl, SO_2, CO_2 or H_2O	
170NBB,AC66,45TM	59%	0%	6.5%	34.5%	N/R	Temperature: 525 °C	[65]
SAN28, A625	37.3%	28%	15.3%	19.3%	N/R	Time: 2-65 Hours	
	Na_2SO_4	K_2SO_4	NaCl	KCl			
T11	49.5%	49.5%	0.5%	0.5%	525 °C		
304L	47.5%	47.5%	2.5%	2.5%	524 °C	Gas: Air	
310	45%	45%	5,%	5%	522 °C	Temperature: 440-590 °C	[66]
A625	40%	40%	10%	10%	518 °C	Time: 6-168 Hours	
	10%	10%	40%	40%	509 °C		
T11,T22,304,HR11N	Na_2SO_4	Na_2CO_3	NaCl	KCl		Gas: Air	
HR3C,SAN28,AC66	59.0%	0%	6.5%	34.5%	N/R	Temperature: 520-530 °C	[67]
45TM,170TMB,A625						Time: 0.2-44 Hours	

As the literature points out, there are many critical factors that influence the corrosion resistance of superheater tube alloys, both above and below the FMT of a typical deposit in a HT/HP recovery boiler. In spite of the relevant field studies conducted in HP recovery boilers using air cooled probes and laboratory studies conducted under controlled conditions, it remains difficult to directly compare the corrosion resistance of candidate tube alloys. Comparisons among the field test results reported are not reliable considering the variable, poorly-defined, albeit real, environmental conditions encountered within the various boilers under study. Comparisons among the controlled laboratory test results reported are not reliable as a consequence of the differences in the testing parameters. Among the documented lab tests, it is difficult to assess, in a quantitative manner, the relative effect of elevated temperature, time at temperature both below and above the FMT, and gas composition, for a given deposit composition and alloy. In addition, more information is required on the possible influence of water vapor on corrosion both above and below the FMT. This is important since soot blowing can increase the local H_2O concentration by 3.5 vol. % [75]. Dissolved H_2O in molten chloride-containing salts has been reported to enhance melt corrosivity [67, 71]. Also, in recently reported corrosion tests, water vapor additions (2 vol. %) were found to increase the corrosion rate of

chromium-containing, nickel-based alloys tested in a simulated reducing low nitrogen oxide (NO_x) coal-fired combustion environment [76,77]. This finding may be relevant in HT/HP recovery boilers under conditions of high carryover.

REFERENCES

(including papers referred to in other parts of the final report)

1. James R. Keiser, Douglas L. Singbeil, Gorti B. Sarma, Joseph R. Kish, Jerry Yuan, Laurie A. Frederick, Kimberly A. Choudhury, J. Peter Gorog, François R. Jetté, Camden R. Hubbard, Robert W. Swindeman, Preet M. Singh, and Philip J. Maziasz, "Cracking and Corrosion of Composite Tubes in Black Liquor Recovery Boiler Primary Air Ports", ORNL/TM-2006/112, October 2006.
2. James R. Keiser, Gorti B. Sarma, Arvind Thekdi, Roberta A. Meisner, Tony Phelps, Adam W. Willoughby, John Zeh, J. Peter Gorog, Shridas Ningileri, Yansheng, Liu and Chenghe Xiao, "Improved Materials and Operation Of Recuperators For Aluminum Melting Furnaces", Final Report for Task 1 of DOE award # DE-FC36-04GO14035 (available from OSTI; OSTI Report No. 919037).
3. A.L. Plumley, E.C. Lewis, and R.G. Tallent, "External Corrosion of Water Wall-Tubes in Kraft Recovery Furnaces," Tappi J, 49(1), 72A (1966).
4. R.G. Tallent, A.L. Plumley, "Recent Research on External Corrosion of Waterwall Tubes in Kraft Recovery Furnaces," Tappi J., 52(10), 1955 (1969).
5. D. Singbeil, L. Frederick, N. Stead, J. Colwell, G. Fonder, "Testing the Effects of Operating Conditions on Corrosion of Water Wall Materials in Kraft Recovery Boilers," 1996 TAPPI Engineering Conference, TAPPI Press, Atlanta, GA, 649 (1996).
6. P.M. Singh, S.J. Al-Hassan, S. Stalder, G. Fonder, "Corrosion in Lower Furnace of Kraft Recovery Boilers - In situ Characterization of Corrosive Environments", Tappi J., 3(2), 21 (2003).
7. A.L. Plumley, W.R. Roczniak, "Recovery Unit Waterwall Protection, A Status Report," Tappi J, 58(9), 118 (1975).
8. W.B.A. Sharp "Composite Furnace Tubes for Recovery Boilers – A Problem Solved," Tappi J., 64(7), 113 (1981).
9. 9. H. Tran, Kraft Recovery Boilers, T.N. Adams, W.J. Frederick, T.M. Grace, M. Hupa, K. Iisa, A.K. Jones, H. Tran (Eds.), TAPPI Press, Atlanta, GA (1998).
10. H. Dykstra, "Recovery Boiler Waterwall Tube Failure Analysis with Implications for Furnace Replacement and New Construction," 1998 TAPPI Engineering Conference, Volume 2, TAPPI Press, Atlanta, GA, p. 431 (1998).
11. P.M. Singh, J. Perdomo, J. Mahmood, "Mid-Furnace Corrosion in Kraft Recovery Boiler," 11th International Symposium on Corrosion in the Pulp and Paper Industry, TAPPI Press, Atlanta, GA (2004).
12. P.M. Singh, V.R. Behrani, "Fireside Corrosion of Carbon Steel Tubes in Kraft Recovery Boiler Mid-Furnace," Corrosion/05, Paper # 197, NACE, Houston, TX (2005).
13. P. McKeough, M. Kurkela, H. Kyllonen, E. Tapola, "New Insights into the Release of Sodium, Sulphur, Potassium and Chlorine during Black-Liquor Combustion and Gasification," LIEKKI 2, Technical Review 1993–1998. Volume 2, M. Hupa (Ed.), Abo Akademi University, Turku, Finland, 855 (1998).
14. 14. D.L. Feuerstein, J.F. Thomas, D.L. Brink, "Malodorous Products from the Combustion of Kraft Black Liquor. I. Pyrolysis and Combustion Aspects," Tappi J., 50(6), 258 (1967).
15. 15. J. Li, A. R. P. Van Heiningen, "Sulfur Emission during Slow Pyrolysis of Kraft Black Liquor," Tappi J, 74(3), 237 (1991).
16. V. Sricharoenchaikul, W.J. Frederick, T.M. Grace, "Sulphur Species Transformations During Pyrolysis of Kraft Black Liquor," J. Pulp and Paper Sci., 23(8), J394 (1997).
17. P.J. Ficalora, T.G. Godfrey, "Technique to Study Corrosion in Fluctuating Gaseous Atmospheres", Oak Ridge National Laboratory Report ORNL/TM-8734 (5900469; DE83014565), Oak Ridge, TN, (1983).

18. M.F. Stroosnijder , W.J. Quadakkers, "Review of High Temperature Corrosion of Metals and Alloys in Sulfidizing/Oxidizing Environments II. Corrosion of Alloys", High Temp. Technol., 4, 141 (1986).
19. J. Stringer, "Mixed Oxidant Corrosion in Coal Combustion and Conversion Systems: Manifestations and Mechanisms", High-Temperature Oxidation and Sulphidation Processes, J.D. Embury (Ed.), Pergamon Press, New York, 257 (1990).
20. B. Gleeson, "Alloy Degradation under Oxidizing-Sulfidizing Conditions at Elevated Temperatures", Mat. Res., 7(1), 61 (2004).
21. F. Gesmundo, D.J. Young, S.K. Roy, "The High-Temperature Corrosion of Metals in Sulfidizing-Oxidizing Environments: A Critical Review," High Temp. Mater. Proc., 8, 149. (2004).
22. H. J. Grabke, R. Lobnig, P. Papaiacovou, Johannesen, A.G. Andersen (Eds.), Selected Topics in High Temperature Chemistry: Defect Chemistry of Solids, Elsevier, New York, 263 (1989).
23. D.L. Douglass, P. Kofstad, A. Rahmel, G.C. Wood, "International Workshop on High Temperature Corrosion," Oxidation of Metals, 45(5-6), 529 (1996).
24. S.J. Al-Hassan, G.J. Fonder, P.M. Singh, "The Effect of Temperature Excursion on Sulfidation of Carbon Steel in 1% H2S Environment," Pulp & Paper Canada, 100(10), 40 (1999).
25. S. Osgerby, "Oxide Scale Damage and Spallation in P92 Martensitic Steel," Materials at High Temperatures, 17(2), 307 (2000).
26. M. Schulte, M. Schutze, "The Role of Scale Stresses in the Sulfidation of Steels," Oxidation of Metals, 51 (1/2), 55 (2002).
27. M. Mäkipää, M. Oksa, P. Pohjanne, "Corrosion Testing of High-Nickel Alloy Composite Tube Materials in Simulated Recovery Boiler Lower Furnace Conditions," 10th International Symposium on Corrosion in the Pulp and Paper Industry, Vol. 1, T. Hakkarainen (Ed.), VTT, Espoo, Finland, 73 (2001).
28. A. Hendry, "The Oxidation Resistance of Nitrided Mild Steel," Corrosion Science, 18(6), 555 (1978).
29. James R. Keiser, Gorti B. Sarma, Kimberly A. Choudhury, François R. Jetté, Richard L. Emerson, Elizabeth F. Walker, Joseph R. Kish, and Douglas L. Singbeil, "Investigation of a Superheater Tube Cracking Problem", TAPPI Engineering, Pulping and Environmental Conference, Philadelphia, PA, August 28-31, 2005.
30. Boardman, B., "Fatigue Resistance of Steels," Metals Handbook, 10th Edition, Volume 1 Properties and Selection: Iron, Steels, and High-Performance Alloys, Lampnam, S.R, Zorc, T.B., Editors, p. 678, ASM International, Materials Park, OH (1990).
31. "SA-210/SA-210M Specification for Seamless Medium-Carbon Steel Boiler and Superheater Tubes," 2004 ASME Boiler and Pressure Vessel Code, Section II – Materials, American Society of Mechanical Engineers, New York, NY (2004).
32. T.N. Adams, Wm.J. Frederick, T.M. Grace, M. Hupa, K. Iisa, A.K. Jones, H. Tran, Editors., Kraft Recovery Boilers, TAPPI Press, Atlanta, GA: p. 310 (1997).
33. D.C. Crowe, W.C. Youngblood, "Recovery Boiler Superheater Corrosion," 9th International Symposium on Corrosion in the Pulp and Paper Industry, CPPA, Montreal, QC: 225 (1998).
34. F. Bruno, "Thermochemical Aspects on Chloride Corrosion in Kraft Recovery Boilers," Paper No. 01426, CORROSION/2001, NACE, Houston, TX (2001).
35. M.Mäkipää, E, Kauppinen, T. Lind, J. Pyykönen, J. Jokiniemi, P. McKeough, M. Oksa, Th. Malkow, R.J. Fordham, D. Baxter, L. Koivisto, K. Saviharju, E. Vakkilainen, "Superheater Tube Corrosion in Recovery Boilers," 10th International Symposium on Corrosion in the Pulp and Paper Industry, Volume 1, VTT, Espoo Finland: 157 (2001).

36. J. Tuiremo, K. Salmenoja, "Control of Superheater Corrosion in Black Liquor Recovery Boilers" 10th International Symposium on Corrosion in the Pulp and Paper Industry, Volume 1, VTT, Espoo Finland: 181 (2001).
37. H. Tran, M. Gonsko, X. Mao, "Effect of Composition on the First Melting Temperature of Fireside Deposits in Recovery Boilers," Tappi Journal, 82(9): 93 (1999).
38. K. Salmenoja, "Field and Laboratory Studies on Chlorine-Induced Superheater Corrosion in Boilers Fired with Biofuels", Report 00-01, Faculty of Chemical Engineering, Abo Akademi, Turku, Finland (2000).
39. K.W. Morris, A.L. Plumley, W.R. Roczniak, "The Effect of Chlorides on Recovery Unit Superheater Wastage: An R&D Progress Report," Pulp and Paper Industry Corrosion Problems, Volume 3, NACE, Houston TX: 47 (1980).
40. D.W. Reeve, H.N. Tran, D. Barham, "Superheater Fireside Deposits and Corrosion in Kraft Recovery Boilers," Tappi Journal, 64(5): 109 (1981).
41. H.N. Tran, D.W. Reeve, D. Barham, "Local Reducing Atmosphere – A Cause of Superheater Corrosion in Kraft Recovery Units," Tappi Journal, 68(6): 102 (1985).
42. R. Backman, M. Hupa, E. Uppstu, "Fouling and Corrosion Mechanism in the Recovery Boiler Superheater Area," Tappi Journal, 70(6): 123 (1987).
43. C. Dees, J. Simonen, H. Tran, "Experience of Recovery Boiler Superheater Corrosion at Willamette Hawesville, 7th International Symposium on Corrosion in the Pulp and Paper Industry, TAPPI Press, Atlanta, GA: 251 (1992).
44. W. Blakemore, M. Ellis, H. Tran, "Experience of Recovery Boiler Superheater Corrosion at Carter Holt Harvey Kinleith," 11th International Symposium on Corrosion in the Pulp and Paper Industry," TAPPI Press, Atlanta, GA: 217 (2004).
45. T.N. Adams, Wm.J. Frederick, T.M.Grace, M. Hupa, K Iisa, A.K. Jones, H. Tran, Editors, Kraft Recovery Boilers, TAPPI Press, Atlanta, GA: p. 247 (1997).
46. S.C. Stultz, J.B. Kitto, Editors, Steam/Its Generation and Use, 40th Edition, Babcock & Wilcox Company, Barberton, OH: 26-10 (1992).
47. M.P. LeBel, "CRU Superheater Experience," Alstom Power Inc., Correspondence to Paprican, May 11, 2005.
48. S.C. Stultz, J.B. Kitto, Editors, Steam/Its Generation and Use, 40th Edition, Babcock & Wilcox Company, Barberton, OH: 6-21 (1992).
49. A. Jaakkola, T. Rose, "Operational Experiences of Austenitic Superheater Tube Bends in Recovery Boilers," Pulp and Paper Industry Corrosion Problems, Volume 4, Swedish Corrosion Institute, Stockholm, Sweden: 82 (1983).
50. 50. J.F. La Fond, A. Verloop, A.R. Walsh, "Engineering Analysis of Recovery Boiler Superheater Corrosion," Tappi Journal, 75(6): 101 (1992).
51. F. Bruno, "The Significance of Superheater Tube Corrosion on the Steam Temperature of Kraft Recovery Boilers," 8th International Symposium on Corrosion in the Pulp and Paper Industry, Swedish Corrosion Institute, Stockholm, Sweden: 138 (1995).
52. D.N. French, Metallurgical Failures in Fossil Fired Boilers, John Wiley & Sons, New York, NY: 248 (1983).
53. P-E. Ahlers, A. Jaakola, "Experiences of Austenitic Superheater Tube Bends in Finnish Recovery Boilers, Black Liquor Recovery Boiler Symposium 1982, Ekono Oy/Finnish Recovery Boiler Committee/Finnish Energy Economy Association, Helsinki, Finland: D7-1 (1982).
54. C. Reid, "Lower Bend Superheater Tube Experience in Coastal Recovery Boilers," Acuren, Correspondence to Paprican, November 5, 2001.
55. "Sandvik Sanicro 28 – Composite Tube for Steam Boiler Application," S-12111-ENG, Sandvik Steel, Sandviken, Sweden (1999).
56. B.K. Trask, "Superheater Corrosion at Scott Maritimes Limited," CPPA Atlantic Branch

Conference 1992, CPPA, Montreal QC (1992).
57. J. McMillan, "Superheater Problems, Their Causes and Solutions," 2004 International Chemical Recovery Conference, Volume 2, TAPPI Press, Atlanta, GA: 953 (2004).
58. T. Odelstam, "Material Evaluation for BLRB Superheater Tubes," Black Liquor Recovery Boiler Symposium 1982, Ekono Oy/Finnish Recovery Boiler Committee/Finnish Energy Economy Association, Helsinki, Finland: D6-1 (1982).
59. A. Fujisaki, H. Takatsuka, M. Yamamura, "World's Largest High Pressure and Temperature Recovery Boiler," 1992 International Chemical Recovery Conference, TAPPI Press, Atlanta, GA: 1 (1992).
60. A. Fujisaki, H. Takatsuka, M. Yamamura, "World's Largest High Pressure and Temperature Recovery Boiler," Pulp & Paper Canada, 95(11): T452 (1994).
61. H. Tran, Y. Arakawa, "Recovery Boiler Technology in Japan," TAPPI 2001 Engineering/Finishing and Converting Conference, TAPPI Press, Atlanta, GA: 49 (2001).
62. Y. Arakawa, Y. Taguchi, T. Meda, Y. Bara, "Experience with High Pressure and High Temperature Recovery Boilers for Two Decades," Pulp & Paper Canada, 106(12): T269 (2005).
63. H. Matsumoto, A. Notomi, T. Nishio, "Advanced Technology for Corrosion Resistant Materials for Recovery Boilers," 1998 International Chemical Recovery Conference, TAPPI Press, Atlanta, GA: 51 (1998).
64. H. Fujikawa, H. Makiura, Y. Nishiyama, „Corrosion Behaviour of Various Steels in Black Liquor Recovery Boiler Environment," Materials and Corrosion, 50: 154 (1999).
65. M. Mäkipää, M. Oksa, L. Koivisto, "Superheater Tube Corrosion in Changing Operation Conditions of Recovery Boilers," CORROSION/2004, Paper No. 01424, NACE, Houston TX (2001).
66. R. Backman, M. Hupa, J. Lagerborn, T. Lepistö, "Influence of Partially Molten Alkali Deposits on Superheater Corrosion in Black Liquor Recovery Boilers," 10th International Symposium on Corrosion in the Pulp and Paper Industry, Volume 1, VTT, Espoo, Finland: 137 (2001).
67. M. Oksa, M. Mäkipää, "Comparative Laboratory Testing of Molten Salt Attack of Superheater Tube Materials," 10th International Symposium on Corrosion in the Pulp and Paper Industry, Volume 2, VTT, Espoo, Finland: 523 (2001).
68. H.J. Grabke, E. Reese, M. Spiegel, "The Effects of Chlorine, Hydrogen Chloride and Sulphur Dioxide in the Oxidation of Steels below Deposits," Corrosion Science, 37: 1023 (1995).
69. R.W. Byers, "Fireside Slagging, Fouling and High Temperature Corrosion of Heat Transfer Surface due to Impurities in Steam-Raising Fuels," Prog. Energy Combust. Sci., 22: 29 (1996).
70. T. Nishio, H. Matsumoto, M. Shinohara, Y. Arkawa, "Influence of Ash Composition on the Corrosion Rate of Superhetaer Tubes," TAPPI 2001 Engineering, Finishing and Converting Conference, TAPPI Press: CD-ROM (2001).
71. M. Mäkipää, T. Malkow, D.J. Baxter, "The Effect of Salt Composition on the Chlorine Corrosion of Low Alloy Steels," CORROSION/2001, Paper No. 01186, NACE, Houston, TX (2001).
72. S.C. Cha, M. Spiegel, "Local Reactions between NaCl and KCl Particles and Metal Surfaces," Corrosion Engineering, Science & Technology, 40(3): 249 (2005).
73. J.R. Kish, C. Reid, D.L. Singbeil, R. Seguin, "Corrosion of High Alloy Superheater Tubes in a Coastal Biomass Power Boiler," CORROSION/2007, Paper No. 07349. NACE, Houston, TX (2007).
74. Y. Shinata, F. Takahashi, K. Hashiura, "NaCl-Induced Hot Corrosion of Stainless Steels," Materials Science and Engineering, 87: 399 (1987).

75. H. Tran, N. Mapara, D. Barham, "The Effect of H2O on Acidic Sulfate Corrosion in Kraft Recovery Boilers," Tappi Journal, 79(11): 155 (1996).
76. L. Paul, G. Clark, M. Eckhardt, "Laboratory and Field Corrosion Performance of a High Chromium Alloy for Protection of Waterwall Tubes from Corrosion in Low NOx Coal Fired Boilers," CORROSION/2006, Paper No. 06473, NACE, Houston, TX (2006).
77. S.D. Kiser, E.B. Hinshaw, T. Orsini, "Extending the Life of Fossil Fired Boiler Tubing with Cladding of Nickel Based Alloy Materials," CORROSION/2006, Paper No. 06474, NACE, Houston, TX (2006).
78. D. Singbeil, L. Frederick, N. Stead, "Testing the Effects of Operating Conditions on Corrosion of Water Wall Materials in Kraft Recovery Boilers", TAPPI 1996 Engineering Conference, TAPPI Press, Atlanta, GA: 649 (1996).
79. R. Backman, M. Hupa, P. Hyoty, "Corrosion due to Acidic Sulphates in Sulphate and Sodium Sulphite Recovery Boilers," Pulp and Paper Industry Corrosion Problems, Volume 4, Swedish Corrosion Institute, Stockholm, Sweden: 76 (1983).
80. S. Mrowec, K. Przybylski, "Defect and Transport Properties of Sulfides and Sulfidation of Metals," High Temperature Materials and Processes, 6(1-2), 1 (1984).
81. J. Klower, F.E. White, "High Temperature Corrosion of Commercial Heat Resistant Alloys under Deposits of Alkali Salts; Recent Laboratory Data," 8th International Symposium on Corrosion in the Pulp and Paper Industry, Swedish Corrosion Institute, Stockholm, Sweden: 179 (1995).
82. Mäkipää, M., Kauppinen, E., Lind, T., Pyykönen, J., Jokiniemi, J., McKeough, P., Oksa, M., Malkow, T., Fordham, R.J., Baxter, D., Koivisto, L., Saviharju, K., Vakkilainen, E., "Superheater Tube Corrosion in Recovery Boilers," Proceedings of the 10th International Corrosion in the Pulp and Paper Industry, Volume 1, Hakkarainen, T. Editor, p. 157, VTT, Espoo, Finland (2001).